The Pennsylvania State University
The Graduate School
Department of Biochemistry and Molecular Biology

STUDY OF THE IRON SULFUR CLUSTER AND POLYPEPTIDE COMPOSITION OF THE PHOTOSYNTHETIC REACTION CENTER FROM *HELIOBACTERIUM MODESTICALDUM*

A Thesis in

Biochemistry and Molecular Biology

by

Mark L. Heinnickel

Submitted in Partial Fulfillment
of the Requirements
for the Degree of

Doctor of Philosophy

May 2007

The thesis of Mark L. Heinnickel was reviewed and approved* by the following:

John H. Golbeck
Professor of Biochemistry and Molecular Biology
Professsor of Chemistry
Thesis Advisor
Chair of Committee

Squire J. Booker
Associate Professor of Biochemistry and Molecular Biology

J. Martin Bollinger
Associate Professor of Biochemistry and Molecular Biology

Donald A. Bryant
Professor of Biochemistry and Molecular Biology

Juliette Lecomte
Professor of Chemistry

Robert Schlegel
Professor of Biochemistry and Molecular Biology
Head of the Department of Biochemistry and Molecular Biology

*Signatures are on file in the Graduate School

ABSTRACT

The Fe/S Clusters and Polypeptide Composition of the Photosynthetic Reaction Center from *Heliobacterium modesticaldum*

The photosynthetic reaction center from *Heliobacterium modesticaldum* (HbRC) was studied using a variety of biochemical and biophysical techniques. The purpose of the work was to obtain a better understanding of the electron transfer cofactors and polypeptides that comprise the HbRC. The major findings include: (1) the HbRC loosely binds a ferredoxin-like protein that harbors two iron-sulfur clusters. This protein, which dissociates from the HbRC when it is passed over an anion exchange resin, was named PshB. HbRC complexes purified in this manner are henceforth referred to as HbRC cores. PshB can also be removed from HbRC complexes at high ionic strength and purified by passage over an ultrafiltration membrane. PshB was shown to restore the light-induced EPR signal of $[F_A/F_B]^-$ (visible at low temperatures), and the characteristic flash-induced kinetic decay of $P798^+$ when recombined with HbRC cores. (2) HbRC cores bind an interpolypeptide iron sulfur cluster termed F_X. When HbRC cores are incubated with sodium dithionite in the presence of light, F_X undergoes a one-electron reduction. Mossbauer and EPR data indicate the reduced cluster has a ground spin state of S=3/2. (3) Analysis of the non-heme iron content shows that HbRC cores bind 21.1 ± 1.1 Bchl *g*/P798. (4) The PshB protein was cloned from *H. modesticaldum* using knowledge of the N-terminal sequence of Fd2, a ferredoxin that had been isolated previously from *Heliobacillis mobilis*. When Fd2 is overexpressed in *Escherichia coli* with a His affinity tag and reconstituted with iron and sulfide, the holoprotein was found to co-purify with HbRC cores when subject to G-75 gel filtration chromatography and Ni-affinity chromatography. Similar to PshB from *H. modesticaldum,* the overexpressed Fd2 holoprotein restores the light-induced EPR signal of $[F_A/F_B]^-$ and the characteristic flash-induced kinetic decay of $P798^+$ when recombined with HbRC cores. This work indicates the function of Fd2 is now properly assigned: instead of representing a soluble ferredoxin, Fd2 is PshB and is normally bound to the HbRC complex.

TABLE OF CONTENTS

LIST OF FIGURES

LIST OF TABLES

ABBREVIATIONS

A_0	primary electron acceptor of Type I photosynthetic reaction center
A_1	quinone intermediate electron acceptor of Type I photosynthetic reaction center
APS	ammonium persulfate
ATP	adenosine triphosphate
Av	*Azotobacter vinelandii*
Bchl	bacteriochlorophyll
Chl	chlorophyll
DEAE	diethyl aminoethyl
F_A	terminal iron sulfur cluster electron acceptor of a Type I photosynthetic reaction center
F_B	terminal iron sulfur cluster electron acceptor of a Type I photosynthetic reaction center
Fd	ferredoxin
Fe/S cluster	iron sulfur cluster
FMO	Fenna-Mathews-Olson protein
F_X	interpolypeptide iron sulfur cluster in a Type I photosynthetic reaction center
HbRC	photosynthetic reaction center from *Heliobacterium modesticaldum*
HbRC core	photosynthetic reaction center from *Heliobacterium modesticaldum* devoid of PshB
Hm	*Heliobacterium modesticaldum*

MOPS	3-(N-morpholino)-propanesulfonic acid
Nd-YAG	neodymium-doped yttrium aluminum garnet
NADPH	reduced nicotinamide adenine dinucleotide phosphate
OEC	oxygen evolving complex
P680	primary donor of photosystem II
P700	primary donor of photosystem I
P700-F_X core	photosystem I devoid of PsaC, PsaD, and PsaE
P798	primary donor of the reaction center from *Heliobacteriaceae*
P840	primary donor of the reaction center from *Chlorobiaceae*
P^+A^-	oxidized primary donor and reduced primary acceptor
PAGE	polyacrylamide gel electrophoresis
Pd-10	desalting column sold by Amersham-Pharmacia
PSI	photosystem I
PSII	photosystem II
Q_A	quinone electron acceptor in Type II photosynthetic reaction center
Q_B	terminal quinone acceptor in Type II photosynthetic reaction center
Q_X	electronic transition in a chlorophyll molecule with a transition dipole moment on the x-axis of the chlorin molecule
Q_Y	electronic transition in a chlorophyll molecule with a transition dipole moment on the y-axis of the chlorin molecule
RC	reaction center

SDS	sodium dodecyl sulfate

ACKNOWLEDGEMENTS

I would like to express my deep appreciation to Dr. Golbeck for all of his patience and enthusiasm in guiding my research and reading my writing. I am especially grateful to him for allowing me the great freedom he granted me in my work. I am also extremely grateful to him for allowing me to attend several conferences, and allowing me to travel to Arizona and Moscow for research purposes. I believe I had the most fulfilling graduate career of any student in my class, and I attribute large amounts of that to him, and the environment he helped create.

I would like to thank Dr. Donald A. Bryant, Dr. Squire J. Booker, Dr. J. Martin Bollinger, and Dr. Juliette Lecomte for their time and support as my committee members. I would especially like to thank Dr. Squire J. Booker for stimulating conversations and assistance with EPR spectroscopy.

I would like to express my gratitude and admiration for the two post-doctorial scientists that aided me in my experiments: Dr. Rufat I. Agalarov and Dr. Gaozhong Shen. Without the help of these two scientists this document would not have been possible. I would also like to acknowledge Rob Cicchillo, Rama Balasubramanian, Bharat Jaganathan, Jané Bogdanov, Mahir Mamedov, Petra Fromme, Raimund Fromme, Sabrina Zimmerman, Julie Maresca, Aline Gomez, and all Golbeck lab members who contributed to my success.

Most importantly I would like to acknowledge my parents and brothers who have always believed in me, even when I didn't. Finally, I would like to acknowledge my beautiful and brilliant fiancée Heather Doyle for all of her support and love.

Mark Heinnickel

State College, PA

Chapter 1

General Introduction

1.1 PHOTOSYNTHESIS

Photosynthesis is the biological process in which solar energy is converted to chemical energy within the membranes of photosynthetic bacteria, plants, and algae. This process consists of a series of light-driven events that begins with the absorption of light and ends with chemical bond formation. The energy harnessed from light, both directly and indirectly, provides all of humanity's food and most of its energy resources. Photosynthesis has not only nourished the organisms that live on this planet, but it also changed the planet itself by producing an atmosphere rich in dioxygen.

The importance of oxygenic photosynthesis can more accurately be understood in its absence. It has been postulated that the extinction of the dinosaurs 65 million years ago was caused indirectly by the crashing of an asteroid into Earth. Massive amounts of dust were ejected into the atmosphere, causing a decrease in the amount of solar radiation that reached the Earth's surface. This resulted in a small decline in photosynthesis for a geologically insignificant time period (months-years). However brief this period, it nevertheless resulted in the eventual extinction of the dinosaurs and many other species on this planet (*1*).

Plants, algae, and cyanobacteria have similar photosynthetic mechanisms and similar components. They all perform oxygenic photosynthesis using chlorophyll-type pigments, and they all use light to drive electrons across a membrane (*1*). The chlorophyll molecules are organized into reaction centers (RCs), which are membrane bound protein-pigment complexes that carry out light-driven electron transfer (*1, 2*). Chlorophyll molecules are also organized into specialized proteins called antenna complexes (*1*). In plants and algae, photosynthesis is localized in specialized organelles called chloroplasts. It is commonly believed that the ancestor of plants and algae engulfed a cyanobacteria-like organism, and over time evolved into the chloroplast (*1*).

Photosynthesis is mediated by two RCs in cyanobacteria, plants, and algae, Photosystem I (PS I) and Photosystem II (PS II). The other major proteins that participate in the photosynthetic process are the cytochrome b_6f complex and ferredoxin:$NADP^+$ oxidoreductase. The cytochrome b_6f complex oxidizes quinonol molecules from PS II, thereby creating a proton gradient that results in ATP production (*1*). The cytochrome b_6f complex provides reducing equivalents for PS I using the soluble copper-containing protein plastocyanin. Ferredoxin:$NADP^+$ oxidoreductase accepts highly reducing electrons from PS I through the mediation of ferredoxin. These low potential reductants are used to reduce $NADP^+$ to NADPH, a stable molecule used for a wide variety of biosynthetic processes in the cell (*1, 2*).

1.1.1 *Reaction Centers*

The first of three steps in the general mechanism of light energy tranduction in the RC involves light harvesting. Pigments absorb light and funnel the exciton to the RC in a highly efficient manner. The antenna molecules transfer energy in the form of electronic excited states from one pigment to another (*1, 2*). The second step involves charge separation in the RC. In plants, algae, and cyanobacteria, the RC contains a special pair of chlorophyll molecules called the primary electron donor (*1*). Once the energy is transferred from the antenna system, the excited singlet state of the primary donor becomes a potent reductant that reduces a nearby electron acceptor to form the charge-separated pair, $P^+ A^-$. (*1, 2*). The third step involves electron transfer from the primary electron acceptor to additional bound secondary and tertiary electron acceptors. These cofactors are placed at very specific distances from one another to ensure rapid electron transfer. Their redox potentials are tuned by the protein milieu to be appropriate for the electron transfer step involved. In practice, the cofactors exist with generally descending redox potentials to guide the electron out of the RC complex to mobile electron transfer carriers (*1*). Consequently, although the electron loses some of its free energy after each electron transfer step, the time of charge separation is extended, thereby preventing charge recombination with $P700^+$ (*1*). The identity of the electron acceptors is the basis for the classification of the different RCs. If the terminal electron acceptor is a bound iron-sulfur cluster (Fe/S cluster), it is termed a Type I RC. If the terminal electron

acceptor is a mobile quinone, it is termed a Type II RC. Plants, algae, and cyanobacteria contain both Type I and a Type II RCs that function in series to oxidize water and reduce $NADP^+$ (*1, 2*).

1.1.2 *Photosytem II, a Type II Reaction Center*

PS II, the light-driven H_2O:plastoquinone oxidoreductase, functions to oxidize water and to reduce plastoquinone. The core subunits D1 and D2 contain the primary and secondary electron donors and acceptors (*1*). The PS II RC in eukaryotes contains as many as 25 polypeptides, while the PS II RC in cyanobacteria contains 21 subunits. The primary electron donor in PS II is composed of two Chl *a* molecules termed P680. Once P680 accepts energy from an electronically excited antenna pigment, it transfers an electron to a pheophytin acceptor (a pheophytin is a chlorophyll molecule missing the magnesium ion). Reduced pheophytin transfers the electron sequentially through two quinone molecules (Q_A and Q_B). Both quinones are stable in the semiquinone state, and following a second electron (and proton) transfer step, Q_B is reduced to the hydroquinol state. The plastiquinol is released within the membrane, and an oxidized plastoquinone molecule enters the Q_B site to continue the process anew. The plastoquinol molecule is oxidized by the cytochrome b_6f complex, which produces a proton gradient for ATP synthesis, and the electron is ultimately passed to PS I via plastocyanin or cytochrome c_6 (*1, 2*).

The most fascinating aspect of PS II is how $P680^+$ is reduced following electron transfer. The reducing equivalents are acquired by oxidizing water to dioxygen in the water splitting complex (OEC) (*1, 2*). Although interesting, this process is not the focus of this thesis, and will not be discussed further.

There are two bacterial groups that possess Type II RCs: purple bacteria and green non-sulfur bacteria. Both have a Type II RC as their lone reaction center. The purple bacterial RC has been studied extensively and was the first membrane protein to be crystallized (*1, 2*).

1.1.3 *Photosystem I, a Type I Reaction Center*

PS I, the light-driven plastoquinone:ferredoxin oxidoreductase, functions to oxidize plastocyanin or cytochrome c_6 and to reduce $NADP^+$. Two of the twelve subunits of PS I, PsaA and PsaB, form a heterodimer; the entire P700-F_x-core binds 90 antenna chlorophylls and six electron transfer chlorophylls. Electron transfer in PS I is initiated when a Chl *a*/*a'* special pair, termed P700, accepts energy from an electronically excited antenna pigment and donates the excited electron to a nearby Chl *a* molecule termed A_0 (*3*). Primary charge separation results in a primary donor cation ($P700^+$) and a primary acceptor anion (A_0^-). A_0^- then passes the electron to a nearby phylloquinone (A_1), which subsequently donates the electron sequentially through three [4Fe-4S] clusters termed F_X, F_A, and F_B (*3*). F_A and F_B are bound by a dicluster, ferredoxin-like protein termed PsaC (*3*). Forward electron transfer from P700 to F_B is complete in ~200 ns (*4*), whereupon it is donated to soluble ferredoxin. The midpoint potential of ferredoxin is sufficiently low to reduce $NADP^+$ to NADPH through the involvement of ferredoxin:$NADP^+$ oxidoreductase (*3*). If ferredoxin and plastocyanin (or cytochrome c_6) are absent, the electron recombines with the primary donor, $P700^+$. The time of this charge recombination varies based on the cofactor the electron inhabits (A_0, A_1, F_X, F_A, or F_B) before it recombines with $P700^+$ (*5*). Figure 1.1 shows the time scales for charge recombination, as well as the redox potential, for each cofactor in PS I.

Two bacterial families possess only Type I RCs: *Chlorobiaceae* and *Heliobacteriaceae* (*6, 7*). Both have a Type I RC as their lone reaction center. The core of these RCs consists of a homodimer instead of a heterodimer (as in PS I).

The RC from the family *chlorobiaceae* is a light-driven cytochrome:ferredoxin oxidoreductase. The RC is composed of a homodimer of the PscA protein, which binds approximately 22 antenna chlorophylls (the vast majority of the chls are contained in a large antenna complex termed the chlorosome). The PscA homodimer also binds the primary electron donor (P840), primary electron acceptor (A_0), and the interpolypeptide Fe/S cluster F_X (*8*). Electron transfer is initiated when a bacteriochlorophyll *a*/*a'* special pair (P840) accepts energy from its antenna complex and donates an excited electron to a nearby Chl *a* molecule (A_0) (*3*). Primary charge separation results in the primary donor

cation ($P840^+$) and the primary acceptor anion (A_0^-). A_0^- then passes the electron sequentially through three [4Fe-4S] clusters termed F_X, F_A, and F_B (*3*). It is uncertain whether a quinone is involved as an intermediate electron transfer cofactor (as in PS I) (*6*). The F_A and F_B iron-sulfur clusters are bound by PscB, a protein with a PsaC-like domain (*8*) The *Chlorobium* RC contains three additional subunits; PscC, PscD, and the Fenna-Mathews-Olson (FMO) protein. PscC is a cytochrome that functions as an electron donor to $P840^+$ (*9*). The function of PscD is said to stabilize the PscB protein, although this is purely supposition (*10*). The FMO protein is a water-soluble antenna protein that contains 40 Bchl *a* molecules (*11*). The function of the RC is to produce reducing equivalents that are used to convert $NADP^+$ to NADPH (*6*).

In contrast to PS I, the RC in heliobacteria has drawn far less attention. It is unclear how many subunits and cofactors exist, and it is unclear if the reducing equivalents are used to reduce NAD^+ or $NADP^+$ (as in PS I) or are used in cyclic electron transfer (as in the purple bacterial RC) (*7*). Future biotechnologies based on photochemical energy conversion stand to profit greatly from a detailed understanding of all photosynthetic RCs. Therefore, a greater understanding of the unique RC from heliobacteria is of utmost importance. The remainder of this chapter, as well as the entire thesis, will focus on the cofactor and polypeptide composition of the RC in heliobacteria.

1.2 *HELIOBACTERIACEAE*

In 1983, Gest and Favinger discovered an entirely new microorganism that had characteristics so unique it eventually led to the creation of a new taxonomic family, *Heliobacteriaceae* (*12*). The microorganism, *Heliobacterium chlorum*, was discovered accidentally when an enrichment medium was prepared incorrectly for a microbiology class at Indiana University. The medium was prepared to culture organisms that could fix dinitrogen under photoheterotrophic conditions from soil on the Indiana University campus. Mistakenly, a small amount of $(NH4)_2SO4$ instead of NH_4Cl was added to the medium to stimulate growth. The sulfate in the medium was reduced by sulfate reducing bacteria to sulfide. The sulfide inhibited the growth of purple non-sulfur bacteria, the photosynthetic bacteria normally cultured in this experiment. A previously unknown

microorganism began to grow in the enrichment culture, forming greenish brown mats. The microorganism, which Gest and Favringer named *Heliobacterium chlorum*, appeared under a microscope as rods with a width of 1 μm and a variable length. The organism was a photoheterotroph, and hence it could not grow on bicarbonate nor could it use hydrogen or sulfide as electron donors. The organism was also quite intolerant of oxygen, and in its presence, turned from a brown color to an emerald green color. Cultures were found to grow much more quickly in the presence of light, although dark growth was possible. The unique aspect of this organism was the presence of an entirely new pigment termed bacteriochlorophyll *g* (Bchl *g*). The organism also contained carotenoids, but in very small amounts, and no β or γ carotenoids (more on these pigments below). Interestingly, the organism did not contain intra-cytoplasmic membranes or chlorosomes, structures commonly found in purple non-sulfur and green sulfur bacteria (*12, 13*).

At the time of its discovery, *H. chlorum* was classified as a green gliding bacterium similar to *Chloroflexus aurantiacus* (*12*). This assignment was based solely on its motility. However, the 16S rRNA sequence showed a greater similarity to gram-positive bacteria than to any photosynthetic organism, even though it stained gram negative (*14, 15*). In 1985, Woese and colleagues found that the oligonucleotide sequence of *H. chlorum* was 85% homologous to *Bacillus subtilis* (more recently the homology between *H. chlorum* and other gram-positive microorganisms has been found to be as high as 87%) (*14, 15*). This finding placed *H. chlorum* in a phylum that previously contained no photosynthetic organisms (*14*).

Although the 16S rRNA of *H. chlorum* has the highest similarity to gram-positive organisms, it has been suggested that an even stronger tie may exist between heliobacteria and cyanobacteria (*15*). This relationship is based on the nature of heliobacteria's photosynthetic apparatus as well as its 16S rRNA (83% similar to *Synechococcus* sp. PCC 6301). Vermaas (*15*) makes the point that there are many more 16S rRNA sequences known from gram positive bacteria than from cyanobacteria, and this larger number of sequences skews the comparison toward gram positive bacteria.

Although the 16S rRNA analysis has been challenged, there are other factors that suggest it is a gram-positive organism. Lipopolysaccharide, a major component of the outer membrane of gram-negative bacteria, is absent in cell extracts (*16*). In addition, the

majority of the fatty acids in the plasma membrane contain branched chains, a feature more characteristic of gram-positive bacteria as opposed to gram negative bacteria (*16*). Using partially hydrolyzed cell wall preparations, the cell wall structure was determined to be A3 type with L,L-diaminopimelate at position 3, D-alanine in position 4, and a glycine interpeptide bridge (*17*). The A3 type cell wall structure is found in other gram-positive bacteria such as *Clostridium perfringens* and *Nocardioides simplex* (*17*). Similar to clostridia, heliobacteria also do not contain the pyruvate dehydrogenase complex but rather have the pyruvate:ferredoxin oxidoreductase complex (*18*). This is a major point considering that pyruvate is the carbon source on which heliobacteria grow optimally (*12, 18-20*). In addition, many strains of heliobacteria have been found to form endospores that resemble those formed by bacteria from the *Bacillaceae* family (*21*). Moreover, the spores formed by heliobacteria contain dipicolinic acid, a key component in endospores of *Bacillaceae* (*21*).

Heliobacteria have been found in every instance to be photoheterotrophic organisms (*12, 20, 22, 23*). They do not contain ribulose 1,5-bisphosphate or ATP citrate-lyase, enzymes used in carbon fixation (*18*). Instead, they have been found to grow only on certain organic substrates including pyruvate, lactate, butyrate, and acetate (*18, 24*). Some strains can grow on sugars and ethanol (*24*). The carbon metabolism of the organism has been found to be highly dependent on light, with the available substrates for growth in the dark limited to pyruvate and lactate (*18, 19*). By analyzing the activities of key enzymes in cell extracts and by analyzing the ^{13}C labeling patterns of certain amino acids of cultures grown in ^{13}C-labeled pyruvate and acetate, heliobacteria were found to utilize carbon using an incomplete reductive carboxylic acid pathway (*17, 18*) (Figure 1.2). Although this pathway can convert pyruvate to 2-oxoglutarate, heliobacteria are unable to grow autotrophically because of the absence of ATP citrate-lyase (*18*). Although heliobacteria can use this pathway for energy transduction as well as for all the metabolites it requires for biosynthesis of its cellular machinery, it has the serious limitation of requiring reduced ferredoxin to convert succinyl CoA into 2-oxoglutarate, and NADH to convert oxalacetate to malate (*18*). These substrates, however, are readily provided as products of photosynthesis. In the absence of photosynthesis, heliobacteria can obtain these intermediates by converting pyruvate to acetyl Co-A and isocitrate to 2-

oxoglutarate, but this is not an efficient process, and it acidifies the medium (*17-19*). Therefore, it appears that photosynthesis is tightly linked to carbon metabolism in heliobacteria, although an alternative light-independent pathway does exist.

Photosynthesis is also important in heliobacteria for the process of nitrogen fixation. Indeed, it has been shown that all species fix nitrogen (*25*), and it has been suggested that in rice fields and hot springs, this is the organism's major ecological role (*26*). It makes good metabolic sense that photosynthesis would be used by a nitrogen-fixing organism, if only because the reaction of fixing nitrogen is so energy intensive (8 electrons and 16 ATPs are required to convert one molecule of N_2 to two molecules of NH_3), Heliobacteria contain a Type I RC (see below) that generates highly reducing compounds such as the ferredoxin necessary for this process. Although it has been shown that heliobacteria can fix dinitrogen in the dark, the process is 83-90% less efficient than in the light, and it only occurs in the presence of pyruvate (*25*). Some strains of heliobacteria have been found to fix dinitrogen in the absence of molybdenum, using iron or iron and vanadium instead (*27*). One particular strain, *Heliobacterium gestii*, was isolated from rice soil, which is an environment that typically has a low molybdenum content because of metal leaching under acidic conditions (*21, 27*). This finding further advances the idea that in rice paddies, nitrogen fixation is the major role of heliobacteria.

In the 23 years following the initial discovery, other heliobacterial strains have been isolated, and all strains have been placed into a new family called Heliobacteriaceae (*26*). The members of this family are divided into four genera: *Heliobacterium*, *Heliobacillus*, *Heliophilum*, and *Heliorestis*. *Heliobacterium, Heliobacillus,* and *Heliophilum* differ from each other in their method of motility (*26*). *Heliorestis* differs from all the other genera because of the ability to grow optimally at alkaline pH and at lower temperatures (*26*). Even though the initial strain was isolated in non-agricultural soil, heliobacterial strains can be isolated reliably from rice fields (*23*). This suggests a possible symbiosis between rice and heliobacteria in which the plants supply the photoheterotrophic heliobacteria with organic compounds and the photoheterotrophic heliobacteria supply the plant with fixed nitrogen (*26*).

1.2.1 *The Heliobacterial Reaction Center*

The photosynthetic RC in heliobacteria (HbRC) shares similarities to PS I in that it has Fe/S clusters as terminal electron acceptors (*7*). This makes it a Type I RC. The majority of the electron transfer cofactors in the HbRC are located on the membrane-embedded PshA protein (*28*). The N-terminus of PshA was found to be blocked, and it was necessary to use peptide fragments from a trypsin digest to first identify and then clone its gene (*28*). The HbRC was judged to be PshA homodimer based on several lines of evidence. Firstly, all protein fragments from the digest were found to correspond to pieces of the PshA sequence (*28*). Secondly, neither northern blot nor Southern blot analysis showed the existence of a second RC protein that would be similar to PshA (*28*). Thirdly, the HbRC was proposed to be a homodimer because the region of highest similarity to PS I is the region where the F_X Fe/S cluster binds (*28*). In PS I, the Fe/S cluster F_X is an interpolypeptide cluster ligated by four cysteines, two of which are supplied by PsaA and two of which are supplied by PsaB (*29*). Hence, the HbRC could not ligate an F_X cluster unless it were a dimer. An approximate molecular weight determined by gel filtration was also consistent with a dimer (*30*).

An HbRC consisting of only the homodimer of PshA has been purified, and it can undergo light induced charge separation (*31-33*). The charge recombination kinetics are similar to those observed in membranes (*30, 31*). The optical absorbance spectrum of the PshA homodimer is also identical to that seen in whole cells and membranes (*30, 31*). The *pshA* gene is located in a gene cluster that does not include any ORFs encoding for proteins that participate in photosynthetic electron transfer (*34*). However, this gene cluster does include genes that code for proteins involved in chlorophyll and carotenoid biosynthesis, as well as genes that code for proteins in the cytochrome *bc* complex (*34*). Based on the biochemical, genetic and spectroscopic observations, several authors have suggested that the only polypeptide in the HbRC is PshA (*31, 35*). There is evidence to contradict this point, but it was not until recently that the PshA-only hypothesis was shown to be incorrect (*36, 37*) (more below, also see Chapters 2 and 4).

Because the HbRC contains far fewer proteins than PS I, it has been suggested to be an evolutionary ancestor to PS I (*28, 38*). The idea has been put forward that a gene duplication event occurred in heliobacteria, leading to a heterodimer (*39*). Because of its

diversity, a heterodimer has the possibility of binding more subunits than a homodimer. In spite of these claims, and despite the biochemical and spectroscopic similarities between PS I and the HbRC, the PshA protein has only a 16.3 and 16.8% identity to the PsaA and PsaB subunits from maize (*28*). The regions of greatest identity lie within the F_X binding region and the hydrophobic section that proceeds it (*28*). However, if just this region and the N-terminal amino acids adjacent to the F_X site (386 amino acids out of 609) are compared to PS I, the sequence identity and similarity are still low (15% and 60%) (*15*). Indeed, this same region shows a larger identity and similarity to CP43 (33% and 72%, respectively), an antenna protein that is a component of PS II (*15*). Therefore, based on these genetic comparisons, the HbRC seems to have an evolutionary relationship with both PS I and PSII, suggesting it may be an evolutionary precursor of both (*39*).

1.2.2 *Pigment Composition of Heliobacteria*

The pigment that distinguishes heliobacteria from other photosynthetic bacteria is Bchl *g* (*26*), which is found only in the *Heliobacteriaceae* (*26*). The structure of Bchl *g* (Figure 1.3a) is a hybrid between Chl *a* and Bchl *b* (Figure 3a and 3b) (*40, 41*). Similar to Bchl *b*, Bchl *g* has a saturated ring II in its core porphyrin structure, and an ethylene group at carbon 8 (Figure 1.3c) (*40, 41*). Similar to Chl *a*, Bchl *g* has a vinyl group at carbon 3 (*40, 41*). In the presence of oxygen and light, ring II isomerizes making carbon 7 an sp^2 hybridized carbon and carbon 8^1 an sp^3 hybridized carbon (*40*). Once ring II has isomerized, Bchl *g* is spectroscopically identical to Chl *a* (*40, 41*). The ethyl group at position 8 is usually a hydroxyethyl in these oxygen isomerized chlorophylls (*40, 42*). This conversion has also been shown to occur under anaerobic conditions in the presence of weak acid (*42*). This isomerization changes the color of the pigment from brownish-green to emerald-green (*12, 40, 41*). The esterifying alcohol in Bchl *g* is farnesol, a C15 alcohol usually esterifed to Bchl *c*, Bchl *d*, and Bchl *e* (the pigments found in green anoxygenic bacteria) (*6, 41*).

The absorbance spectrum of Bchl *g* is unique and gives heliobacteria an evolutionary advantage in certain environments. Cells and isolated membranes have similar absorbance spectra with peaks at 368, 409, 575, and 787 nm (Figure 1.3, brown)

(*40*). The first two peaks are due to Soret transitions, whereas the last two are due to Q_x and Q_y transitions, respectively (*40, 41*). (Soret and Q transitions refer to different $\pi \rightarrow \pi^*$ transitions in the chlorophyll molecule; Q_x and Q_y refer to the orientations of the transition dipole moment in the chlorin molecule (*43*)). The absorbance spectrum of Bchl *g* allows heliobacteria to harvest near-ultraviolet and near-infrared light in its terrestrial environment (*12*).

Two additional Chl molecules are found in heliobacteria. A 13^2 epimer of Bchl *g* termed Bchl *g*' is found in the HbRC and a 'special pair' functions as the primary electron donor (more below) (*44, 45*). At position 13^2, which is in ring V on the chlorophyll molecule, Bchl *g*' has a proton and a carboxymethyl group in a different stereochemical position with respect to the Bchl g molecule (*45*). The 8^1-OH Chl a_F, a Chl *a* with a farnesol tail, is also found in the HbRC where it functions as the primary electron acceptor (*46*) (see below, absorbance spectrum Figure 1.3, green). The bioynthesis of this Chl in heliobacteria most likely proceeds by a non oxygen-requiring pathway because it can be formed under anaerobic conditions in the absence of light (*19*).

The primary (>95%) carotenoid in heliobacteria 4,4-is diaponeurosporene (*47*), a C30 acyclic compound with nine conjugated double bonds and one non-conjugated double bond. Heliobacteria, which have lower levels of carotenoids compared to other phototrophic bacteria, are the only phototrophs known to contain diapocarotenoids (*12, 47*). It has been suggested that the small content of carotenoids is the reason that heliobacteria are sensitive to oxygen (*12*). Even though 4,4-diaponeurosporene has not been directly shown to be involved in any cellular process, its presence in the HbRC implies that it may be involved in triplet scavenging and other forms of photoprotection (*30, 31*).

The last photosynthetic cofactor found in heliobacteria is menaquinone-9, although trace amounts of menaquinone-7, menaquinone-8, and menaquinone-10 are also present (*48*). The presence of this quinone implies a link between heliobacteria and green bacteria. Green sulfur bacteria have been found to contain menaquinone-7, whereas green non-sulfur bacteria have been found to contain menaquinone-10 (*6, 48*). The presence of menaquinone in heliobacteria implies a link with gram-positive bacteria, which have only been found to contain quinones of the naphthoquinone type (*48*). The role of

menaquinone-9 in the organism is under intense debate. Menaquinone-9 has been shown to be involved in the cytochrome *bc* complex, but it may also be involved in the HbRC (see below).

1.2.3 *The Primary Electron Donor*

The primary electron donor in heliobacteria was first described in 1985 and was named P798 (*49, 50*) because the wavelength of maximal bleaching following light excitation was at 798 nm. The flash-induced difference spectrum of P798 immediately drew attention as it appeared to be spectroscopically similar (in terms of shape) to the flash-induced difference spectrum of P700 in PS I, with the provision that it was red shifted by 100 nm (*51*). Soon after its discovery, EPR studies showed that P798 forms a radical following illumination (*52*). The linewidth of the organic radical was 0.95 mT, which is approximately the same linewidth of $P860^{+}$, a Bchl *a* special pair in the bacterial RC (*52*). The redox potential of P798 was measured to be +225 to +240 mV (*52*). This redox potential is more reducing than any other primary electron donor, either from a Type I or Type II RC, and the key to this redox potential may involve cysteines that ligate P798 (*32*).

Bchl *g*′ was found in membranes and purified HbRCs by pigment analysis using HPLC (*44, 45*). Based on its similarity with PS I, which contains a Chl *a*′ molecule in the primary donor (*3*), the hypothesis was put forward that P798 was also composed of Bchl *g*′ molecules (*45*). Bchl *g*′ was present in purified HbRCs, where it was found to be more difficult to remove from lyophilized complexes with organic solvent than Bchl *g* (*44*). This result is consistent with the notion that Bchl *g*′ is the primary donor: it is expected to be located deep in the protein and difficult to remove (*44*). It was generally accepted that P798 would need to be a homodimer of Bchl *g*′ because the proteins involved in the HbRC are identical (*28, 45*).

1.2.4 *The Primary Electron Acceptor*

The spectroscopic properties of the primary electron acceptor were also first described in 1985 (*49*). Flash-induced difference spectroscopy performed on membranes showed a transient bleaching at 670 nm that decayed in 600 to 800 ps (*49*). This

bleaching did not correspond to the decay of the primary donor, thus indicating it was not a backreaction but rather represented forward donation to an electron acceptor (*49*). Because of its absorbance maximum, it was concluded the transient signal could not be from a Bchl *g* antenna molecule. In the presence of dithionite at a high pH, this component recombines with $P798^+$ in 17 ns (*49*). This indicates that the acceptor has a very low redox potential, although its precise value is unknown.

This acceptor, named A_0, was believed to account for the flash-induced absorbance change at 670 nm in membranes and HbRCs (*49*). Although the pigment was first believed to be BChl *c (49)*, its spectral properties more resembled that of Chl *a* after purification by HPLC (*46*). Further analysis by HPLC and NMR revealed the pigment was slightly different from Chl *a*. The pigment was more polar than Chl *a*, and its molecular weight was 17 mass units heavier than Chl *a (46)*. This new pigment contained a farnesyl tail, as opposed to Chl *a*, which contains a phytyl tail. NMR analysis showed the pigment was in fact 8^1-hydroxy-chlorophyll *a* with a farnesyl tail (8^1-OH-Chl a_F) (*46*). The existence of 8^1-OH-chl a_F as the primary acceptor in heliobacteria demonstrates a clear evolutionary link between the HbRC and PS I (where Chl *a* is also the primary acceptor (*3, 46*)). Pigment analysis showed that the HbRC contains 17 Bchl *g*/ 8^1-OH-chl a_F, and this ratio is similar to the Bchl *g*/Bchl *g* ratio (*45, 46*). Because the HbRC is a homodimer, it is assumed that there are identical electron transfer pathways on both subunits. It is therefore likely that each subunit has an 8^1-OH-Chl *a* molecule positioned as a primary acceptor (*43*).

1.2.5 *Intermediate Electron Acceptors: A_1 and F_X*

The reduced primary electron acceptor A_0^- is re-oxidized in 600-800 ps. The oxidation results in forward electron transfer to a secondary electron acceptor. The identity of the secondary acceptor in the HbRC is, however, in dispute. The fact that a quinone intermediate may not exist is what makes RCs from *Heliobacteriaceae* and *Chlorobiaceae* potentially different from PS I (*7*).

It is clear the HbRC contains menaquinone-9 (*48*). By analogy with PS I, it was proposed that menaquinone-9 could function as the secondary electron acceptor (*3*). Early evidence appeared to support this hypothesis. When the HbRC was frozen in the presence

of light and a chemical reductant (a process referred to as photoaccumulation), a radical that was attributed to a semiquinone was detected by EPR at both X-band and Q-band (*53*). An ENDOR signal attributed to a semiquinone radical was also detected (*54*). Furthermore, the low temperature charge recombination kinetics could be deconvoluted into a biphasic decay (*36*). The hypothesis used to explain this result presupposed the existence of two different electron acceptors, both of which followed A_0, which were undergoing charge recombination at these temperatures (*36*). Moreover, a redox titration of purified PshA homodimers best fit two different cofactors, implying that two acceptors are present following A_0 (*55*).

However, there is equally good evidence to contradict the assertion that menaquinone-9 functions as a secondary electron acceptor. Kleinherenbrink and colleagues extracted the quinones from lyophilized membranes and found that the HbRC was still active, provided the ether was completely removed before the protein was redissolved in buffer (*56*). The ether extraction had no effect on forward electron transfer or on charge recombination at either room temperature or low temperature in either the msec or nsec time scale. These data suggested that menaquinone-9 did not participate in the electron transfer pathway (*56*).

Time-resolved optical spectroscopy performed in the ps, ns, and μs time scales have not provided any evidence that a menaquinone is reduced on a single flash (*57, 58*). Transient EPR spectroscopy performed at X-band (9 GHz) and K-band (24 GHz) also fails to show the involvement of a semiquinone radical after a laser flash (*59*). Photovoltage measurements indicate that only two electron transfer steps occur in membranes following a laser flash (*58*). This is in contrast to PS I, in which three electron transfer steps occur in the P700-F_X core (P700➞A_0➞A_1➞F_X). Because a primary donor, a primary acceptor, and an F_X-like Fe/S cluster have been found in HbRCs, it appears that the intermediate electron acceptor A_1 is missing (more on the F_X-like Fe/S cluster below) (*49*). These results have persuaded many researchers to suggest that the iron-sulfur cluster F_X, rather than the quinone A_1, is the secondary electron acceptor in the HbRC, and that the menaquinone has either an undetermined function or is involved in an alternative electron transfer pathway (*57, 60*).

All of the above techniques revolve around the hypothesis that menaquinone functions as a non-covalently bound cofactor, and that it accumulates to spectroscopically detectable levels, similar to phylloquinone in PS I (*3*). It is possible that the menaquinone could be bound covalently to PshA, thus making it resistant to removal by organic solvent. It is also possible that the reduction of the quinone occurs at a faster rate than its reoxidation, making the reduced semiquinone state spectroscopically undetectable. The covalently bound menaquinone hypothesis was tested in 1993 when peptide fragments of PshA were all found to have the same mass as predicted by the the *pshA* gene, thus excluding the existence of a covalently bound cofactor (*28*). The idea of a spectroscopically undetectable intermediate was tested by Brettel et al. using double flash experiments (*58*). Membranes were incubated with neutral red, an artificial electron donor capable of reducing $P798^+$ in 700 μs, which is much faster than the 12 ms decay of $P798^+$ in membranes. On multiple flashes, all of the terminal electron acceptors could be sequentially reduced, thereby allowing the number of acceptors to be determined. It was found that after the cofactor that decays in 12 ms had been reduced, the next flash resulted in a 17 ns decay, a lifetime that matches that of the recombination of $P798^+$ with the primary acceptor A_0^- (*49*). This implies there exists no spectroscopically undetectable intermediate between A_0 and the cofactor that decays in 12 ms. (The argument will be made below that the 12-ms kinetic phase represents the $P798^+ F_X^-$ backreaction.)

The existence of the Fe/S cluster F_X was at first only implied by the amino acid sequence of the PshA protein, which contains an F_X binding motif (*28*). Kleinherenbrink and colleagues shortly thereafter provided optical evidence for the presence of F_X (*61*). In this experiment membranes were treated with urea to remove any PsaC-like protein that might exist. The treatment did not eliminate the charge recombination with $P798^+$, but it did cause in loss of the EPR signals of F_A and F_B, thus indicating removal of a bound ferredoxin. A flash-difference spectrum was constructed in the presence of an artificial electron acceptor that would quickly remove electrons from the (now) terminal acceptor. In its presence, $P798^+$ I would be generated, and in its absence $P798^+ I^-$ would be generated (where I is the unidentified cofactor). When the spectrum of $P798^+I$ was subtracted from that of $P798^+I^-$, a spectrum was generated for I^- that resembled the difference spectrum of an Fe/S cluster (*62*). The spectrum was broad and featureless, yet

showed a very slight maximum at 430 nm. Assuming a 1:1 molar ratio of $P798^+$ to I^-, a differential molar extinction coefficient for I^-/I was calculated. The value, 10-11 mM^{-1} cm^{-1}, compares favorably to the molar extinction coefficient for F_X^-/F_X in PS I (*63*). In support of this finding, the purified PshA homodimer contains acid labile sulfide and non-heme iron, indicating the presence of an intact Fe/S cluster apart from F_A and F_B (*31*).

In spite of these observations, no EPR signal could be detected that would correspond to an F_X^- -like iron-sulfur cluster (*31, 61*). A recent EPR study performed on membranes has since claimed to show the presence of an F_X like Fe/S cluster (*33*). In this experiment, membranes from *H. modesticaldum* were incubated with dithionite at pH 8, frozen in the dark and illuminated at 4 to 10 K. A light-minus-dark difference spectrum revealed a signal at $g_x = 2.040$, $g_y = 1.911$, and $g_z = 1.896$, which was only observable at very low temperatures and high microwave powers. Curiously, the signal was not present in purified HbRC complexes that lacked F_A and F_B. One distinct possibility is that the signal detected in membranes is an artifact of cavity heating by the light source; relief of power saturation would allow the resonances from the chemically-reduced F_A^- and F_B^- to become larger in the light, thereby resulting in a light-minus-dark difference spectrum. Earlier, an EPR signal had been published on the Fe/S clusters in heliobacteria using a similar technique (*64*), and was noted as an artifact in a later publication (*36*).

1.2.6 *The Terminal Electron Acceptors F_A/F_B*

The first observation that the HbRC may contain EPR-detectable Fe/S clusters was made in 1985 (*52*). Membranes were shown to exhibit large EPR signals near $g = 2$ that were characteristic of Fe/S clusters. Although these Fe/S clusters were not reducible with light, they were shown to have a low redox potential, similar to F_A and F_B in PS I (*52*). This finding led some to propose that Fe/S clusters were the terminal electron acceptors in heliobacteria (*51*). In 1990, Nitschke and colleagues discovered that it was possible to reduce the iron-sulfur clusters at cryogenic temperatures using light, but a very intense light source was required (*36*). It was proposed that this was because the HbRC contains a small antenna complement (*36*). This study also showed that there were two light reducible iron-sulfur clusters, and that they were distinguishable on the basis of

their *g*-factors. This study proved that the terminal electron acceptors in heliobacteria were indeed iron-sulfur clusters similar to F_A and F_B in PS I (*36*).

Further information on the F_A and F_B clusters remained elusive. F_A and F_B do not have optical signatures that clearly distinguish them from other cofactors in the HbRC, most notably from Fe/S cluster F_X. In addition, the charge recombination kinetics between the primary donor, $P798^+$, and $[F_A/F_B]^-$ proved difficult to determine (however, see chapter 2). Indeed, Amesz and co-workers suggested that electron transfer to the iron-sulfur clusters was irreversible at room temperature in membranes (*37*). However, in flash excitation experiments, it is important that a period of time elapses between the flashes to ensure that the electron acceptors are completely oxidized, since otherwise the yield of charge separation will diminish on successive flashes (see Chapter 2).

Published reports of purified HbRCs, which consist of homodimers of the PshA protein, do not indicate the presence of EPR-observable iron-sulfur clusters (*30, 31, 33*). These preparations have the same charge recombination kinetics as found in membranes and detergent-solubilized membranes (when measured without significant time intervals between the flashes). These observations have led some researchers to speculate that the HbRC consists solely of the PshA homodimer, and that F_A and F_B are contained on a protein that only transiently associates with the PshA homodimer (*31*).

Further hindering the study of F_A/F_B is the absence of knowledge of the polypeptide that binds these acceptors. In PS I, F_A/F_B are bound by a ferredoxin-like protein termed PsaC (*3*). A similar PsaC-like protein had not been found as an integral component of the HbRC (*30, 31*). Sequencing of the open reading frames surrounding the *pshA* gene revealed no homologue of *psaC* (*34*). It is believed that a PsaC-like protein would be oxygen sensitive because it is known that even after brief exposure to air, the light-induced EPR resonances of the iron-sulfur clusters disappear (*61*). It would also appear that the PsaC-like protein would be sensitive to ionic detergents such as deriphat 160c and sucrose monolaurate (*31, 32*). These detergents have been used in past studies to purify the PshA homodimer, and it comes as no surprise that they might have also removed this hypothetical protein.

1.2.7 *Antenna Composition of Heliobacteria*

The antenna Chls in heliobacteria are thought to reside exclusively on the PshA protein (*30, 31*). Using a freeze-etching electron microscopic technique, cell membranes were found to have no specialized membrane structures such as cytoplasmic invaginations, thylakoids, or chlorosomes (*12, 50, 65*). The antenna pigments consist primarily of Bchl *g* and carotenoids (*30, 31*). The number of Bchl *g* molecules that function as antenna in the HbRC is uncertain. The first attempt to determine the Bchl/P798 ratio came about in 1985 when Nuijs and colleagues compared, in membranes, the amplitude of Bchl *g* absorbance to the amplitude of the flash-induced bleaching at 798 nm that was attributed to the primary donor (*49*). The value obtained was 30 Bchl *g*/ P798. A similar approach was employed by Trost and Blankenship, who concluded that there were 24 to 27 Bchl *g*/P798 in purified HbRCs (*31*). One potential weakness of this approach is that the extinction coefficients of Bchl *g* and P798 are assumed to be identical, which may not be the case. Indeed, recent reports have shown the extinction coefficients of Bchl *g* and P798 are significantly different. Using methylene blue, an artificial electron acceptor with a well-known molar extinction coefficient, the number of HbRCs that participate in charge separation can be calculated by the number of molecules reduced on a single-turnover flash (*61*). The molar extinction coefficient of Bchl *g* was determined to be 76 mM^{-1} cm^{-1} after purification from membranes by HPLC (*46*). The molar extinction coefficient for P798 was determined to be 240 mM^{-1} cm^{-1} (*61*). Using these values, the Bchl *g*/ P798 can be calculated to be 17-23. The most cited value for Bchl *g*/P798 molecules is 35, attained by Kobayashi et al. (*45*) using HPLC to separate the pigments. Here, the Bchl *g* to Bchl *g*□ratio was found to be 17.3:1 in membranes. Assuming the presence of two Bchl *g*□/HbRC, this value yields 35 Bchl *g*/HbRC. It is interesting that this value also corresponds to the number of histidines (17) found in PshA (*28*). This is relevant because in PS I many of the antenna Chls are ligated by histidines (*29*).

The absorbance of Chl molecules, much like the pK_a of amino acids, can be changed by the protein milleu. Although absorbance spectra between 750 and 810 nm of whole cells at room temperature exhibit only one peak, three spectroscopically-distinct Bchl *g* molecules exist at low temperatures (*66*). At 4 K, the three spectroscopically

identifiable species are Bchl *g* 776, Bchl *g* 793, and Bchl *g* 808 (the numbers correspond to their absorbance maximum in nm) (*66*). The function of these Bchl *g* molecules may be to funnel energy to the HbRC efficiently, based on a thermodynamically downhill flow of energy. Fluorescence emission from the HbRC at room temperature and low temperature is exclusively from Bchl *g* 808 (*66*). This indicates that the energy dissipation to the longest wavelength Bchl *g* is efficient even at low temperatures. Time-resolved optical spectroscopy shows that energy transfer between these pigments is rapid (*67, 68*). Fluorescence emission from Bchl *g* occurs 22 ps after a laser flash, indicating a fast spectral equilibration (*69*).

1.2.8 *Cyclic Electron Transfer: the Cytochrome bc Complex and the Cytochrome c_{553} Complex*

One of the first reported observations on heliobacteria membranes was that following a laser flash, a bleaching can be observed at 553 nm that decays biphasically with $t_{1/2}$ of 6 and 20 ms (*50, 52*). A flash difference spectrum revealed that it is most likely derived from a cytochrome that donates electrons to $P798^+$ (*52*). This forward electron donation was observed to be much faster in whole cells than in membranes (*70*). When membrane proteins were analyzed by SDS-PAGE and stained using tetra-methyl benzidine (TMBZ), three heme-containing proteins could be identified. The molecular masses of these proteins are 50 kDa, 29 kDa, and 18 kDa (*50, 71*).

All three cytochromes can donate electrons to $P798^+$ either directly or indirectly (*71-73*). In whole cells, a cytochrome *c* donates to the primary acceptor in 100 to 600 µs following a laser flash (*70*). This oxidized cytochrome is reduced in 100 ms, and this reduction occurs simultaneously with the oxidation of cytochrome *b*, which has been shown to be a component of the cytochrome *bc* complex (*73*). This process is inhibited by stigmatellin, a potent cytochrome *bc* inhibitor (*73, 74*). If the repetition rate of the flashes is changed to 4 ms so that the primary donor can be oxidized many times before the cytochrome *bc* complex can reduce any of the donating cytochrome *c* molecules, the number of molecules donating to an HbRC can be calculated to be 5-6 cytochromes *c* and 1-3 cytochromes b (*71*).

The only heme binding proteins in heliobacteria are located in the membrane (*50*). The 29 kDa heme binding protein is associated with the cytochrome *bc* complex (*71*), which, in addition to cytochrome *b*, contains a Rieske Fe/S cluster (*73, 75*). The 50 kDa and 18 kDa heme binding proteins have been proposed to represent the *c*-type cytochromes involved with forward donation to $P798^+$ (*72*). There is some evidence for the identification of the 18-kDa cytochrome *c* as the genuine donor. The gene for this protein has been sequenced and has been named *petJ* (*76*). The *petJ* product forms a complex with two other proteins forming an entity termed the cytochrome c_{553} complex (*76*). These proteins have approximate molecular weights of 35 kDa and 30 kDa. The gene sequences of the two other proteins in this complex are unknown. If the detergent used in this purification is non-ionic, the cytochrome c_{553} complex is associated with yellowish-green pigments (*72*). If the cytochrome c_{553} complex is purified with an ionic detergent, the color is brownish-red, consistent with the presence of a cytochrome (*76*). The *petJ* gene and the *pshA* gene are in an gene cluster, which also contains genes for the cytochrome *bc* complex, and for Chl and carotenoid synthesis (*34*). Indeed, the 18 kDa protein is the most abundant c-type cytochrome in heliobacteria (*50*). It should be stressed there is no evidence for forward electron donation to $P798^+$ from this protein *in vitro*, so its participation as an electron donor requires confirmation.

Although it is clear that electrons from the cytochrome *bc* complex are ultimately donated to the HbRC, the source of the electrons is unclear (*73*). It has been suggested that electrons are transferred to a ferredoxin-like protein and then to an oxidoreductase that would provide reducing equivalents, most likely menaquinol, for the cytochrome bc complex (*73*). Two ferredoxin-like proteins have been discovered that could mediate this process (*77*). In addition, the redox potential of the Rieske Fe/S protein (*75*) in the cytochrome *bc* complex (*73*) seems to be well suited to oxidize menaquinol. A slightly modified scheme adopted from Kramer et al. (*73*) is shown in Figure 1.5 to outline this hypothesis. The identification of an oxidoreductase that would function in this manner, as well as the cytochrome protein that actually donates to $P798^+$, would be paramount in providing evidence for this process.

1.3 REFERENCES

1. Blankenship, R. E. (2002) *Molecular Mechanisms of Photosynthesis*, Blackwell Science Ltd, London, United Kingdom.
2. Berg, J. M., Tymoczko, J.L., Stryer, L. (2001) *Biochemistry*, 5th ed., W. H. Freeman and Company, New York, NY.
3. Brettel, K., and Leibl, W. (2001) Electron transfer in photosystem I, *Biochim Biophys Acta 1507*, 100-14.
4. Leibl, W., Toupance, B., and Breton, J. (1995) Photoelectric characterization of forward electron transfer to iron-sulfur centers in photosystem I, *Biochemistry 34*, 10237-44.
5. Shinkarev, V. P., Zybailov, B., Vassiliev, I. R., and Golbeck, J. H. (2002) Modeling of the P700+ charge recombination kinetics with phylloquinone and plastoquinone-9 in the A_1 site of photosystem I, *Biophys J 83*, 2885-97.
6. Hauska, G., Schoedl, T., Remigy, H., and Tsiotis, G. (2001) The reaction center of green sulfur bacteria**,** *Biochim Biophys Acta 1507*, 260-77.
7. Neerken, S., and Amesz, J. (2001) The antenna reaction center complex of heliobacteria: composition, energy conversion and electron transfer, *Biochim Biophys Acta 1507*, 278-90.
8. Buttner, M., Xie, D. L., Nelson, H., Pinther, W., Hauska, G., and Nelson, N. (1992) Photosynthetic reaction center genes in green sulfur bacteria and in photosystem I are related, *Proc Natl Acad Sci U S A 89*, 8135-9.
9. Okkels, J. S., Kjaer, B., Hansson, O., Svendsen, I., Moller, B. L., and Scheller, H. V. (1992) A membrane-bound monoheme cytochrome *c*551 of a novel type is the immediate electron donor to P840 of the *Chlorobium vibrioforme* photosynthetic reaction center complex, *J Biol Chem 267*, 21139-45.
10. Tsukatani, Y., Miyamoto, R., Itoh, S., and Oh-Oka, (2004) H. Function of a PscD subunit in a homodimeric reaction center complex of the photosynthetic green sulfur bacterium *Chlorobium tepidum* studied by insertional gene inactivation. Regulation of energy transfer and ferredoxin-mediated $NADP^+$ reduction on the cytoplasmic side, *J Biol Chem 279*, 51122-30.
11. Hager-Braun, C., Xie, D. L., Jarosch, U., Herold, E., Buttner, M., Zimmermann, R., Deutzmann, R., Hauska, G., and Nelson, N. (1995) Stable photobleaching of P840 in *Chlorobium* reaction center preparations: presence of the 42-kDa bacteriochlorophyll *a* protein and a 17-kDa polypeptide, *Biochemistry 34*, 9617-24.
12. Gest, H., Favringer, JL. (1983) *Heliobacterium chlorum*, an anoxygenic brownish-green photosynthetic bacterium containing a "new" form of bacteriochlorophyll, *Arch of Microbiol Volume 136*, 11-16.
13. Gest, H. (1994) Discovery of heliobacteria, *Photosynth Res 41*, 17-21.
14. Woese, C. R., Debrunner-Vossbrinck, B. A., Oyaizu, H., Stackebrandt, E., and Ludwig, W. (1985) Gram-positive bacteria: possible photosynthetic ancestry, *Science 229*, 762-5.
15. Vermaas, W. (1994) Evolution of heliobacteria: Implications for photosynthetic reaction center complexes, *Photosynth Res 41*, 285-294.

16. Beck, H., Hegeman, G., White, D. (1990) Fatty acid and lipopolysaccharide analysis of three Heliobacterium spp, *FEMS Microbiol Lett 69*, 229-232.
17. Pickett, M. W., Weiss, N., Kelly, D.J. (1994) Gram-positive cell wall structure of the A3(gamma) type in heliobacteria, *FEMS Microbiology Letters 122*, 7-12.
18. Pickett, M. W., Williamson, M. P. N., Kelly, D.J. (1994) An enzyme and 13C-NMR study of carbon metabolism in heliobacteria, *Photosynth Res 41*, 75-88.
19. Kimble, L. K., Stevenson, A.K., and Madigan, M.T. (1994) Chemotrophic growth of heliobacteria in darkness, *FEMS Microbiology Letters 115*, 51-56.
20. Kimble, L. K., Mandelco, L., Woese, C.R., and Madigan, M.T. (1995) *Heliobacterium modesticaldum*, sp-nov, a thermophilic heliobacterium of hot-springs and volcanic soils, *Arch of Microbiol 163*, 259-267.
21. Omerod, J. G., Kimble, L.K., Nesbakken, T., Torgersen, Y.A., Woese, C.R., Madigan, M.T. (1996) *Heliophilum fasciatum* gen. nov. sp. nov. and *Heliobacterium gestii* sp. nov.: endospore-forming heliobacteria from rice field soil, *Arch Microbiol 165*, 226-234.
22. Beer-Romero, P., Gest, H. (1987) *Heliobacillus mobilis*, a peritrichously flagellated anoxyphototropyh containing bacteriochlorophyll *g*, *FEMS Microbiology Letters 41*, 109-114.
23. Stevenson, A. K., Kimble, L.K., Woese, C.R., Madigan, M.T. (1997) Characterization of new phototrophic heliobacteria and their habitats, *Photosynth Res 53*, 1-12.
24. Ormerod, M. T. M. a. J. G. (1995) *Anoxygenic Photosynthetic Bacteria*, Vol. Volume 2, Kluwer Academic Publishers, Dordrecht.
25. Kimble, L. K., Madigan, M.T. (1992) Nitrogen fixation and nitrogen metabolism in heliobacteria, *Arch Microbiol 158*, 155-161.
26. Madigan, M. T. (2001) *Bergy's Manual of Systematic Bacteriology*, Vol. Volume I, 2nd ed., Springer-Verlag, New York, NY.
27. Kimble, L. K., Madigan, M.T. (1992) Evidence for an alternative nitrogenase in *Heliobacterium gestii*, *FEMS Microbiology Letters 100*, 255-260.
28. Liebl, U., Mockensturm-Wilson, M., Trost, J. T., Brune, D. C., Blankenship, R. E., and Vermaas, W. (1993) Single core polypeptide in the reaction center of the photosynthetic bacterium *Heliobacillus mobilis*: structural implications and relations to other photosystems, *Proc Natl Acad Sci U S A 90*, 7124-8.
29. Jordan, P., Fromme, P., Witt, H. T., Klukas, O., Saenger, W., and Krauss, N. (2001) Three-dimensional structure of cyanobacterial photosystem I at 2.5 A resolution, *Nature 411*, 909-17.
30. van de Meent, E., Kleinherenbrink, FAM., Amesz, J. (1990) Purification and properties of an antennae-reaction center complex from heliobacteria, *Biochim Biophys Acta 1015*, 223--230.
31. Trost, J. T., and Blankenship, R. E. (1989) Isolation of a photoactive photosynthetic reaction center-core antenna complex from *Heliobacillus mobilis*, *Biochemistry 28*, 9898-904.
32. Noguchi, T., Fukami, Y., Oh-oka, H., and Inoue, Y. (1997) Fourier transform infrared study on the primary donor P798 of *Heliobacterium modesticaldum*: cysteine S-H coupled to P798 and molecular interactions of carbonyl groups, *Biochemistry 36*, 12329-36.

33. Miyamoto, R., Iwaki, M., Mino, H., Harada, J., Itoh, S., and Oh-Oka, H. (2006) ESR signal of the iron-sulfur center F(X) and its function in the homodimeric reaction center of *Heliobacterium modesticaldum*, *Biochemistry 45*, 6306-16.
34. Xiong, J., Inoue, K., and Bauer, C. E. (1998) Tracking molecular evolution of photosynthesis by characterization of a major photosynthesis gene cluster from *Heliobacillus mobilis*, *Proc Natl Acad Sci U S A 95*, 14851-6.
35. Fyfe, P. K., Jones, M. R., and Heathcote, P. (2002) Insights into the evolution of the antenna domains of Type-I and Type-II photosynthetic reaction centres through homology modelling, *FEBS Lett 530*, 117-23.
36. Nitschke, W., Setif, P., Liebl, U., Feiler, U., and Rutherford, A. W. (1990) Reaction center photochemistry of *Heliobacterium chlorum, Biochemistry 29*, 11079-88.
37. Smit, H., Amesz, J., van der Hoeven, M. (1987) Electron transport and triplet formation in membranes of the photosynthetic bacterium *Heliobacterium chlorum*, *Biochim Biophys Acta 893*, 232-240.
38. Nitschke, W., and Rutherford, A. W. (1991) Photosynthetic reaction centres: variations on a common structural theme? *Trends Biochem Sci 16*, 241-5.
39. Olson, J. M., and Blankenship, R. E. (2004) Thinking about the evolution of photosynthesis, *Photosynth Res 80*, 373-86.
40. Brockmann, H., Lipinski, A. (1983) Bacteriochlorophyll *g*. A new bacteriochlorophyll from *Heliobacterium chlorum*, *Arch Microbiol 136*, 17-19.
41. Michalski, T. J., Hunt, J. E., Bowman, M. K., Smith, U., Bardeen, K., Gest, H., Norris, J. R., and Katz, J. J. (1987) Bacteriopheophytin *g*: Properties and some speculations on a possible primary role for bacteriochlorophylls *b* and *g* in the biosynthesis of chlorophylls, *Proc Natl Acad Sci U S A 84*, 2570-2574.
42. Kobayashi, M., Hamano, T., Akiyama, M., Watanabe, T., Inoue, K., Oh-Oka, H., Amesz, J., Yamamura, M., Kise, H. (1998) Light-independant isomerization of bacteriochlorophyll *g* to chlorophyll *a* catalyzed by weak acid in vitro, *Anal Chim Acta 365*, 199-203.
43. Amesz, J. (1995) The heliobacteria, a new group of photosynthetic bacteria, *J Photochem Photobiol B: Biol 30*, 89-96.
44. Kobayashi, M., Watanabe, T., Ikegami, I., van de Meent, E. J., and Amesz, J. (1991) Enrichment of bacteriochlorophyll *g*' in membranes of *Heliobacterium chlorum* by ether extraction. Unequivocal evidence for its existence *in vivo*, *FEBS Lett 284*, 129-31.
45. Kobayashi, M., van de Meent, E. J., Erkelens, C., Amesz, J., Ikegami, I., and Watanabe, T. (1991) Bacteriochlorophyll *g* Epimer as a Possible Reaciton Center Component of Heliobacteria, *Biochim Biophys Acta 1057*, 89-96.
46. van de Meent, E., Erkelens, C., van Veelen, D.A., and Amesz, J. (1991) Identification of 8^1-hydroxychlorophyll *a* as a functional reaction center pigment in heliobacteria, *Biochim Biophys Acta 1058*, 356-62.
47. Takaichi, S., Inoue, K., Akaike, M., Kobayashi, M., Oh-oka, H., Madigan, M.T. (1997) The major carotenoid in all known species of heliobacteria is the C30 carotenoid 4,4'-diaponeurosporene, not neurosporene, *Arch Microbiol 168*, 277-281.

48. Hirashi, A. (1989) Occurance of menaquinone as the sole isoprenoid quinone in the photosynthetic bacterium *Heliobacterium chlorum*, *Arch Microbiol 151*, 378-379.
49. Nuijs, A. M., Dorssen, R. J., Duysens, L. N., and Amesz, J. (1985) Excited states and primary photochemical reactions in the photosynthetic bacterium *Heliobacterium chlorum*, *Proc Natl Acad Sci U S A 82*, 6865-6868.
50. Fuller, R. C., Sprague, S.G., Gest, H., Blankenship, R.E. (1985) A unique photosynthetic reaction center from *Heliobacterium chlorum*, *FEBS Lett 182*, 345-349.
51. Barber, J. (1985) A new type of photosynthetic reaction centre, *Trends Biochem Sci 10*, 17-19.
52. Prince, R., Gest. H. Blankenship, RE. (1985) Thermodynamic properties of the photochemical reaction center of *Heliobacterium chlorum, Biochim Biophys Acta 810*, 377-384.
53. Brok, M., Vasmel, H., Horikx, J., Hoff, A. (1986) Electron transport components of *Heliobacterium chlorum* investigated by EPR spectroscopy at 9 and 35 GHz, *FEBS Lett 194*, 322-326.
54. Muhiuddin, I. P., Rigby, S. E., Evans, M. C., Amesz, J., and Heathcote, P. (1999) ENDOR and special TRIPLE resonance spectroscopy of photoaccumulated semiquinone electron acceptors in the reaction centers of green sulfur bacteria and heliobacteria, *Biochemistry 38*, 7159-67.
55. Trost, J. T., Brune, D. C., and Blankenship, R. E. (1992) Protein sequences and redox titrations indicate that the electron acceptors in reaction centers from heliobacteria are similar to Photosystem I, *Photosynth Res 32*, 11-22.
56. Kleinherenbrink, F. A., Ikegami, I., Hiraishi, A., Otte, SCM., Amesz, J. (1993) Electron transfer in menaquinone depleted membranes of *Heliobacterium chlorum, Biochim Biophys Acta 1142*, 69-73.
57. Lin, S., Chiou, H. C., and Blankenship, R. E. (1995) Secondary electron transfer processes in membranes of *Heliobacillus mobilis*, *Biochemistry 34*, 12761-7.
58. Brettel, K., Leibl, W., and Leibl, U. (1998) Electron transfer in the heliobacterial reaction center: Evidence against a quinone-type electron acceptor functioning analogous to A_1 in photosystem I, *Biochim. et Biophys. Acta 1363*, 175-81.
59. van der Est, A., Hager-Braun, C., Leibl, W., Hauska, G., and Stehlik, D. (1998) Transient electron paramagnetic resonance spectroscopy on green-sulfur bacteria and heliobacteria at two microwave frequencies, *Biochim. Biophys. Acta 1409*, 87-98.
60. Kleinherenbrink, F. A. M., Amesz, J. (1993) Stoichiometries and rates of electron transfer and charge recombination in *Heliobacterium chlorum*, *Biochim Biophys Acta 1143*, 77-83.
61. Kleinherenbrink, F. A., Chiou, H. C., LoBrutto, R., and Blankenship, R. E. (1994) Spectroscopic evidence for the presence of an iron-sulfur center similar to F_X of Photosystem I in *Heliobacillus mobilis, Photosynth Res 41*, 115-23.
62. Ke, B. (1973) The primary electron acceptor of Photosystem I, *Biochim Biophys Acta 301*, 1-33.

63. Parrett, K. G., Mehari, T., Warren, P., Golbeck, J.H. (1989) Purification and properties of the intact P-700 and F_X containing Photosystem I core protein, *Biochim Biophys Acta 973*, 324-332.
64. Fischer, M. (1990) Photosynthetic electron transfer in *Heliobacterium chlorum* studied by EPR spectroscopy, *Biochim Biophys Acta 1015*, 471-481.
65. Miller, K., Jacob, J., Smith, U., Kolaczkowski, S., Bowman, M. (1986) *Heliobacterium chlorum*: cell organization and structure, *Arch Microbiol 146*, 111-114.
66. van Dorssen, R. J., Vasmel, H., Amesz, J. (1985) Antenna organization and energy transfer in membranes of *Heliobacterium chlorum*, *Biochim Biophys Acta 809*, 199-203.
67. Liebl, U., Lambry, J. C., Leibl, W., Breton, J., Martin, J. L., and Vos, M. H. (1996) Energy and electron transfer upon selective femtosecond excitation of pigments in membranes of *Heliobacillus mobilis*, *Biochemistry 35*, 9925-34.
68. Liebl, U., Lambry, J. C., Breton, J., Martin, J. L., and Vos, M. H. (1997) Spectral equilibration and primary photochemistry in *Heliobacillus mobilis* at cryogenic temperature, *Biochemistry 36*, 5912-20.
69. Kleinherenbrink, F. A., Hastings, G., Wittmerhaus, B. P., and Blankenship, R. E. (1994) Delayed fluorescence from Fe-S type photosynthetic reaction centers at low redox potential, *Biochemistry 33*, 3096-105.
70. Vos, M. H., Klaassen, H.E., van Gorkom, H.J. (1989) Electron transport in *Heliobacterium chlorum* whole cells studied by electroluminescence and absorbance difference spectroscopy, *Biochim Biophys Acta 973*, 163-169.
71. Nitschke, W., Liebl, U., Matsuura, K., and Kramer, D. M. (1995) Membrane-bound c-type cytochromes in *Heliobacillus mobilis*. In vivo study of the hemes involved in electron donation to the photosynthetic reaction center, *Biochemistry 34*, 11831-9.
72. Nitschke, W., Schoepp, B., Floss, B., Schricker, A., Rutherford, A. W., and Liebl, U. (1996) Membrane-bound c-type cytochromes in *Heliobacillus mobilis*. Characterisation by EPR and optical spectroscopy in membranes and detergent-solubilised material, *Eur J Biochem 242*, 695-702.
73. Kramer, D. M., Schoepp, B., Liebl, U., and Nitschke, W. (1997) Cyclic electron transfer in *Heliobacillus mobilis* involving a menaquinol-oxidizing cytochrome bc complex and an RCI-type reaction center, *Biochemistry 36*, 4203-11.
74. Oh-Oka, H., Iwaki, M., and Itoh, S. (2002) Electron donation from membrane-bound cytochrome c to the photosynthetic reaction center in whole cells and isolated membranes of *Heliobacterium gestii*, *Photosynth Res 71*, 137-47.
75. Liebl, U., Pezennec, S., Riedel, A., Kellner, E., and Nitschke, W. (1992) The Rieske FeS center from the gram-positive bacterium PS3 and its interaction with the menaquinone pool studied by EPR, *J Biol Chem 267*, 14068-72.
76. Albert, I., Rutherford, A. W., Grav, H., Kellermann, J., and Michel, H. (1998) The 18 kDa cytochrome c553 from *Heliobacterium gestii*: gene sequence and characterization of the mature protein, *Biochemistry 37*, 9001-8.
77. Hatano, A., Seo, D., Kitashima, M., Sakurai, H., Inoue, K. (2005) Purification of two ferredoxins and cloning of these genes from the photosynthetic bacterium *Heliobacterium mobilis*, Allen Press, Lwrence, KS, USA.

1.4 FIGURE LEGENDS

Figure 1.1 Charge recombination rates and redox potentials of the cofactors in PS I (values are adapted from (*5*)).

Figure 1.2 Carbon fixation pathways in heliobacteria (adapted are from (*18*)). Numbers correspond to the enzymes that catalyze the reactions (1) PEP synthase (2) PEP carboxykinase (3) malate dehydrogenase (4) fumarase (5) fumarate reductase (6) succinate: acetyl CoA transferase (7) 2-oxoglutarate: ferredoxin oxidoreductase (8) pyruvate: ferredoxin oxidoreductase (9) NADP-linked isocitrate dehydrogenase

Figure 1.3 (a-c) Structures of Bchl *g (* 3a), Chl *a* (3b), and Bchl *b (*3c). Numbering is according to the IUPAC system.

Figure 1.4 Absorption spectrum of Bchl *g* (brown) and Bchl *g* after a 2 hr exposure to light and oxygen (green).

Figure 1.5 A slightly modified scheme adapted from Kramer el al. (*73*) shows electron transfer pathways in membranes from heliobacteria. Question marks indicate parts of the pathway that are unknown. MK stands for menaquinone-9.

Figure 1.1

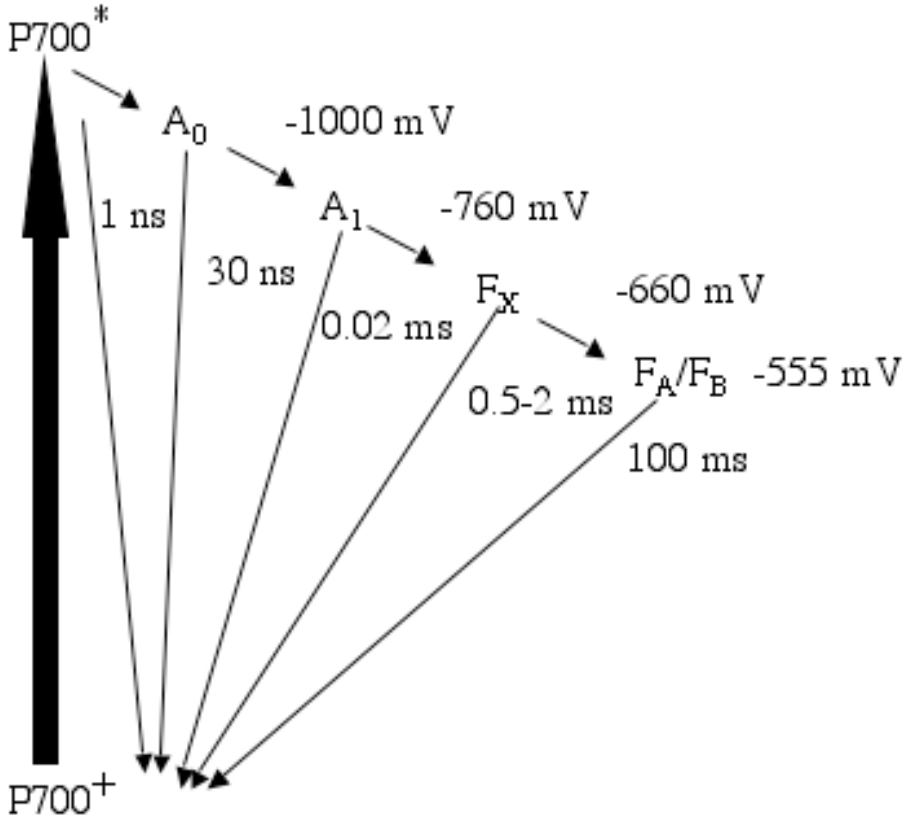
P700*
A0
-1000 mV
A1
-760 mV
FX
-660 mV
FA/FB
-555 mV
1 ns
30 ns
0.02 ms
0.5-2 ms
100 ms
P700+

Figure 1.2

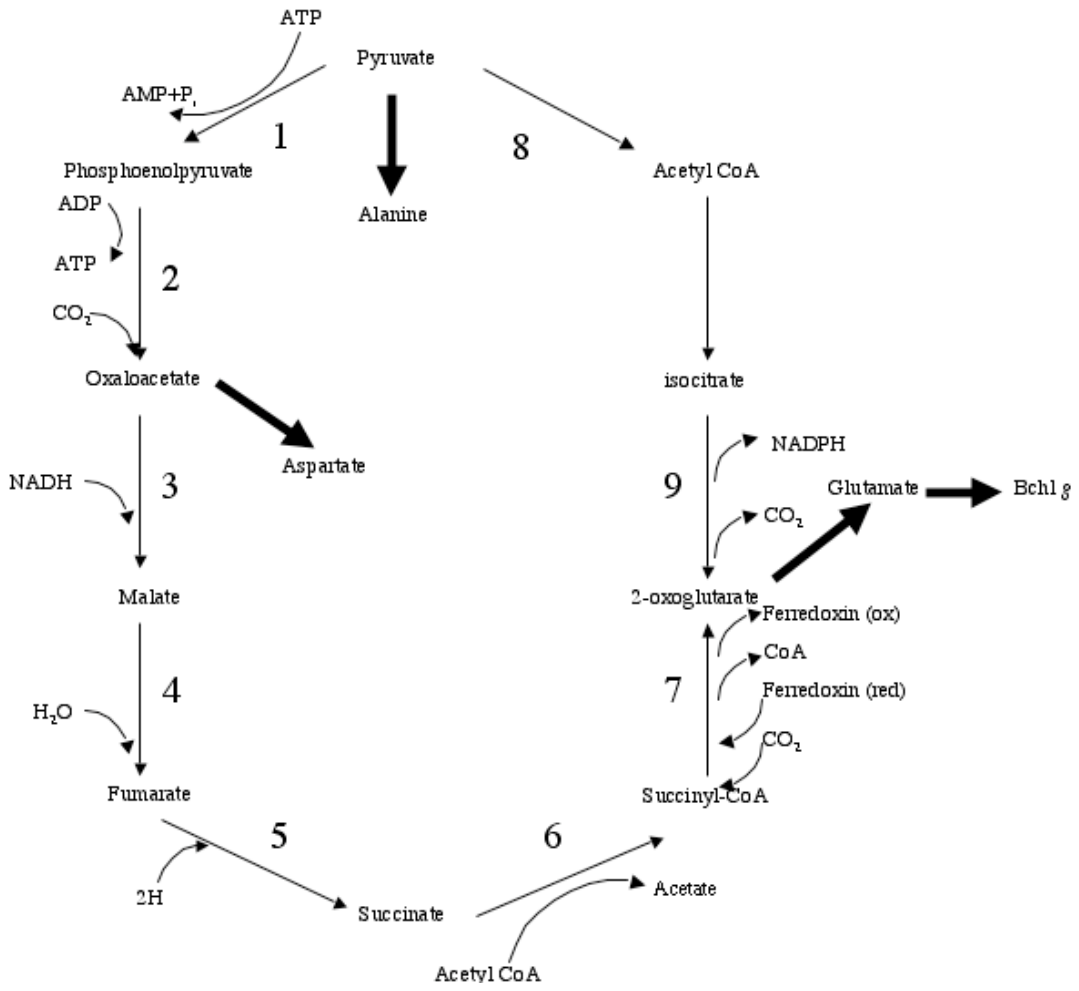
ATP
Pyruvate
AMP+P$_i$
1
8
Phosphoenolpyruvate
Alanine
Acetyl CoA
ADP
ATP
2
CO_2
Oxaloacetate
isocitrate
Aspartate
NADPH
NADH
3
9
Glutamate
Bchl *g*
CO_2
Malate
2-oxoglutarate
Ferredoxin (ox)
CoA
4
7
H_2O
Ferredoxin (red)
CO_2
Fumarate
Succinyl-CoA
5
6
2H
Succinate
Acetate
Acetyl CoA

Figure 1.3

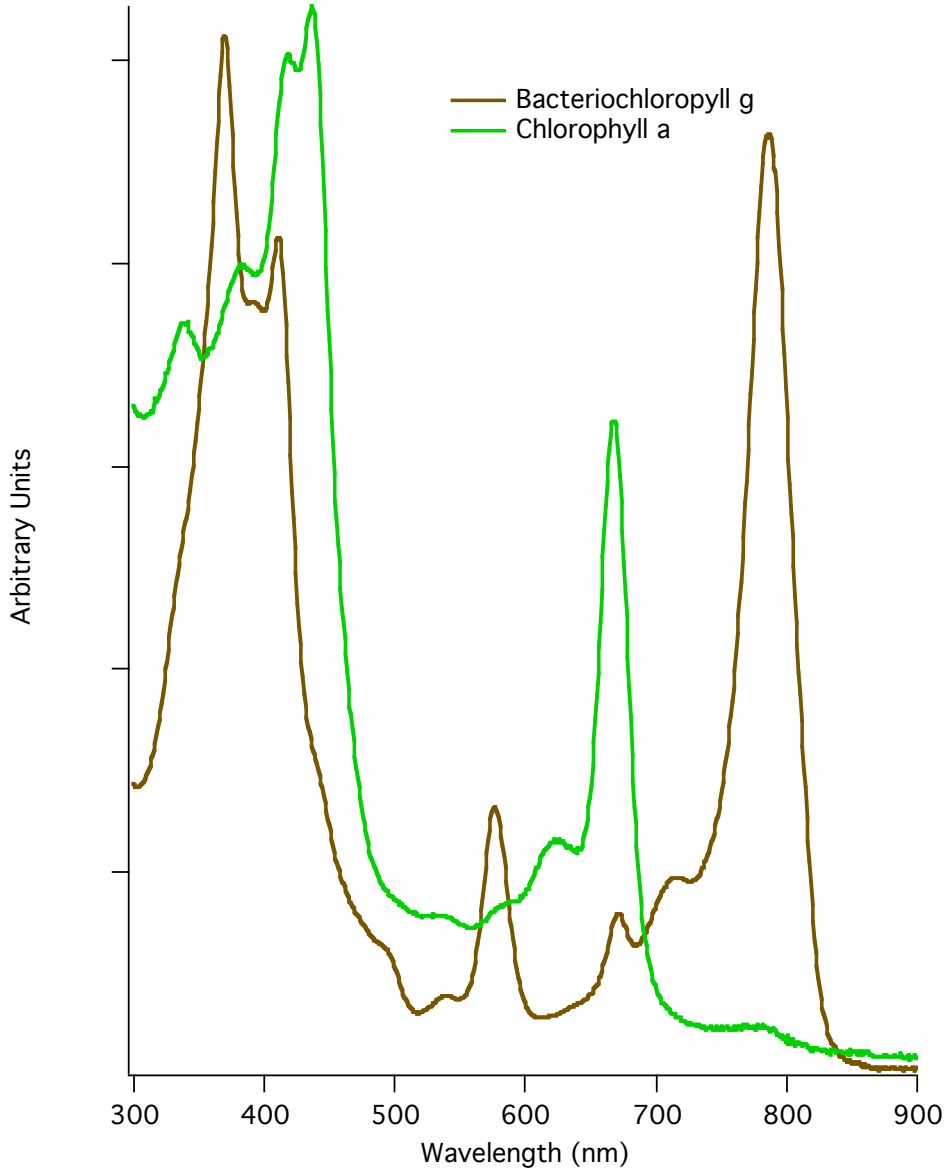
Bacteriochloropyll g
Chlorophyll a
Arbitrary Units
300
400
500
600
700
800
900
Wavelength (nm)

Figure 1.4a

Bacteriochlorophyll *g*

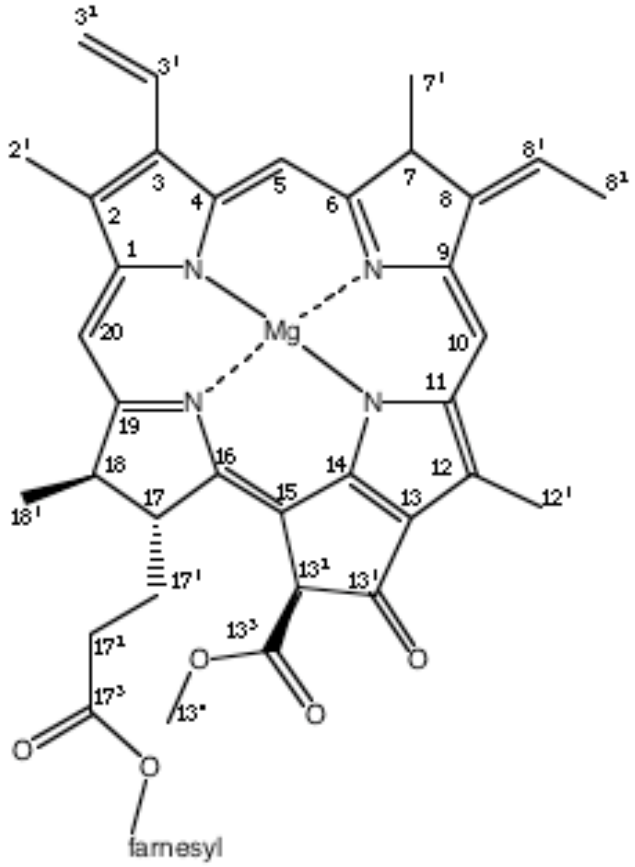

Figure 1.4b

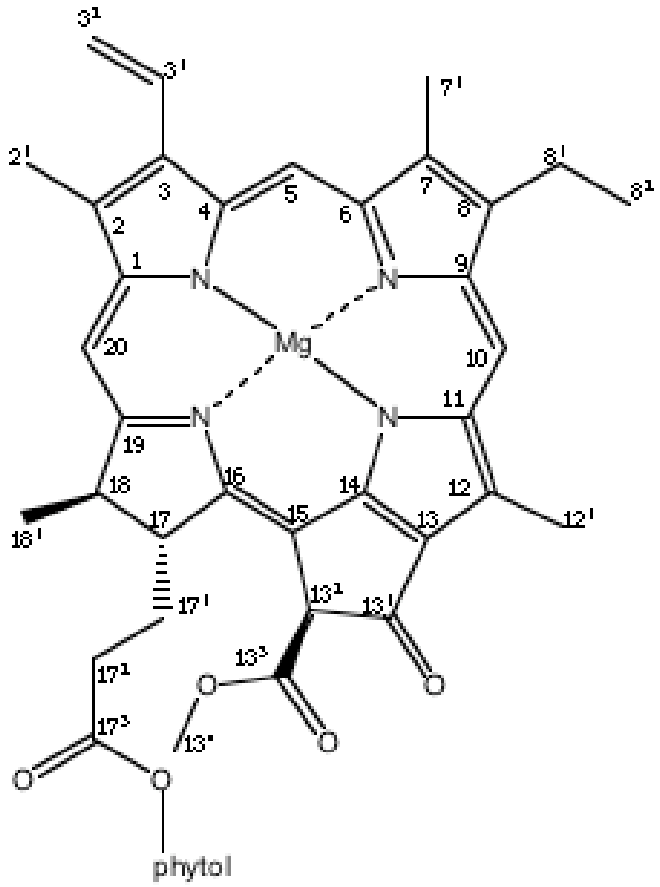

Figure 1.4c

Bacteriochlorophyll *b*

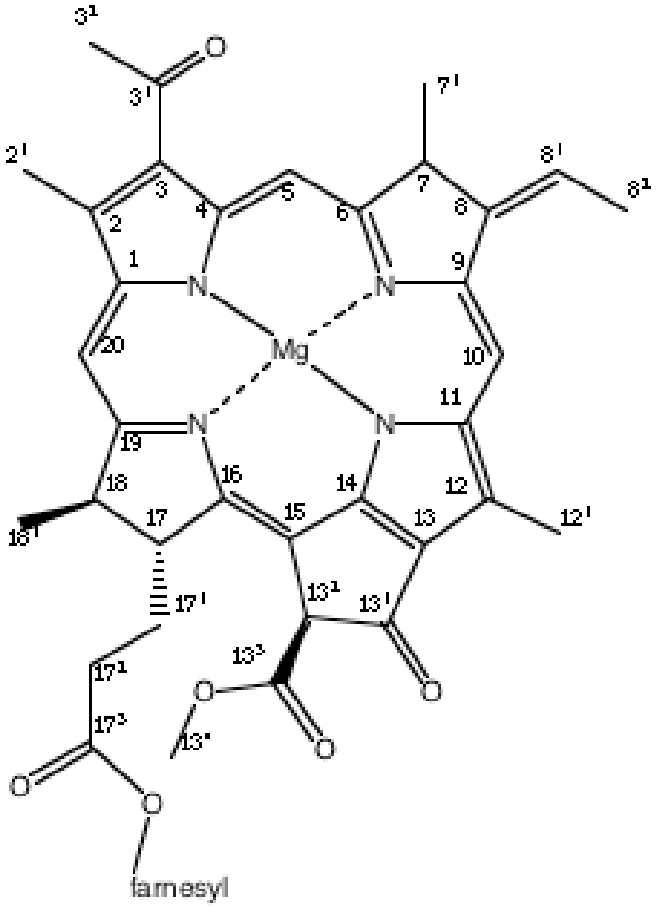

Figure 1.5

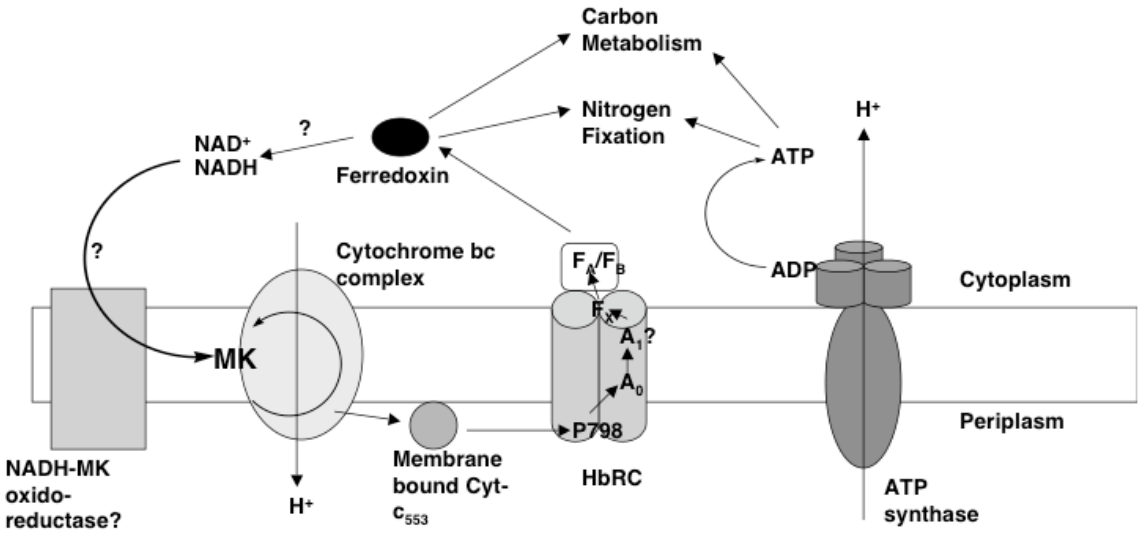
Carbon
Metabolism
Nitrogen
Fixation
H+
NAD+
NADH
?
Ferredoxin
ATP
?
Cytochrome bc
complex
FA/FB
ADP
Cytoplasm
FX
A1?
MK
A0
Periplasm
P798
NADH-MK
oxido-
reductase?
H+
Membrane
bound Cyt-
c553
HbRC
ATP
synthase

Chapter 2

Resolution and Reconstitution of a Bound Fe/S Protein (PshB) from the Photosynthetic Reaction Center of *Heliobacterium modesticaldum*

[Published as a paper titled "Resolution and Reconstitution of a Bound Fe/S Protein (PshB) from the Photosynthetic Reaction Center of *Heliobacterium modesticaldum*" by Mark Heinnickel, Gaozhong Shen, Rufat Agalarov, and John H. Golbeck (2005) Biochemistry 44 (29), 9950-9960]

2.1 ABSTRACT

The light-induced EPR signals of the Fe/S clusters seen in membranes from *Heliobacterium modesticaldum* are not present in purified HbRCs. It has been proposed that the Fe/S clusters reside on a protein that dissociates from the HbRC during purification. In this chapter, I offer evidence to support this assertion and I show reasons why the protein that binds the terminal electron acceptors does not purify with the HbRC. The HbRC was isolated from membranes using *n*-dodecyl-_-D-maltopyranoside followed by sucrose density gradient ultracentrifugation. The low temperature EPR spectra of whole cells, isolated membranes, and HbRC complexes were found to be similar, showing a single Fe/S cluster with *g*-values of 2.067, 1.933 and 1.890 after illumination at 20 K, and a complex spectrum attributed to exchange interaction from two Fe/S clusters after illumination during freezing. The protein containing the Fe/S clusters was removed from the HbRC by washing with 1.0 M NaCl and purified by ultrafiltration over a 30-kDa cut-off membrane. Analysis of the filtrate by SDS PAGE showed a major band at ~8 kDa that was weakly stained with Coomassie Brilliant Blue and strongly stained with silver. The optical spectrum of the oxidized Fe/S protein showed a maximum at 410 nm and the EPR spectrum of the reduced Fe/S protein showed a complex set of resonances similar to those found in 2[4Fe-4S] ferredoxins. The HbRC core was purified by DEAE ion exchange chromatography and resolved by SDS PAGE. The purified HbRC was composed of a band at ca. 40 kDa, which was identified as PshA, and several additional proteins. The isolated Fe/S protein was shown to rebind spontaneously to purified HbRC cores, and the light-induced EPR signals of the Fe/S clusters were recovered. The flash-induced kinetics of the HbRC complex showed two kinetic phases at room temperature, one with a lifetime of 75-ms and the other with a lifetime of 15-ms. The 75-ms component was lost when the Fe/S protein was removed from the HbRC complex, and it was regained when the Fe/S protein was rebound to HbRC cores. Thus, the 75-ms kinetic phase is derived from recombination of a terminal Fe/S cluster with $P798^{+}$, and the 15-ms kinetic phase is derived from recombination with an earlier acceptor, probably F_X. I have suggested that the bound Fe/S protein present in the HbRC be designated PshB.

2.2 INTRODUCTION

The major focus of research in photosynthesis is to understand the mechanisms that plants and bacteria use to convert sunlight into chemical bond energy. All known photosynthetic RCs can be divided into two main groups: Type I, in which an Fe/S cluster is the terminal electron acceptor, and Type II, in which a quinone is the terminal electron acceptor. Each of these two types of RCs can be subdivided into two additional subgroups: PS II and the bacterial RC are members of the Type II group, and PS I and the homodimeric RCs of *Heliobactericae* and *Chlorobaecea* are members of the Type I group. The latter are the only homodimeric RCs known in nature (*1, 2*). Atomic resolution structures are available for the purple bacterial RC (*3*) and for PS I (*4*) and models are becoming available for PS II based on X-ray data taken at a resolution of 3.5 to 3.8 Å (*5, 6*). However, no detailed structural information is yet available for the Type I homodimeric RCs.

Heliobacteria are strictly anaerobic, spore-forming members of the Firmicutes. They are photoheterotrophic organisms that grow on a very limited range of carbon sources (*7*). Heliobacteria contain a unique photosynthetic pigment called bacteriochlorophyll *g*, which contains a vinyl group on ring I and an ethylidine group on ring II. These features give the microorganism its characteristic absorbance spectrum that confers a selective advantage in dealing with its specific growth environment (*7, 8*). Even though heliobacteria stain Gram negative, an analysis of the G-C content of its 16S ribosomal RNA indicates that these microorganisms are Gram positive. This makes them the first identified Gram-positive microorganisms to perform photosynthesis (*9*). Unlike cyanobacteria, which have two types of photosynthetic RCs, heliobacteria have only one type, with Fe/S clusters as the terminal electron acceptors. This places them in the Type I class of RC (*10*).

In the twenty-four years that have followed their discovery, research on heliobacteria has proceeded at a steady pace. The HbRC was shown to contain 35-40 antenna bacteriochlorophyll *g* molecules (*11, 12*) and a primary donor consisting of a bacteriochlorophyll *g* dimer (*13*). The primary acceptor (A_0) is an 8^1-hydroxy chlorophyll *a* molecule (*14*). Although it was suggested that the PshA homodimer

contained all of the HbRC antenna chlorophylls (*15*), it is still uncertain whether additional chlorophyll proteins are associated with the RC complex. The participation of a quinone is controversial, with some studies arguing for (*16*) and some against (*17-19*) its role as intermediate electron transfer cofactor. An Fe/S cluster similar to F_X has been detected in urea-treated HbRCs using time-resolved optical spectroscopy (*20*) and Fe/S clusters similar to F_A and F_B have been detected in membranes by EPR spectroscopy (*21, 22*). However, the absence of a gene that codes for a low molecular mass Fe/S protein in the major gene cluster that codes for the photosynthetic proteins has led to difficulties in identifying a protein that plays a similar role to PsaC in harboring the terminal Fe/S clusters in HbRCs (*23*).

The primary aim of this work is to begin characterization of the protein that contains the bound Fe/S clusters. One of the problems in studying this organism has been the difficulty of isolating intact HbRCs. Heliobacteria are strict anaerobes, and the Fe/S clusters are particularly unstable in the presence of oxygen. I approached this issue using a strategy similar to earlier studies from the Golbeck laboratory that involved the Type I RCs from *Chlorobium tepidum (24)*. I first characterized the light-induced EPR spectra of the terminal Fe/S clusters in freshly frozen whole cells of *Heliobacterium modesticaldum*, a moderate thermophile that grows optimally at 50^{o}-52^{o} C (*25*). I then used these spectra as a benchmark to optimize the isolation conditions for membranes and HbRCs, with the retention of the light-induced EPR spectrum of the Fe/S clusters as the primary criterion of intactness. This guaranteed that the properties of the bound Fe/S clusters were from an undamaged protein.

I report here that in addition to the PshA homodimer, the isolated HbRC complex contains at least one additional protein. It is an 8-kDa Fe/S protein, that can be removed from the HbRC complex at moderate ionic strength. The resolved Fe/S protein can be rebound to the purified HbRC cores, thus regaining light-induced charge separation between P798 and the Fe/S clusters. The spectroscopic properties of the HbRC complex, the HbRC core, and the isolated Fe/S protein are described below.

2.3 MATERIALS AND METHODS

2.3.1 *Growth of Heliobacterial Cultures*

A culture of *Heliobacterium modesticaldum* was generously provided by Dr. Michael Madigan (Southern Illinois University). Liquid cultures of *H. modesticaldum* were grown anaerobically in PYE media as described in (*25*) except that resazurin, an oxygen reporter dye, was added to a final concentration of 0.001%. Banks of eight fluorescent bulbs provided white light illumination. The medium was degassed and allowed to incubate in an anaerobic chamber with an atmosphere of 10% hydrogen and 90% nitrogen (Coy Labs, Grass Lake, MI) until it was devoid of oxygen, as indicated by the color of the resazurin. The media was sealed in Hungate bottles and autoclaved. The bottles were inoculated using the Hungate technique and the culture was allowed to grow at 43° C. Growth at a temperature lower than the optimum resulted in fewer broken cells (*26*). Banks of eight fluorescent bulbs provided white light illumination.

2.3.2 *Isolation of HbRC Complexes*

All manipulations were performed anaerobically. Plasticware and glassware were placed in the anaerobic chamber three hours prior to use and tested with a resazurin solution to verify that any residual oxygen had been removed. Cells grown to late-exponential phase were harvested anaerobically at 10,000 x *g* and resuspended in 50 mM MOPS buffer, pH 7. Whole cells were lysed by sonication, and membranes were pelleted by centrifugation at 200,000 x *g*. A variety of detergents were used to solubilize the membranes, including Triton X-100, digitonin, Deriphat 160c, *n*-dodecyl-_-D-maltopyranoside and *n*-octyl-_-D-glucopyranoside. Based on the efficiency of solubilization, the stabilization of the chlorophyll-containing RC complexes, and retention of the light-induced EPR resonances of the Fe/S clusters, *n*-dodecyl-_-D-maltopyranoside was chosen as the optimum detergent. Membranes were solubilized with 1% *n*-dodecyl-_-D-maltopyranoside for one hour; intact membranes were removed by centrifugation at 200,000 x *g*. The supernatant was loaded onto a 5 to 20% sucrose gradient and centrifuged at 28,000 rpm in an SW-28 rotor for 16 hrs (~150,000 x *g*). A brownish-green colored fraction was collected from the gradient.

2.3.3 *Purification of the Bound Fe/S Protein*

HbRCs isolated by sucrose density untracentrifugation were incubated with 1 M NaCl for one hour and ultrafiltered over a 30-kDa molecular weight cutoff membrane (PM30, Millipore). The proteins that passed through the membrane were collected, and the process was repeated a second time. The filtrate, which contained low molecular mass proteins, was concentrated over a 3-kDa molecular weight cutoff membrane (YM-3, Millipore) and desalted on a PD-10 column (Amersham Biosciences). The HbRC core that was retained on the ultrafiltration membrane was also desalted on a PD-10 column and concentrated over a 30-kDa molecular weight cutoff membrane (PM-30, Millipore). Fe/S clusters were reconstituted anaerobically according to the following protocol. The resolved Fe/S protein was incubated for 20 minutes with 100 mM _-mercaptoethanol in 50 mM Tris buffer (pH 8.3). Ferrous ammonium sulfate was added dropwise to a final concentration of 180 μM and the solution was allowed to incubate for 20 minutes. After the mixture turned a slightly brown color, sodium sulfide was added dropwise to a final concentration of 180 μM and the solution was allowed to incubate overnight at 4°C. The reconstituted Fe/S protein was desalted by ultrafiltration over a YM-3 membrane to remove all iron and sulfide and concentrated in the same step.

2.3.4 Low Temperature X-band EPR Spectroscopy

Low temperature EPR spectroscopy was performed using a Bruker ECS-106 X-band spectrometer equipped with an Oxford liquid helium cryostat and temperature controller. The spectrometer conditions were: temperature, 20 K; power, 126 mW; microwave frequency, 9.47 GHz; receiver gain, 2 x 10^4; modulation amplitude, 10 G at 100 kHz. Spectra were obtained by averaging ten scans. HbRCs were concentrated to an absorbance of ~75 OD at 788 nm and loaded into the EPR sample tubes. To assure that oxygen had not damaged the sample, the absorbance at 788 nm, which is a measure of Bchl *g*, needed to be at least five times greater than the absorbance at 670 nm, which is a measure of Chl *a*, otherwise the sample was discarded. Samples were chemically reduced with 10 mM sodium hydrosulfite in 100 mM glycine at pH 10.0. In all cases, the oxidized spectrum (no additions) was subtracted from the reduced spectrum to yield a difference

spectrum. A 250 W tungsten lamp focused to fill the grid of the resonator did not provide sufficient light to elicit the full amplitude of the Fe/S resonances. An argon ion laser was used instead, which was operated at 2.5 W in all-lines mode, and a 3-fold beam expander was used to fill the grid of the resonator. Light-induced electron transfer was assayed according to one of two protocols. One electron can be promoted from P798 to the Fe/S clusters by illuminating the sample frozen in darkness and illuminated at 20 K. Two or more electrons can be promoted from P798 to the Fe/S clusters by freezing the sample slowly during illumination. The latter was accomplished by fitting the EPR tube with a vacuum adaptor and illuminating the tube with an argon ion laser outside of the EPR resonator under conditions that allowed the sample to be frozen slowly to 77 K. The sample was then quickly transferred to the EPR resonator, which was maintained at 20 K.

2.3.5 *Time Resolved Optical Spectroscopy in the Visible and near-IR*

The kinetics of $P798^+$ reduction were measured by monitoring the flash-induced absorbance after a laser flash. In brief, the sample was probed with a continuous measuring beam at 798 nm isolated from a 150 W tungsten-halogen lamp with a 1/4 meter monochromator. A shutter allowed the light to reach the sample 10 ms prior to the laser flash. The beam was monitored using a reverse-biased Si photodiode that was shielded from stray light with an 800 nm interference filter. The signal from the photodiode was amplified by a Tektronix AM502 differential amplifier and digitized using a DSA601 Tektronix digital oscilloscope. The data were sent to a Macintosh computer via an IEEE-488 bus (National Instruments). The electronic bandwidth of the detection system was fixed at 1 MHz. The sample was excited by a Nd-YAG laser operating in the second harmonic (λ = 532 nm) with a 7 ns pulse duration and an energy of ~ 2 mJ/cm^2. Typically 8 to 10 transients were recorded and averaged. Samples were placed in a quartz anaerobic cuvette with an optical path of 10 mm. The samples were in 50 mM MOPS pH 7.0 buffer at an absorbance of 0.5 OD at 788 nm. The kinetic traces were analyzed by fitting a multiexponential decay using the Marquardt least-squares algorithm (Igor Pro, Lake Oswego, OR).

2.4 RESULTS

2.4.1 *Isolation of an Intact HbRC Retaining the Light-Induced EPR Signals of Fe/S Clusters*

Low temperature X-band EPR spectra of freshly frozen cells of *H. modesticaldum* are depicted in Figure 2.1. The one-electron reduced EPR spectrum (Figure 2.1 A, trace a), generated by illuminating dark-adapted cells at 20 K, is rhombic, with *g*-values of 2.067, 1.933, and 1.890. These resonances are typical of a reduced Fe/S protein and appear to be derived either from a single Fe/S cluster or from two (or more) Fe/S clusters that have identical *g*-values. The signal does not diminish after the light is turned off, indicating that charge separation with $P798^{+}$ is irreversible at low temperatures. The amplitude of the signal is maximal at 20 K (-2 dB microwave power) and disappears completely above 35 to 40 K. The relative number of spins represents 3% of that found after chemical reduction (Figure 2.1 C, trace a), indicating that either electron transfer to the Fe/S clusters is inefficient at 20 K or that self-shielding and scatter in the whole cells prevent light from reaching the majority of the Chls. The rapid spin relaxation properties, inferred from the temperature and microwave power dependencies, are more characteristic of a [4Fe-4S] cluster than a [2Fe-2S] cluster. The two-electron reduced EPR spectrum, generated either by illuminating cells during freezing to 77 K (Figure 2.1 B, trace a) or by reducing the cells with sodium hydrosulfite at pH 10.0 (Figure 2.1 C, trace a), is complex, showing apparent *g*-values of 2.52, 1.97, 1.93 and 1.90. Note that the light- and chemically-reduced spectra are virtually identical, indicating that additional Fe/S proteins in the cellular milieu do not contribute significantly to the spectrum of the chemically reduced sample. Note also that the *g*-anisotropy of the spectrum, as indicated by the lowfield and highfield turning points, is narrower than that of the one-electron reduced spectrum. The amplitude of the signal is maximum at 20 K (-2 dB microwave power) and disappears completely above 35 to 40 K; at all but the lowest temperatures, the resonances remain unchanged. This complex EPR spectrum is attributed to an exchange interaction that occurs between the two [4Fe-4S] clusters that are typically

located 12.5 Å apart in dicluster ferredoxins. Because the Fe/S clusters can be reduced by illumination at 20 K, a temperature at which diffusion and protein motion are limited, these resonances are attributed to a Fe/S protein bound to the HbRC.

The one-electron reduced EPR spectrum of isolated membranes (Figure 2.1 A, trace b) is similar to that of whole cells (Figure 2.1 A, trace a), and is nearly identical to that reported for isolated membranes from *Heliobacterium chlorum* (*21*). The relative number of spins, calculated by comparing the areas under the integrated spectra, represents 12% that found after chemical reduction (Figure 2.2 C, trace b), a value similar to that reported in isolated membranes from *H. chlorum* (*21*). The assumed light-induced two-electron reduced EPR spectrum of isolated membranes (Figure 2.1 B, trace b) is slightly different from the chemically reduced spectrum (Figure 2.1 C, trace b), particularly the *g*-values of the highfield and lowfield resonances. Considering the different *g*-anisotropies of the one-electron and the two-electron reduced spectra, the light-induced sample of the membranes appears to represent an admixture. This could come about if there were a mixed population of one-electron and two-electron reduced spectra owing to incomplete reduction of the Fe/S clusters during the photoaccumulation protocol.

The isolation of intact HbRCs depends on the use of detergents to dissolve the membrane and render the hydrophobic membrane proteins soluble. Two criteria were employed for screening the efficacy of detergents: one is the ability to isolate the HbRC on a sucrose density gradient, and the other is the retention of the intact light-induced EPR resonances of the Fe/S clusters. I found that among the variety of detergents tested (see *Materials and Methods*) *n*-dodecyl-_-D-maltopyranoside was the most effective at fulfilling these criteria. HbRCs recovered from the sucrose gradients prepared under anaerobic conditions were brown in color due to the retention of Bchl *g*. However, HbRCs recovered from the sucrose gradients prepared under aerobic conditions were green in color owing to the (partial) conversion (oxidation) of Bchl *g* to Chl *a.* The light-induced Fe/S clusters were present in the brown samples that were prepared anaerobically whereas they were missing in the green sample prepared aerobically. This visual indicator of color has proven to be an excellent marker for exposure of the HbRC to oxygen. The EPR spectra in the brown sample, measured under one-electron reducing

conditions (Figure 2.1 A, trace c) and two-electron reducing conditions (Figures 2.1 B, trace c; and 2.1 C, trace c), were similar to those measured in membranes. Thus, the Fe/S clusters are judged to be intact after detergent treatment and purification by sucrose density ultracentrifugation. (*21*). Interestingly, the relative number of spins represents as much as 41% that found after chemical reduction (Figure 2.1 C, trace c). Because both of the [4Fe-4S] clusters in the Fe/S protein are reduced by chemical reduction, whereas only one can be reduced by illumination at 20 K, this indicates that nearly 82% of the terminal Fe/S cluster can be reduced in isolated HbRCs by illumination at low temperature.

2.4.2 *Loss of the Light-Induced EPR signal of Fe/S Clusters at High Ionic Strength*

I found that the light-induced EPR resonances of the Fe/S clusters were present when the HbRCs were subject to chromatography by gel filtration but that they were missing when the HbRCs were passed over a DEAE ion-exchange column. Because both types of chromatography were carried out under anaerobic conditions (the HbRCs remained brown in color), I reasoned that either the Fe/S protein was sensitive to ionic strength or the Fe/S clusters were degraded. To study this effect further, membranes that were solubilized with *n*-dodecyl-_-D-maltopyranoside were incubated with various concentrations of NaCl for 5 min. The samples were flash-frozen to 77 K, and the light-induced EPR spectra of the Fe/S clusters were measured at 20 K. I found that relatively low concentrations of NaCl led to a marked reduction in the amplitude of the light-induced Fe/S resonances. At 100 mM NaCl (Figure 2.2 trace b), 250 mM NaCl (Figure 2.2, trace c) and 500 mM NaCl, (Figure 2.2, trace d), the amplitude of the light-induced spectrum was reduced to 46%, 26%, and <5% of the control (Figure 2.2, trace a), respectively. The relative spin concentrations were determined by comparing the peak to trough intensities of the midfield resonance at g = 1.925. HbRCs that were isolated by sucrose density ultracentrifugation showed an identical loss of the light-induced Fe/S resonances as the ionic strength was increased. In contrast, the light-induced Fe/S resonances of isolated membranes were resistant to loss at high ionic strength. Thus, *n*-dodecyl-_-D-maltopyranoside must be present for the effect to be observed. The intensity of the radical at g = 2.002 derived from $P798^{+}$ is generally lower when the Fe/S clusters are not observed. However, these signals cannot be used to quantify the amount of

oxidized primary donor because the organic radical is saturated at the temperature and power required to measure the Fe/S clusters.

2.4.3 *Properties of the HbRC Core Isolated by Ion-Exchange Chromatography*

The HbRCs isolated by sucrose density ultracentrifugation were passed over a DEAE-Sepharose CL-6B ion-exchange column that had been pre-equilibrated with 50 mM MOPS buffer. The HbRCs were not retained on the column, but rather flowed through in the void volume. The EPR spectra of the DEAE-purified HbRCs showed that the EPR resonances of the bound Fe/S clusters were completely missing regardless of whether the sample was illuminated (Figure 2.1 A, trace d and Figure 2.1 B, trace d) or reduced with sodium hydrosulfite (Figure 2.1 C, trace d). The presence of the radical at g = 2.002 derived from $P798^{+}$ shows that the HbRC core is intact and that light-induced charge separation occurs between P798 and an earlier electron acceptor.

To determine whether the Fe/S protein is attached to the HbRC but devoid of Fe/S clusters, I attempted reconstitution of the Fe/S clusters by treating the DEAE-purified HbRCs with 2-mercaptoethanol, ferrous ammonium sulfate and sodium sulfide (see *Materials and Methods*). No EPR resonances of the Fe/S clusters were detected regardless of whether the sample was illuminated or chemically reduced with sodium hydrosulfite (data not shown). Similar to soluble 2[4Fe-4S] ferredoxins and to PsaC of PS I, the bound Fe/S protein in the HbRC is likely to be negatively charged at pH 7.0. If the Fe/S protein is in equilibrium between the HbRC-bound and unbound states, a fraction should be retained at any given time by the anion-exchange resin. As the HbRC passes through the column, it will be become successively depleted of the Fe/S protein until a purified HbRC core is attained. (I did not attempt to recover the isolated Fe/S protein from the ion-exchange column.) The DEAE-purified particles will henceforth be referred to as HbRC cores.

The HbRC cores were treated with 1% (w/v) SDS, subject to SDS PAGE analysis, and the gel stained with Coomassie Brilliant Blue R-250 (Figure 2.3). The major band with an apparent mass of ca. 40 kDa is the PshA reaction center protein (*27*). Its predicted mass, derived from the sequence of the *pshA* gene from *H. mobilis* is 68 kDa (*28*); thus, this hydrophobic membrane protein runs anomalously on SDS PAGE (*28, 29*).

This is a common feature of integral membrane proteins, including PsaA and PsaB of PS I, which tend to unfold incompletely and to bind larger amounts of SDS than soluble proteins. The HbRC also contains two strongly-stained protein bands with apparent masses between 25 and 30 kDa, and two lightly-stained protein bands with apparent masses around 20 kDa and 10 kDa. (Details of the polypeptides in the HbRC complex and HbRC core are beyond the scope of this study and will be published elsewhere.) When the HbRC cores are subject to chromatography over a DEAE-Sepharose CL-6B column under aerobic conditions, the color turns from brown to green, but the protein composition remains identical to that shown in Figure 2.3. Hence, none of the low molecular mass polypeptides are released from the HbRC core owing to exposure to oxygen.

2.4.4 *Isolation and Characterization of the Bound Fe/S Protein by SDS PAGE*

To determine the mass of the resolved Fe/S protein, detergent solubilized membranes were treated with 1 M NaCl for 10 min and the solution was ultrafiltered over a 30-kDa cut-off membrane. The HbRC cores, which were retained above the membrane, were desalted over a PD-10 column and stored for later use. The low molecular mass proteins, which were present in the filtrate, were collected, concentrated over a 3-kDa ultrafiltration membrane, and desalted over a PD-10 column. The protein composition of the filtrate was analyzed by SDS-PAGE. As shown in Figure 2.4A, the filtrate contains one major protein band with a molecular mass of ca. 9 kDa. The band stains poorly with Coomassie Brilliant Blue R-250, but it stains intensely brown with silver. I attribute this difference to a relative lack of amino acids that bind the organic dye and to the presence of a large number of cysteines that are capable of binding silver. Based on the large content of this protein with respect to all other bands in the filtrate, it can be assumed that this 9 kDa protein is the Fe/S cluster binding protein. Based on mass alone, the bound Fe/S protein in *Heliobactericae* is therefore more similar to PsaC of PS I than it is to PscB of *Chlorobaecea*. I suggest that the bound Fe/S protein in the RC of heliobacteria be named PshB and the gene be named *pshB* according to the recommendations in ref. (*30*). This would be consistent with the nomenclature used in the RC of *Chlorobium*, another homodimeric Type I RC, in which the bound Fe/S protein is termed PscB (*31*).

2.4.5 *Characterization of PshB by Optical and EPR Spectroscopy*

The optical spectrum of the oxidized PshB protein shows a relatively featureless absorption in the blue region with a pronounced shoulder at 410 nm (Figure 2.4B). The relative lack of absorbance from 500 nm to 700 nm is characteristic of ferredoxins that contains [4Fe-4S] rather than [2Fe-2S] clusters. The addition of sodium hydrosulfite results in a loss of about one-half of the absorbance between 350 nm and 450 nm (not shown), a feature also characteristic of dicluster ferredoxins.

Figure 2.5A (trace a) shows the EPR spectrum of the concentrated filtrate after incubation with 33 mM sodium hydrosulfite at pH 10.0. The spectrum closely resembles that seen in whole cells, membranes and HbRC complexes after chemical reduction (compare with Figure 2.1C, traces a-c). To determine whether any damage had occurred to the Fe/S clusters, the filtrate was incubated with 2-mercaptoethanol, ferrous ammonium sulfate, and sodium sulfide, for 18 hours (see *Materials and Methods*). As shown in Figure 2.5A (trace b), the EPR spectrum was identical except that the amplitude of the signal was nearly 5-times larger. This shows not only that the majority of the Fe/S clusters in the isolated PshB protein are denatured, but that it is possible to reconstitute the Fe/S clusters in the PshB apoprotein. Figure 2.5B compares the EPR spectrum of the reconstituted and concentrated filtrate after reduction with 10 mM sodium hydrosulfite at pH values of 7.0 and 10.0, where the redox potential of the aqueous solution is fixed by the H^+/H_2 couple, and should be -420 mV and -600 mV, respectively. The EPR spectrum of the chemically-reduced sample at pH 7.0 resembles the one-electron light-induced spectrum (compare Figure 2.1A, traces a-c) and the spectrum of the chemically-reduced sample at pH 10.0 resembles the two-electron photoaccumulated (compare Figure 2.1B, traces a-c) or chemically reduced spectra of whole cells, membranes and HbRC complexes (compare Figure 2.1C, traces a-c). This result indicates that the two Fe/S clusters in the heliobacterial Fe/S protein are in solution more widely separated in redox potential than are F_A and F_B in PsaC of PS I (see also ref. (*21*)).

2.4.6 *Reconstitution of the HbRC Core with the Resolved Fe/S Protein*

The next goal was to determine whether the isolated PshB protein could be rebound to purified HbRC cores. In the first set of experiments, detergent-treated membranes were treated with 1 M NaCl and ultrafiltered over a 30-kDa membrane; the retentate, which contained the HbRC cores, and the filtrate, which contained the PshB protein, were collected. As shown in Figure 2.6A, the amplitude of the light-induced EPR signal generated by illumination of the HbRC cores at 20 K was ca. 5-fold lower than in the intact HbRC complexes (compare trace a, trace b). As shown earlier, this loss is due to the loss of the PshB protein. When the isolated PshB protein is added to the HbRC cores in 3-fold molar excess, the light-induced EPR signal increases, but the degree of recovery varied from preparation-to-preparation (not shown). However, when the PshB protein was pretreated with 2-mercaptoethanol, ferrous ammonium sulfate, and sodium sulfide for 18 hours to reconstitute the Fe/S clusters, the amplitude of the light-induced EPR signal recovered to a value similar to that of the intact HbRC complex (Figure 2.6A, trace c). Note that a light-induced organic radical, derived from $P798^{+}$, is visible at g = 2.003 in all samples.

In the second set of experiments, a DEAE-purified HbRC core was treated similarly. As shown in Figure 2.6B, the light-induced EPR signal generated by illumination of the HbRC cores at 20 K (trace a) or by chemical reduction with sodium hydrosulfite (see Figure 2.1C, trace d) was completely devoid of resonances from Fe/S clusters. After incubating the DEAE-purified HbRC cores with a 7-fold molar excess of the PshB protein, the amplitude of the EPR signals from the Fe/S clusters generally increased. Again, when the PshB protein was pretreated with 2-mercaptoethanol, ferrous ammonium sulfate, and sodium sulfide for 18 hours to reconstitute the Fe/S clusters, the amplitude of the EPR signals increased to a value 70% that of the intact HbRC complex (compare traces c and b). The addition of a larger molar excess of the reconstituted PshB protein to the HbRC core did not increase the amplitude of the light-induced signal. Thus, a small population of the HbRC cores may be irreversibly damaged by either salt treatment or by passage through the ion-exchange column. Note again that a light-induced organic radical is also visible at g = 2.003 in all samples. These reconstitution

experiments prove that the HbRC core is largely intact after removal of the PshB protein and that the latter can be spontaneously rebound, leading to the recovery of the light-induced EPR signals of the terminal Fe/S clusters.

2.4.7 *Time Resolved Optical Spectroscopy of Resolved and Reconstituted HbRC Complexes*

The charge recombination kinetics between the primary donor, $P798^{+}$, and the bound Fe/S clusters acceptors were measured using time-resolved optical spectroscopy in the near-IR. My primary goal was to correlate the lifetimes of the charge-separated states in the HbRC complexes and HbRC cores with the presence and absence of the PshB protein. As shown in Figure 2.7A, the charge recombination kinetics in the HbRC complex is biphasic, with lifetimes of 73 ms and 17 ms. These will henceforth be referred to as the slow and fast kinetic components. In the first set of experiments, detergent-treated membranes were incubated with 1 M NaCl, and the retentate, which contained the HbRC cores, as well as the filtrate, which contained the PshB protein, were collected. The PshB protein was treated with 2-mercaptoethanol, ferrous ammonium sulfate, and sodium sulfide for 18 hours to reconstitute any damaged or lost Fe/S clusters (*See Materials and Methods)*. The flash-induced absorbance change in the retentate that contains the HbRC cores (Figure 2.7B) shows a significant loss in amplitude of the slow kinetic component, which now accounts for 27% of the signal, and an equivalent gain in amplitude of the slow kinetic component, which now accounts for 67% of the total amplitude. There are no significant kinetic events on the microsecond timescale. When the filtrate is added to the HbRC cores in a 10-fold molar excess, the slow kinetic component is partially regained and the fast kinetic component is partially lost (Figure 2.7C). Note that the total absorbance change is diminished by 18% after salt washing and by 32% after rebinding of PshB.

In the second set of experiments, DEAE-purified HbRC cores were used in the reconstitution experiments. As shown in Figure 2.8B, only the fast kinetic component is retained, and it accounts for 97% of the total amplitude (compare, Figure 2.8A). This matches the total loss of the light-induced EPR signals of the Fe/S signals in the DEAE-purified HbRC core (see Figure 2.6B, trace a). When the filtrate was added back to the

HbRC core, a significant fraction of the slow kinetic component is restored at the expense of the fast kinetic component. Note that the total absorbance change is diminished by 14% after purification by DEAE ion-exchange chromatography and after rebinding of the PshB protein. The slightly lower amplitude of both the optical (Figures 2.7 and 2.8) and EPR (Figure 2.6) signals after reconstitution may be due to damage to an early acceptor incurred during the salt-wash and/or DEAE-ion exchange chromatographic steps.

2.5 DISCUSSION

The primary aim of this study was to initiate a detailed characterization of the cofactors and proteins that comprise the photosynthetic RC in *Heliobactericae*. I chose to study *H. modesticaldum*, a moderate thermophile that grows optimally at 50°-52° C, because the RC from this organism would likely be more thermostable than one from a mesophile. The HbRC is a Type I RC with a homodimeric core; it does not harbor a tightly bound cytochrome, and it does not contain chlorosomes, the FMO protein, or any other type of extended antenna system as found in species of *Chlorobium (31)*. Given the absence of these structures, the HbRC should be ideal for study of a prototypical homodimeric RC. However, current knowledge of the HbRC is incomplete, particularly with respect to the polypeptide composition and the full complement of electron acceptors. To paraphrase Amesz (*10*), with the exception of the primary charge separation steps, limited progress has been made in the last several years on the HbRC, either with respect to its polypeptide composition, the components of the electron acceptor chain, or the kinetics of forward and backward electron transfer. What is known with certainty concerns primarily the initial charge-separated state. The primary electron donor, $P798^{+}$, is a dimer of Bchl *g*' (the 13^2 epimer that now appears to be a common feature of all Type I reaction centers) and, as might be expected in a homodimeric RC, the cation is delocalized over both Bchl *g* molecules (*22, 26*). The primary electron acceptor is Chl *a* 670, an 8^1-hydroxy Chl *a* molecule. Charge separation between P798 and A_0 occurs within 25 ps after a flash, but this value may instead represent energy transfer from the thermally-populated antenna; the actual time of charge separation is

estimated to be within 1 or 2 ps (*32, 33*). Forward electron transfer from A_0^- occurs in 600 ps at room temperature (*34*) and if blocked, the resulting charge recombination between $P798^+$ and A_0^- occurs in 17 ns.

There are only a few reliable reports that describe the properties of the bound Fe/S clusters in Heliobacteria. There is optical evidence for an F_X-like cluster in isolated membranes (*20*) but not for F_A- or F_B-like clusters. Conversely, there exists EPR evidence for a light-induced Fe/S cluster (*22*), as well as a more detailed report of EPR resonances comparable to F_A and F_B of PS I (*21*), but not for an F_X-like cluster (*20, 27*). No single methodology reveals the presence of all three Fe/S clusters in either cells, membranes or isolated HbRCs. Taken at face value, these data can be fit into a model such that the Fe/S clusters in the HbRC are equivalent to F_X, F_B and F_A in PS I. The issue, however, is further complicated by a report that the major photosynthesis gene cluster from *H. mobilis* does not contain a gene that codes for a PsaC (or PscB)-like protein (*23*). There also have been few, if any, reports of a PsaC (or PscB)-like protein in membranes or HbRCs, either as a band on a SDS-polyacrylamide electrophoresis gel or as a purified protein. No doubt, the lack of evidence on many of the components of the electron transport chain is due to the sensitivity of the terminal Fe/S clusters to oxygen and, as I have found in this study, an instability of the Fe/S protein to moderate ionic strength in the presence of detergent. It is therefore likely that the combined deleterious effect of oxygen, detergent, and ionic strength is the reason that the PshB protein has not been previously reported. It should be noted that the conditions under which the HbRC complex was purified in ref. (*27*) probably resulted in the removal of the PshB protein.

I therefore considered it timely to investigate the detailed properties of the bound Fe/S clusters in Heliobacteria, paying particular attention to the need to maintain anaerobic conditions throughout the purification procedure. My studies indicate that PshB, the bound Fe/S protein in the HbRC, has a mass of ca. 9 kDa and that it contains two [4Fe-4S] clusters. The PshB protein in the HbRC is therefore more similar to PsaC of PS I than to PscB of the *Chlorobium* RC. The interaction spectrum observed at low redox potentials or after photoaccumulation is also characteristic of ferredoxins that contain two closely-spaced [4Fe-4S] clusters, including PsaC of PS I. However, the linewidths of the individual *g*-components of the reduced Fe/S clusters in PshB are considerably broader

than the resonances of F_A^-/F_B^- in PS I. Indeed, the *g*-values and the linewidths of the resonances in the bound and the unbound forms of the reduced PshB protein are quite similar, and compare favorably with *unbound* PsaC. When PsaC docks onto the F_x-core in PS I, the spectroscopic properties of F_A and F_B change, and linewidths of the individual *g*-components narrow (*35*). The addition of PsaD leads to further narrowing of the individual *g*-components to become similar to those of the wild-type. In contrast, when PshB docks to the HbRC core, the magnetic properties of the cluster(s) remain relatively unaltered. It is not known if the HbRC has a subunit comparable to PsaD; however, the salt-treatment removes primarily the 8-kDa Fe/S protein, PshB. The HbRC does contain several additional, prominent polypeptides with molecular weights ranging from 15 to 25 kDa, but these proteins are tightly associated with the PshA homodimer and are not removed by treatment with high ionic strength. They can be removed when membranes are solubilized using Triton X-100 (data not shown), and they are also apparently removed using the detergent Deriphat 160c, which results in a HbRC that contains only a single-subunit, the PshA protein (*27*).

The results suggest that the PshB protein associates with the PshA homodimer in the HbRC in a manner unlike that of PsaC with the PsaA/PsaB heterodimer in PS I. The facile removal of the bound Fe/S protein in HbRCs with 1 M NaCl is in striking contrast to the need for 7.8 M urea or high concentrations of chaotropic agents (*i.e.*, 2 M $NaClO_4$) to remove PsaC from PS I. The salt-based removal of the bound Fe/S protein from the HbRC leaves a population of the Fe/S clusters intact, whereas the chaotrope-based removal of PsaC from PS I completely destroys the F_A and F_B clusters. The tight binding of PsaC can be explained by the X-ray crystal structure of PS I (*4*). The core region of PsaC is bound to the F_X region of the PsaA/PsaB heterodimer through at least 8 ionic contacts (*35*): $Arg65_{PsaC}$ and $Lys51_{PsaC}$ are bridged to $Asp555_{PsaB}$ and $Asp566_{PsaB}$, and $Arg\ 52_{PsaC}$ is bridged to $Asp579_{PsaA}$ and $Asp568_{PsaA}$. In addition, the C-terminal region of PsaC is bound in a hydrophobic pocket on the PsaB protein and anchored by two H-bonds, one from $Tyr\ 80_{PsaC}$ to $Pro703_{PsaB}$ and one from $Thr73_{PsaC}$ to $Lys702_{PsaB}$. Even though many residues in the F_X core region are conserved between PshA and PsaA/PsaB, particularly the Cys, Gly and Pro residues, $Asp566_{PsaB}$ and $Asp579_{PsaA}$ are replaced by a neutral Leu in PshA, and $Asp555_{PsaB}$ and $Asp568_{PsaA}$ are replaced by a basic Lys in PshA

(*28*). When this work was completed, I did not yet have the sequence of PshB with which to attempt comparison modeling. Nevertheless, these differences imply a different mode of binding of PsaC to the heterodimeric PsaA/PsaB core and PshB to the homodimeric PshA core.

There are other notable differences between the properties of the HbRC and PS I. Firstly, the relatively low number of antenna chlorophylls in the HbRC (reported to be ca. 35- 40/P798 in the HbRC *vs* 100/P700 in PS I) required us to use a higher intensity of light to achieve maximum amplitude of the Fe/S resonances. This requirement is either due to the relatively low number of Bchl *g* molecules that are associated with the HbRC (*26*) or to the reported inefficiency of electron transfer to the Fe/S clusters at low temperatures (*21*). Secondly, illumination of the HbRCs at 20 K results in the generation of a single rhombic signal, whereas in PS I, the same protocol results in the generation of two rhombic signals, F_A^- and F_B^-, in a ca. 3:1 ratio. One possible explanation is that because of the expected high symmetry of the HbRC, the two [4Fe-4S] clusters in PshB have identical EPR spectra and cannot be distinguished when only one is reduced in a given PshB protein. Another possibility is that the two [4Fe-4S] clusters have dissimilar EPR spectra, but that the two Fe/S clusters have sufficiently different redox potentials such that the equilibrium favors population of only the higher potential Fe/S cluster. The assessment that the two Fe/S clusters have widely different redox potentials is supported by an EPR study of a sample that was chemically reduced at different pH values. The addition of sodium hydrosulfite to PshB at pH 7.0, where the solution potential is -420 mV, leads to the chemical reduction of a single Fe/S cluster, whereas the same treatment at pH 10.0, where the solution potential is ca. -600 mV, leads to the chemical reduction of both Fe/S clusters. Were the two Fe/S clusters identical, there should have been a complex interaction spectrum present at both pH 7.0 and 10.0. A complete redox titration and a detailed comparison of the redox potentials of the Fe/S clusters when PshB is bound and unbound to the HbRC core will be reported elsewhere.

Time-resolved optical spectroscopy performed on the HbRC complex and the HbRC core allows us to assign with relative certainty the kinetic phases derived from charge recombination with $P798^+$. The partial elimination of the 70-ms kinetic component uncovered by time-resolved optical spectroscopy after salt washing is in

agreement with the partial loss of the light-induced Fe/S resonances by EPR spectroscopy. Indeed, the total elimination of the 70-ms kinetic component after DEAE ion-exchange chromatography is in complete agreement with the EPR data. These results provide a compelling argument for assigning the slow, 70-ms kinetic component to charge recombination between P798 and the terminal Fe/S cluster bound to PshB. The HbRC core prepared by DEAE ion-exchange chromatography shows a single monophasic, 15 ms lifetime component by time-resolved optical spectroscopy that I attribute to the recombination of $P798^+$ with an earlier electron acceptor. The identity of this acceptor, however, is not obvious from the spectroscopic results. It is unlikely to be A_0 because if forward electron transfer from A_0^- to the next electron acceptor is blocked, charge recombination between $P798^+$ and A_0^- occurs in 17 ns. If the fast, 15-ms kinetic component in the HbRC core represents charge recombination from a quinone, then the charge-separated state between $P798^+$ and Q^- would be stable for periods two- to three-orders of magnitude longer than the comparable charge-separated state in PS I. If it represents charge recombination from F_X, then the charge-separated state between $P798^+$ and F_X would be stable for periods up to 15 times longer than the comparable charge-separated state in PS I. The 15 ms lifetime, however, is strikingly similar to the 14-ms (aerobic) or 20-ms (anaerobic) decay measured in a HbRC core isolated from *Heliobacillus mobilis* membranes after treated with 6 M urea. The spectrum of this electron acceptor, extracted by taking the difference of the flash-induced absorbance changes in the presence and absence of benzyl viologen, showed a bleaching in the blue between 400 nm and 800 nm attributed to Fe/S cluster F_X (*20*). This agrees with the circumstantial evidence for the existence of F_X from the FPCLGPAYGGTC sequence in the PshA protein that likely corresponds to the FPCDGPCRGGTC binding site for F_X in PS I (*28*). Nevertheless, we were unable to measure an EPR spectrum of an Fe/S cluster in the $g = 2$ region after photoaccumulation of the HbRC core in the presence of sodium hydrosulfite at pH 10.0 (see also (*20*)). This could be because the F_X cluster has unusual relaxation properties or a ground spin state greater than S = 1/2; both would make detection by EPR difficult. Further work is directed towards obtaining EPR evidence for the existence of F_X in the purified HbRC core.

2.6 SUMMARY

Heliobacteria contain a bound Fe/S protein similar to PsaC in PS I. By studying the EPR spectra of HbRC complexes that were subjected to various purification protocols, I found the bound Fe/S protein could be removed by chromatography on an anion exchange column. The bound Fe/S protein can also be removed from the HbRC complexes by treatment with 1 M NaCl in the presence of *n*-dodecyl-_-D-maltopyranoside. The removed protein contains two Fe/S clusters, and these clusters can be re-inserted into the apoprotein by incubation with iron, sulfide, and 2-mercaptoethanol under anaerobic conditions. The ability to restore functional electron transfer to the terminal Fe/S clusters after combining the Fe/S protein with HbRC cores indicates that the preceding electron acceptor, the presumed F_X cluster, is relatively stable. In HbRC complexes, the 75-ms kinetic phase after a saturating laser flash is derived from recombination of a terminal Fe/S cluster with $P798^+$. In HbRC cores, the 15-ms kinetic phase is derived from recombination with an earlier acceptor, most likely F_X. Following convention established in the field, I suggest that the bound Fe/S protein present in the HbRC be designated PshB.

2.7 REFERENCES

(1) Blankenship, R. E. (1994) Protein structure, electron transfer and evolution of prokaryotic photosynthetic reaction centers, *Antonie Van Leeuwenhoek 65*, 311-329.

(2) Nitschke, W., and Rutherford, A. W. (1991) Photosynthetic reaction centres: variations on a common structural theme?, *Trends Biochem Sci 16*, 241-5.

(3) Deisenhofer, J., Epp, O., Miki, K., Huber, R., and Michel, H. (1984) X-ray structure analysis of a membrane protein complex. Electron density map at 3 A resolution and a model of the chromophores of the photosynthetic reaction center from *Rhodopseudomonas viridis*, *J Mol Biol 180*, 385-98.

(4) Jordan, P., Fromme, P., Witt, H. T., Klukas, O., Saenger, W., and Krauß, N. (2001) Three-dimensional structure of cyanobacterial photosystem I at 2.5 A resolution, in *Nature 411*, pp 909-917.

(5) Ferreira, K. N., Iverson, T. M., Maghlaoui, K., Barber, J., and Iwata, S. (2004) Architecture of the photosynthetic oxygen-evolving center, *Science 303*, 1831-8.

(6) Zouni, A., Witt, H. T., Kern, J., Fromme, P., Krauss, N., Saenger, W., and Orth, P. (2001) Crystal structure of photosystem II from *Synechococcus elongatus* at 3.8 A resolution, *Nature 409*, 739-43.

(7) Madigan, M. T., and Ormerod, J. G. (1995) Taxonomy, physiology, and ecology of heliobacteria, in *Anoxygenic photosynthetic bacteria* (Blankenship R. E., Madigan, M. T., Bauer, C. E., Ed.) pp 17-30, Kluwer, Dordrecht.

(8) Brockmann, H., and Lipinski, A. (1983) Bacteriochlorophyll *g*. A new bacteriochlorophyll from *Heliobacterium chlorum*, *Arch. Microbiol. 136*, 17-19.

(9) Woese, C. R., Debrunner-Vossbrinck, B. A., Oyaizu, H., Stackebrandt, E., and Ludwig, W. (1985) Gram-positive bacteria: possible photosynthetic ancestry, *Science 229*, 762-5.

(10) Neerken, S., and Amesz, J. (2001) The antenna reaction center complex of heliobacteria: composition, energy conversion and electron transfer, *Biochim Biophys Acta 1507*, 278-90.

(11) Kobayashi, M., van de Meent, E. J., Erkelens, C., Amesz, J., Ikegami, I., and Watanabe, T. (1991) Bacteriochlorophyll *g* epimer as a possible reaction center component of heliobacteria, *Biochim Biophys Acta 1057*, 89-96.

(12) Van de meent, E. J., Kleinherenbrink, F. A. M., and Amesz, J. (1990) Purification and properties of an antenna-reaction center complex from heliobacteria, *Biochim Biophys Acta 1015*, 223-230.

(13) Prince, R., Blankenship, RE, Gest, H. (1985) Thermodynamic properties of the photochemical reaction center of *Heliobacterium chlorum*, *Biochim Biophys Acta 810*, 377-384.

(14) van de Meent, E. J., Kobayashi, M., Erkelens, C., van Veelen, PA., Amesz, J. (1991) Identification of 8'-hydroxychlorophyll a as a functional reaction center pigment in heliobacteria, *Biochim et Biophys Acta 1058*, 356-62.

(15) Amesz, J. (1995) The heliobacteria, a new group of photosynthetic bacteria, *J Photochem Photobiol B: Biol 30*, 89-96.

(16) Muhiuddin, I. P., Rigby, S. E., Evans, M. C., Amesz, J., and Heathcote, P. (1999) ENDOR and special TRIPLE resonance spectroscopy of photoaccumulated semiquinone electron acceptors in the reaction centers of green sulfur bacteria and heliobacteria, *Biochemistry 38*, 7159-67.

(17) Brettel, K., Leibl, W., and Liebl, U. (1998) Electron transfer in the heliobacterial reaction center: evidence against a quinone-type electron acceptor functioning analogous to A_1 in photosystem I, *Biochim Biophys Acta 1363*, 175-181.

(18) Kleinherenbrink, F. A. M., Ikegami, I., Hiraishi, A., Otte, S. C. M., and Amesz, J. (1993) Electron transfer in menaquinone-depleted membranes of *Heliobacterium chlorum*, *Biochim Biophys Acta 1142*, 69-73.

(19) van der Est, A., Hager-Braun, C., Leibl, W., Hauska, G., and Stehlik, D. (1998) Transient electron paramagnetic resonance spectroscopy on green-sulfur bacteria and heliobacteria at two microwave frequencies, *Biochim Biophys Acta 1409*, 87-98.

(20) Kleinherenbrink, F. A., Chiou, H. C., LoBrutto, R., and Blankenship, R. E. (1994) Spectroscopic evidence for the presence of an iron-sulfur center similar to Fx of Photosystem I in *Heliobacillus mobilis*, *Photosynth Res 41*, 115-23.

(21) Nitschke, W., Setif, P., Liebl, U., Feiler, U., and Rutherford, A. W. (1990) Reaction center photochemistry of *Heliobacterium chlorum*, *Biochemistry 29*, 11079-88.

(22) Prince, R. C., Gest, H., and Blankenship, R. E. (1985) Thermodynamic properties of the photochemical reaction center of *Heliobacerium chlorum*, *FEBS Lett 182*, 345-349.

(23) Xiong, J., Inoue, K., and Bauer, C. E. (1998) Tracking molecular evolution of photosynthesis by characterization of a major photosynthesis gene cluster from *Heliobacillus mobilis*, *Proc Nat Acad Sci Usa 95*, 14851-14856.

(24) Vassiliev, I. R., Ronan, M. T., Hauska, G., and Golbeck, J. H. (2000) The bound electron acceptors in green sulfur bacteria: resolution of the g-tensor for the F(X) iron-sulfur cluster in *Chlorobium tepidum*, *Biophys J 78*, 3160-9.

(25) Kimble, L. K., Mandelco, L., Woese, C. R., and Madigan, M. T. (1995) *Heliobacterium modesticaldum*, sp-nov, a thermophilic Heliobacterium of hot-springs and volcanic soils, *Arch Microbiol 163*, 259-267.

(26) Noguchi, T., Fukami, Y., OhOka, H., and Inoue, Y. (1997) Fourier transform infrared study on the primary donor P798 of *Heliobacterium modesticaldum*: Cysteine S-H coupled to P798 and molecular interactions of carbonyl groups, *Biochemistry 36*, 12329-12336.

(27) Trost, J. T., and Blankenship, R. E. (1989) Isolation of a photoactive photosynthetic reaction center-core antenna complex from *Heliobacillus mobilis*, *Biochemistry 28*, 9898-904.

(28) Liebl, U., Mockensturmwilson, M., Trost, J. T., Brune, D. C., Blankenship, R. E., and Vermaas, W. (1993) Single core polypeptide in the reaction center of the photosynthetic bacterium *Heliobacillus mobilis* - Structural implications and relations to other photosystems, *Proc Natl Acad Sci USA 90*, 7124-7128.

(29) Trost, J. T., Brune, D. C., and Blankenship, R. E. (1992) Protein sequences and redox titrations indicate that the electron acceptors in reaction centers from heliobacteria are similar to Photosystem I, *Photosynth Res 32*, 11-22.

(30) Bryant, D. (1994) Gene nomenclature recommendations for green photosynthetic bacteria and heliobacteria, *Photosynth Res 41*, 27-28.
(31) Hauska, G., Schoedl, T., Remigy, H., and Tsiotis, G. (2001) The reaction center of green sulfur bacteria, *Biochim Biophys Acta 1507*, 260-77.
(32) Lin, S., Chiou, H. C., Kleinherenbrink, F. A. M., and Blankenship, R. E. (1994) Time-resolved spectroscopy of energy and electron transfer processes in the photosynthetic bacterium *Heliobacillus mobilis*, *Biophys J 66*, 437-445.
(33) Liebl, U., Lambry, J. C., Breton, J., Martin, J. L., and Vos, M. H. (1997) Spectral equilibration and primary photochemistry in *Heliobacillus mobilis* at cryogenic temperature, *Biochemistry 36*, 5912-20.
(34) Lin, S., Chiou, H. C., and Blankenship, R. E. (1995) Secondary electron transfer processes in membranes of *Heliobacillus mobilis*, *Biochemistry 34*, 12761-12767.
(35) Antonkine, M. L., Jordan, P., Fromme, P., Krauss, N., Golbeck, J. H., and Stehlik, D. (2003) Assembly of protein subunits within the stromal ridge of Photosystem I. structural changes between unbound and sequentially PS I-bound polypeptides and correlated changes of the magnetic properties of the terminal iron sulfur clusters, *J Mol Biol 327*, 671-97.

2.8 FIGURE LEGENDS

Figure 2.1: EPR spectra of whole cells, membranes and RCs of *Heliobacterium modesticaldum*. Spectrometer conditions: temperature, 20 K; power, 126 mW; microwave frequency, 9.47 Ghz; receiver gain, 2 x 10^4. **A**) Difference spectrum between a sample illuminated at 20 K and a dark-adapted sample. **B**) Difference spectrum between a sample frozen in the presence of light and a dark-adapted sample. **C**) Difference spectrum between a chemically reduced and an oxidized (no treatment) sample. The sample was reduced with 33 mM sodium hydrosulfite in 100 mM glycine (pH 10.0) buffer. **a)** Whole cells, **b)** Isolated membranes, **c)** HbRCs isolated by sucrose gradient ultracentrifugation, **d)** HbRCs purified from DEAE ion-exchange chromatography.

Figure 2.2: EPR spectra of salt-washed membranes from *Heliobacterium modesticaldum*. The membranes were solubilized using *n*-dodecyl-_-D-maltopyranoside and were either untreated **(a)** or treated with **(b)** 100 mM, **(c)** 250 mM or **(d)** 500 mM NaCl for 5 min. The samples were then flash-frozen to 77 K and placed in the resonator at 20 K. Light-induced EPR signals were generated by illuminating dark-adapted samples at 20 K with a 2.5-W argon ion laser for 1 min. The spectra depicted are the difference between the illuminated and dark-adapted samples. Spectrometer conditions: temperature, 20 K; power, 126 mW; microwave frequency, 9.47 GHz; receiver gain, 2 x 10^4. The optical absorbance at 788 nm was 75 OD.

Figure 2.3: SDS polyacrylamide gel electrophoresis of the isolated RC complexes from cells of *Heliobacterium modesticaldum*. The HbRC complexes were isolated by sucrose gradient ultracentrifugation and further purified by DEAE ion-exchange chromatography. The sample lane was loaded with the equivalent of 2 μg Bchl. The proteins were resolved in a 12% (w/v) polyacrylamide gel and visualized by staining with Coomassie Brilliant Blue R-250.

Figure 2.4: Protein composition and optical absorption spectrum of the filtrate from 250 to 700 nm of salt-washed HbRCs. **A)** SDS-PAGE followed by staining with silver.

Molecular mass standards are in the left lane, the filtrate is in the right lane. The molecular masses of the standards are depicted. **B)** Optical absorption spectrum of the filtrate containing the oxidized PshB protein.

Figure 2.5: EPR spectra of the the PshB-containing filtrate from salt-washed HbRCs. **(A)** EPR spectrum before **(a)** and after **(b)** reconstitution of the Fe/S clusters with 2-mercaptoethanol, $Fe(NH_4)_2(SO_4)_2$ and Na_2S. The samples were incubated in 33 mM sodium hydrosulfite in 100 mM glycine (pH 10) buffer. **(B)** EPR spectrum of the reconstituted filtrate at pH 7.0 **(a)** and pH 10.0 **(b)**. The samples were reduced with 10 mM sodium hydrosulfite.

Figure 2.6: EPR spectra of reconstituted HbRC complexes from HbRC cores and the PshB protein. **(A)** Difference spectrum between a sample illuminated at 20 K and a dark-adapted sample. **(a)** The HbRC core prepared by addition of 1 M NaCl followed by ultrafiltration and concentration over a YM-30 membrane; **(b)** the reconstituted HbRC complex prepared by adding a 3-fold molar excess of PshB protein to the HbRC cores, and **(c)** the intact HbRC complex isolated by sucrose density ultracentrifugation. **(B)** Difference spectrum between a sample illuminated at 20 K and a dark-adapted sample. **(a)** The HbRC cores after DEAE ion-exchange chromatography, **(b)** the reconstituted HbRC complex prepared by adding a 7-fold molar excess of the PshB protein to the HbRC cores purified by DEAE ion-exchange chromatography, and **(c)** the HbRC complex isolated by sucrose gradient ultracentrifugation. Light-induced EPR signals were generated by illuminating dark-adapted samples at 20 K with a 2.5-W argon ion laser for 1 min. The spectra depicted are the difference between the illuminated and dark adapted samples. The optical absorbance at 788 nm was 75 OD.

Figure 2.7: Flash induced absorption changes of $P798^+$ reduction detected at 798 nm: **(A)** Decay kinetics of the HbRC complexes isolated by sucrose density ultracentrifugation. **(B)**, Decay kinetics of the HbRC cores after addition of 1 M NaCl followed by ultrafiltration and concentration over a YM-30 membrane **(C)** Decay kinetics after

incubating the HbRC cores isolated by 1M NaCl washing with a 10-fold molar excess of the PshB-containing filtrate. The optical absorbance at 788 nm was 0.5 OD.

Figure 2.8: Flash induced absorption changes of $P798^{+}$ reduction detected at 798 nm: **(A)** Decay kinetics of the HbRC complexes isolated by sucrose density ultracentrifugation. **(B)**, Decay kinetics of the HbRC cores purified by DEAE ion-exchange chromatography. **(C)** Decay kinetics after incubating the HbRC cores purified from DEAE ion-exchange chromatography with a 10-fold molar excess of the PshB-containing filtrate. The optical absorbance at 788 nm was 0.5 OD.

Figure 2.1

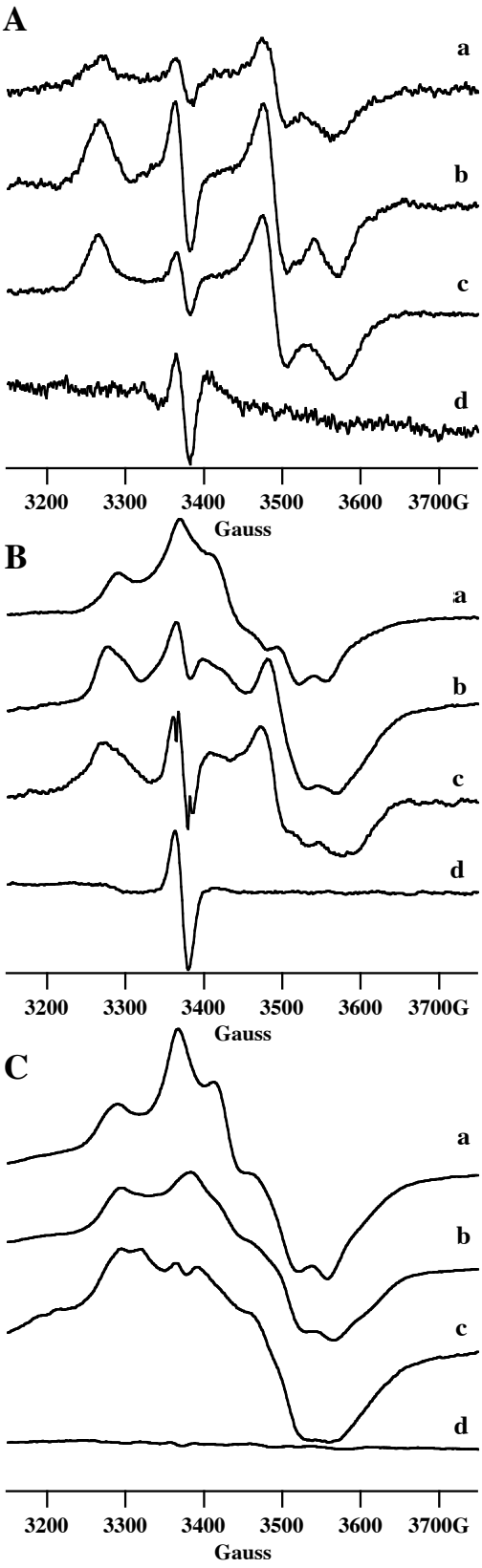
A
a
b
c
d
3200
3300
3400
3500
3600
3700G
Gauss
B
a
b
c
d
3200
3300
3400
3500
3600
3700G
Gauss
C
a
b
c
d
3200
3300
3400
3500
3600
3700G
Gauss

Figure 2.2

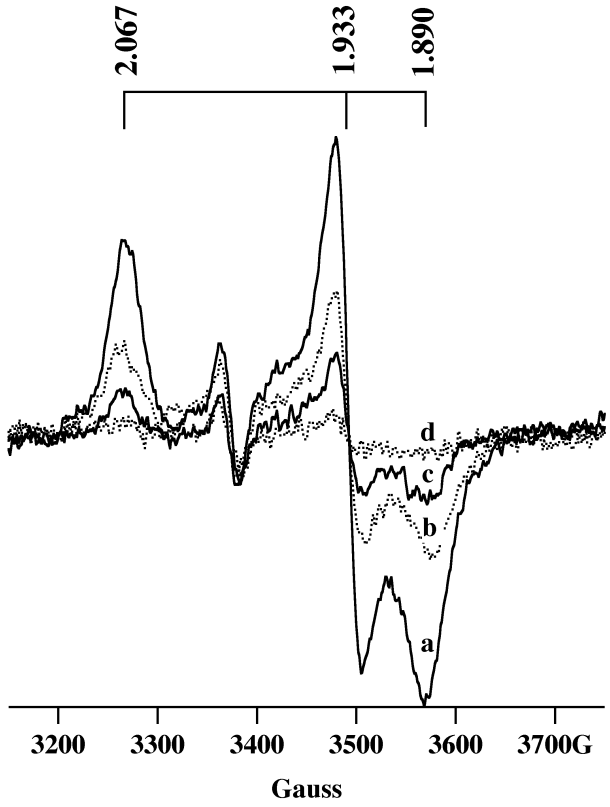

Figure 2.3

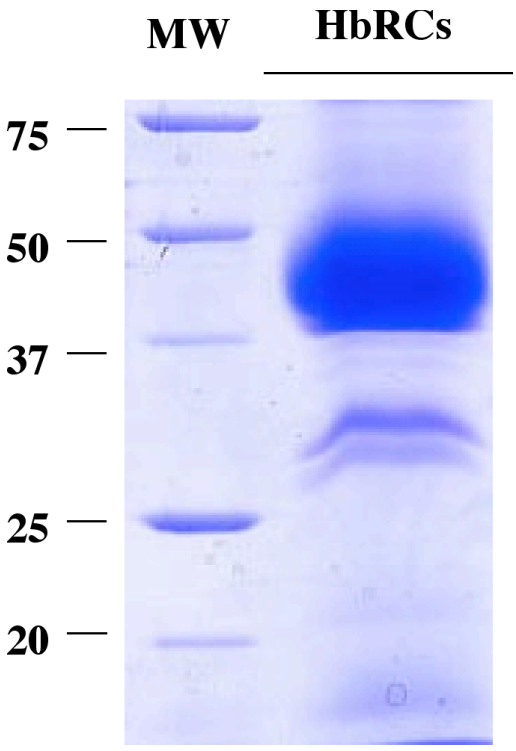

Figure 2.4

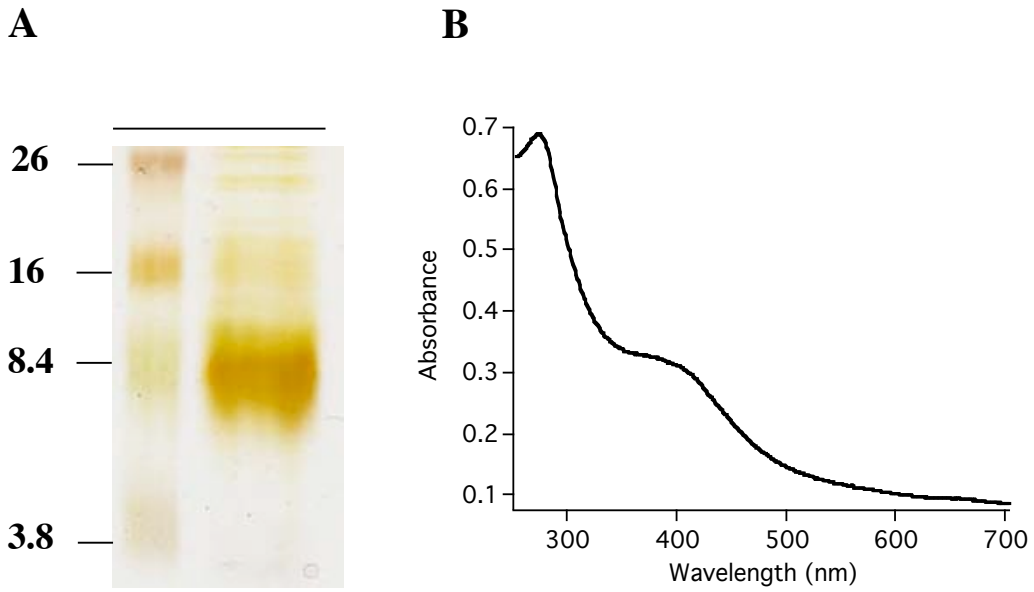
A
B
26
16
8.4
3.8
0.7
0.6
0.5
0.4
0.3
0.2
0.1
Absorbance
300
400
500
600
700
Wavelength (nm)

Figure 2.5

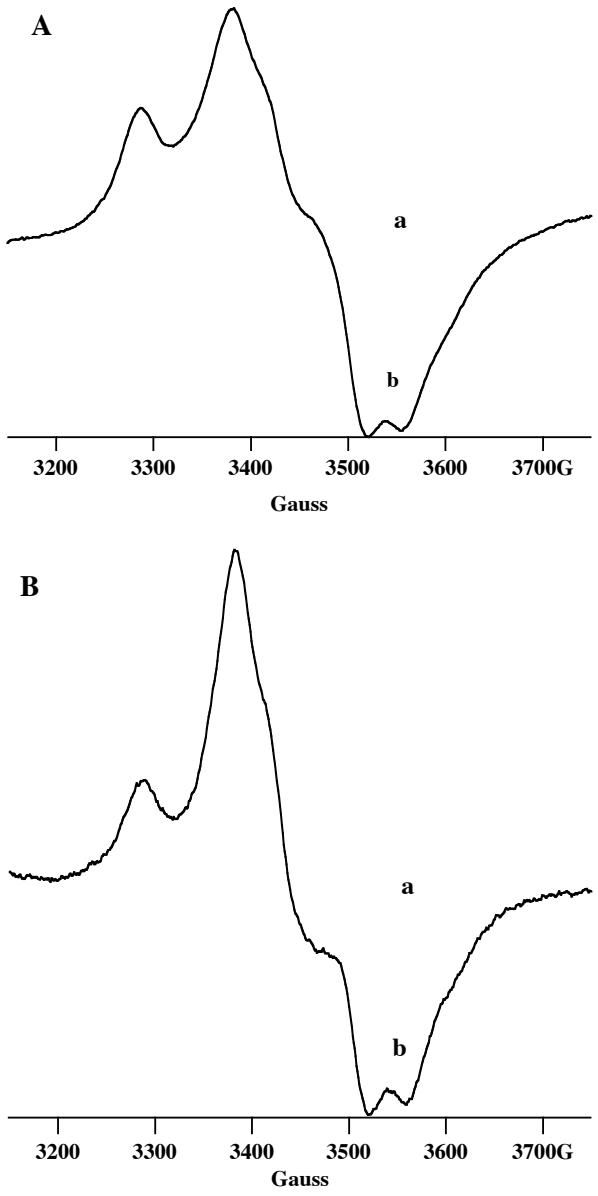
A
a
b
3200
3300
3400
3500
3600
3700G
Gauss
B
a
b
3200
3300
3400
3500
3600
3700G
Gauss

Figure 2.6

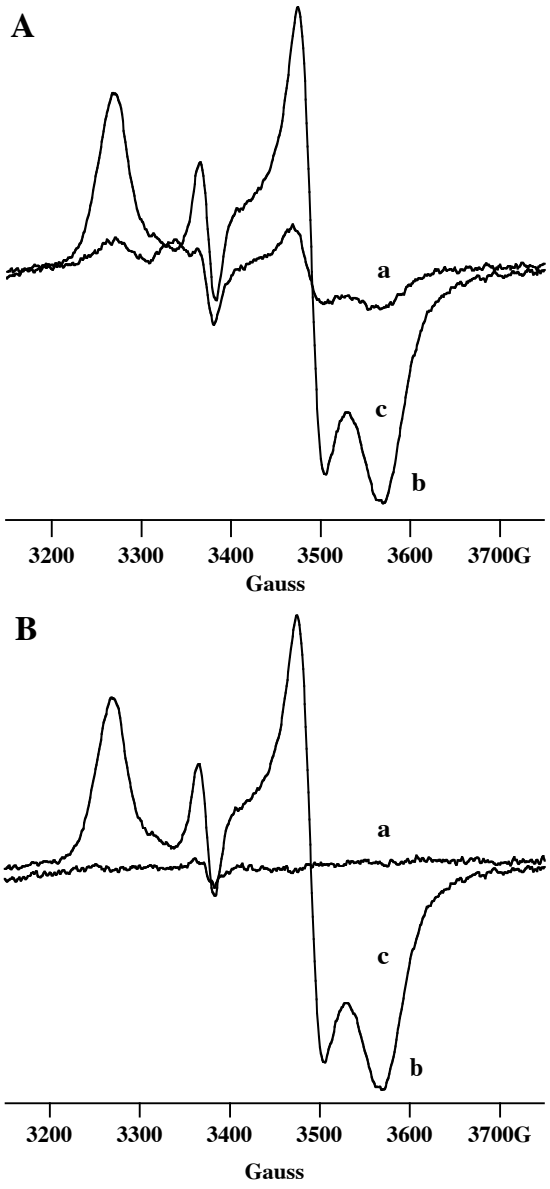
A
a
c
b
3200
3300
3400
3500
3600
3700G
Gauss
B
a
c
b
3200
3300
3400
3500
3600
3700G
Gauss

Figure 2.7

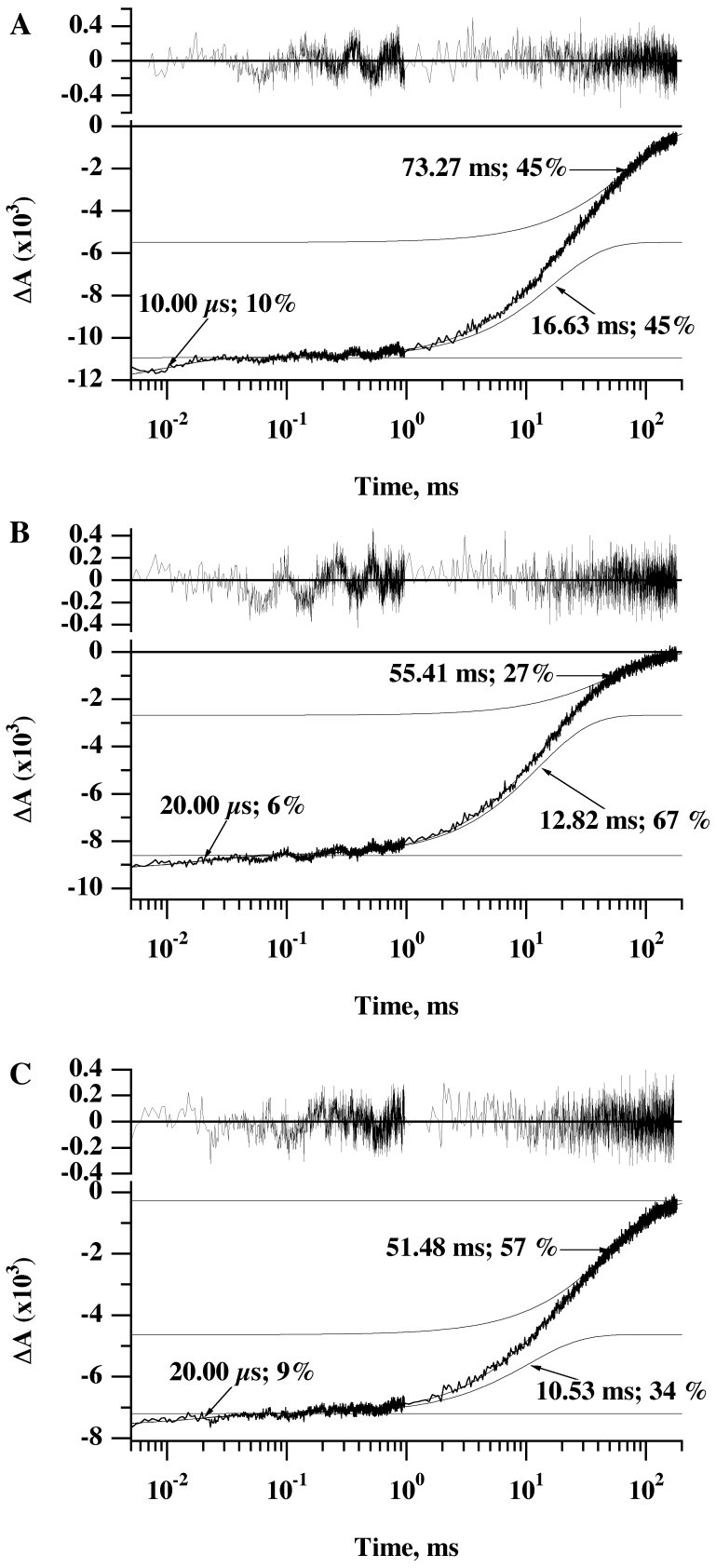
A
0.4
0
-0.4
0
-2
-4
-6
-8
-10
-12
ΔA (x10³)
73.27 ms; 45%
10.00 μs; 10%
16.63 ms; 45%
10⁻²
10⁻¹
10⁰
10¹
10²
Time, ms
B
0.4
0.2
0
-0.2
-0.4
0
-2
-4
-6
-8
-10
ΔA (x10³)
55.41 ms; 27%
20.00 μs; 6%
12.82 ms; 67 %
10⁻²
10⁻¹
10⁰
10¹
10²
Time, ms
C
0.4
0.2
0
-0.2
-0.4
0
-2
-4
-6
-8
ΔA (x10³)
51.48 ms; 57 %
20.00 μs; 9%
10.53 ms; 34 %
10⁻²
10⁻¹
10⁰
10¹
10²
Time, ms

Figure 2.8

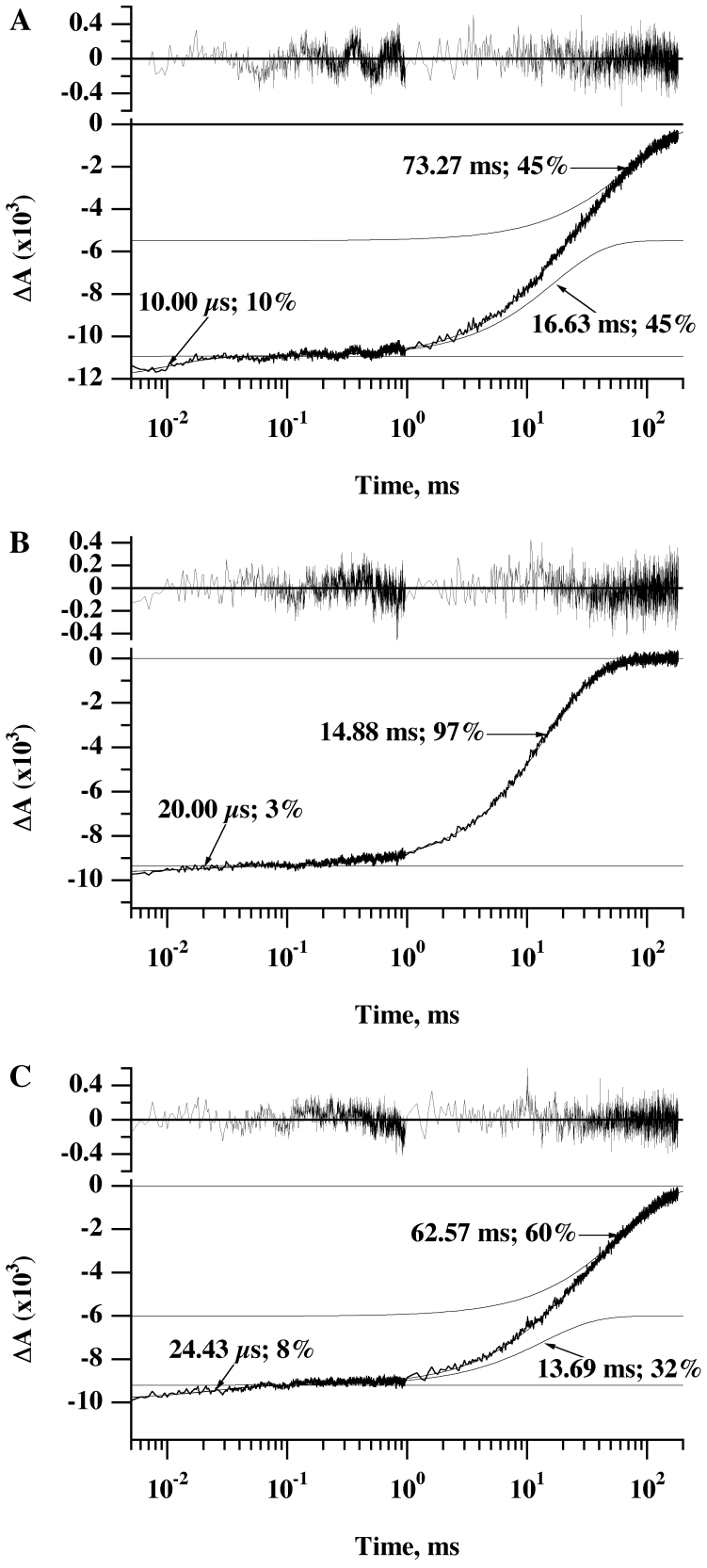
A
0.4
0
-0.4
0
-2
-4
-6
-8
-10
-12
ΔA (x10³)
73.27 ms; 45%
10.00 μs; 10%
16.63 ms; 45%
10⁻²
10⁻¹
10⁰
10¹
10²
Time, ms
B
0.4
0.2
0
-0.2
-0.4
0
-2
-4
-6
-8
-10
ΔA (x10³)
14.88 ms; 97%
20.00 μs; 3%
10⁻²
10⁻¹
10⁰
10¹
10²
Time, ms
C
0.4
0
-0.4
0
-2
-4
-6
-8
-10
ΔA (x10³)
62.57 ms; 60%
24.43 μs; 8%
13.69 ms; 32%
10⁻²
10⁻¹
10⁰
10¹
10²
Time, ms

Chapter 3

The Identification of F_X in the Heliobacterial Reaction Center as a [4Fe-4S] Cluster with a Ground Spin State of S = 3/2

Published in part as a paper titled "The Identification of F_X in the Heliobacterial Reaction Center as a [4Fe-4S] Cluster with a Ground Spin State of S = 3/2" by Mark Heinnickel, Rufat Agalarov, Nina Svensen, Carsten Krebs, and John H. Golbeck. (2006) Biochemistry 45 (21), 6756 - 6764

3.1 ABSTRACT

In the previous chapter, I showed that PshB, the protein containing the terminal F_A/F_B acceptors, could be removed from the HbRC by chromatography on a DEAE anion exchange column. The resulting HbRC core showed a light-induced 15-ms charge recombination from $P798^+$ and an unidentified acceptor. Similar kinetics had previously been ascribed to charge recombination between the interpolypeptide Fe/S cluster, F_X, and the primary donor, P798. However a functional Fe/S cluster comparable to F_X had not been detected by EPR spectroscopy. I report here that when HbRC cores are incubated with sodium dithionite in the presence of light, the 15-ms charge recombination is replaced with a kinetic transient in the sub-μs time domain, consistent with the reduction of an electron acceptor. Concomitantly, a broad and intense EPR signal arises around g = 5 along with a minor set of resonances around g = 2 similar to the spectrum of the $[4Fe\text{-}4S]^{1+}$ cluster in the Fe-protein of *Azotobacter vinelandii* nitrogenase, which exists in two conformations having ground spin states of $S = 3/2$ and $S = 1/2$. The Mössbauer spectrum in the as-isolated HbRC core shows that all of the Fe is present in the form of a $[4Fe\text{-}4S]^{2+}$ cluster. After reduction with sodium dithionite in the presence of light, approximately 65% of the Fe appears in the form of a $[4Fe\text{-}4S]^{1+}$ cluster; the remainder is in the $[4Fe\text{-}4S]^{2+}$ state. Analysis of the non-heme iron content of HbRC cores indicates an antenna size of 21.6 ± 1.1 BChl *g*/P798. The HbRC therefore contains a [4Fe-4S] cluster that is coordinated between the PshA homodimer; in contrast to F_X in other Type I reaction centers, this [4Fe-4S] cluster exhibits an $S = 3/2$ ground spin state.

3.2 INTRODUCTION

Type I homodimeric reaction centers, particularly the class present in *Heliobacteriaceae*, are among the most poorly understood of all photosynthetic complexes. Three-dimensional X-ray crystal structures exist at atomic resolution for the purple non-sulfur bacterial reaction center (*1, 2*) and for cyanobacterial PS I (*3*), and the protein backbone and cofactor arrangement is known from near-atomic resolution X-ray data for higher plant PS I (*4*) and cyanobacterial PS II (*5-7*). In contrast, the number and identities of electron transfer cofactors as well as the number and identities of polypeptides that constitute the HbRC remain obscure.

What is known with certainty concerns the early light-induced reactions. The primary electron donor, P798, is a dimer of Bchl *g*' (the 13^2 epimer that now appears to be a common feature of all Type I RCs) and the cation is delocalized over both molecules (*8, 9*). The primary acceptor is Chl *a* 670, an 8^1-hydroxy Chl *a* molecule. Charge separation between P798 and A_0 occurs within 25 ps after a flash, but this may represent energy transfer from the thermally populated antenna; the actual time of charge separation is estimated to be within 1 or 2 ps (*10, 11*). Forward electron transfer from A_0^- occurs in 600 ps at room temperature and if blocked, charge recombination between $P798^+$ and A_0^- occurs in 17 ns, repopulating the triplet state of P798.

In contrast, less is known about the intermediate and tertiary electron acceptors. Membranes contain large quantities of menaquinone-9 (as well as some menaquinone–8 and menaquinone–10), but isolated HbRCs have been reported to contain as little as one molecule or less (*12*). EPR (*13*) and ENDOR (*14*) studies show a photoaccumulated signal consistent with a semiquinone radical, but optical kinetic and photovoltage experiments (*15*) have failed to confirm a functional quinone intermediate. A broad and featureless optical difference spectrum in urea-treated membranes of *Heliobacillus mobilis* provides the only evidence for an F_X-like Fe/S cluster (*16*), the existence of which is nevertheless implied by a conserved FPCxGPxxGGTC motif on the PshA reaction center polypeptide (*17*). However, the presence of F_X could not be confirmed by EPR spectroscopy in membranes of *Heliobacterium chlorum*, in spite of the fact that a well-defined set of resonances show the presence of F_A- and F_B-like Fe/S clusters (*18*).

In the last chapter, I described a series of systematic experiments aimed at re-examining the issue of the participation of Fe/S clusters in the photosynthetic reaction center of *Heliobacterium modesticaldum (Hm*), a thermophile that grows in hot springs and volcanic soils (*19*). I showed that the intact photosynthetic reaction center of *Hm* (HbRC) could be isolated from membranes using *n*-dodecyl-_-D-maltopyranoside and partially purified on a sucrose density gradient (*20*). The low-temperature EPR spectrum of a sample that was illuminated at 20 K exhibits a rhombic spectrum, with *g*-values of 2.067, 1.933 and 1.890, which is attributed to a single $[4Fe\text{-}4S]^{1+}$ cluster. The EPR spectrum of a sample that was continuously illuminated during freezing is more complex and exhibits multiple resonances spanning *g*-values from 2.04 to 1.90; these features were assigned to two $[4Fe\text{-}4S]^{1+}$ clusters that are dipolarly coupled. The low molecular mass protein containing the Fe/S clusters, which was termed PshB, could be dissociated from the HbRC by washing with 1.0 M NaCl and removed by ultrafiltration over a 30-kDa cut-off membrane. The resulting HbRC core, which was further purified by ion exchange chromatography, could rebind PshB, resulting in the recovery of light-induced EPR signals of the F_A- and F_B-like Fe/S clusters (*20*).

The isolation of an intact, functional HbRC core provided an opportunity to study the electron acceptor that immediately precedes F_A and F_B. The flash-induced kinetics of the intact HbRC complex show two kinetic phases at room temperature, one with a lifetime of ca. 75 ms and the other with a lifetime of ca. 15 ms. The 75-ms component is lost when PshB is removed from the HbRC complex, and it is regained when PshB is rebound to HbRC cores (*20*). Thus, the 15-ms kinetic phase is derived from recombination of $P798^+$ with an earlier acceptor that remained unidentified, but which was proposed to be F_X. However, I was unable to measure an EPR spectrum of an Fe/S cluster after photoaccumulation of HbRC cores in the presence of sodium dithionite at pH 10.0 (see also (*16*). These conditions should have allowed me to detect F_X. I suggested that this could be because the F_X cluster has exceedingly rapid relaxation properties or an unusual ground spin state; both would make detection by EPR difficult. The work presented here is directed toward obtaining unequivocal EPR and Mössbauer evidence for the presence of F_X in HbRC cores.

3.3 MATERIALS AND METHODS

3.3.1 *Isolation of HbRC Cores*

Cultures of *Heliobacterium modesticaldum* were generously provided by Dr. Michael Madigan (Southern Illinois University). Liquid cultures of *Hm* were grown anaerobically in PYE media as described in (*19*) except that 50 µmoles of $^{57}FeSO_4$ was added to the growth medium. Resazurin, an oxygen reporter dye, was also added to a final concentration of 0.001%. All manipulations were performed anaerobically. Plasticware and glassware were placed in the anaerobic chamber three hours prior to use and tested with a resazurin solution to verify that any residual oxygen had been removed. Cells grown to late-exponential phase were harvested at 10,000 x *g* and resuspended in 50 mM MOPS buffer, pH 7. Whole cells were lysed by sonication, and membranes were pelleted by centrifugation at 200,000 x *g*. Membranes were solubilized with 1% *n*-dodecyl-_-D-maltopyranoside for one hour, and intact membranes were removed by centrifugation at 200,000 x *g*. Solubilized membranes were passed over a diethylaminoethyl cellulose ion-exchange column equilibrated in 50 mM MOPS, pH 7.0. The flowthrough contained the HbRC cores, which were concentrated by ultrafiltration to 15 mM Bchl *g* (1200 OD at 788 nm) and divided into three aliquots: one was diluted 1500-fold and used for time-resolved optical studies, and the other two were used without dilution for EPR studies and Mössbauer studies. The identical sample of ^{57}Fe-containing HbRC cores was therefore used for all of the spectroscopic studies described in this paper.

3.3.2 *Bacteriochlorophyll and Iron Analyses*

Bacteriochlorophyll *g* was measured in acetone using a previously published molar extinction coefficient (*21*). A 10-µl aliquot of HbRC cores was added to 990 µL of acetone, the sample was vortexed and spun at 10,000 x *g*, and the optical density of the supernatant was measured at 762 nm. Non-heme iron was measured according to a previously described protocol (*22*) with minor modifications. A 300-µL aliquot of HbRC cores was added to 300 µL of reagent A (4.5% sodium dodecyl sulfate, 1.5% saturated solution of sodium acetate) and 300 µl of reagent B (273 mM ascorbic acid, 8.45 mM

sodium meta-bisulfate, 6.6% saturated solution of sodium acetate), the mixture was incubated at 37 °C for 15 minutes. A total of 15 μL of reagent C (36 mM of 3-(2-pyridyl)-5,6-di(2-furyl)-1,2,4-triazine-5',5'-disulfonic acid, sodium salt, also known as ferene) was added and the optical density was measured at 593 nm. A control was prepared without adding reagent C, and the optical density was measured similarly. The difference between the sample and control represented the optical density from the iron-ferene complex. The standard curve was constructed from a freshly prepared solution of $Fe^{II}(NH_4)_2(SO_4)_2 \bullet 6H_2O$.

3.3.3 *Time Resolved Optical Spectroscopy.*

The kinetics of reduction of the primary electron donor were measured by monitoring the flash-induced absorbance change at 798 nm. The sample was placed in a 1 cm x 1 cm quartz cuvette. Actinic illumination was provided by a Nd-YAG laser (Quanta-Ray DCR-11, Spectra-Physics, Mountain View, CA) operated in the second harmonic (= 532 nm) with a 7-ns duration and an energy of ~ 2 mJ/cm^2. The measuring beam was derived from a 400-W tungsten-halogen lamp (Model 66057, Oriel Corp, Stratford, CT). Light from the lamp was passed sequentially through a _ meter monochromator (Model 82-410, Jarrell-Ash. Co, Waltham, MS) and a shutter (Uniblitz Model T132, Vincent Associates, Rochester, NY). The beam was monitored using a biased Si photodiode (PIN10D, UDT Sensors, Inc., Hawthorne, CA) shielded from stray light by a narrow-band interference filter centered at 800 nm (Corion). The shutter was opened 20 ms before the onset of the laser flash. The signal from the photodiode was amplified with a AM502 differential amplifier (Tektronix, Beaverton, OR), digitized with a DSA601 digital oscilloscope (Tektronix, Beaverton, OR), and processed on a Power Macintosh computer (Model 9500, Apple Computer, Cupertino, CA) that was interfaced to the digitizer via an IEEE-488 bus (PCI-GPIB, National Instruments, Austin, TX). The electronic bandwidth of the detection system was 1 MHz. Typically 8 to 10 transients were averaged. Kinetic traces were analyzed by fitting the multi-exponential decay using the Marquardt least-squares algorithm program in Igor Pro (Wavemetrics, Lake Oswego, OR). The samples were suspended in 50 mM MOPS (pH 7.0) to 0.8 OD at 788 nm.

3.3.4 *EPR Spectroscopy*

Low-temperature EPR spectroscopy was performed using an ECS-106 X-band spectrometer (Bruker Biospin, Billerica, MS) equipped with an ESR900 liquid helium cryostat and an ITC-4 temperature controller (Oxford Instruments, Billerica, MS). The HbRC cores were loaded into the EPR sample tubes along with 33 mM sodium dithionite, and 100 mM glycine, pH 10.0. The samples were photoaccumulated by fitting the EPR tube with a vacuum adaptor and illuminating the sample with a 3-Watt Series 2000 argon ion laser (Spectra Physics, Mountain View, CA) in an outboard glass dewar under conditions that allowed the sample to be frozen slowly to 77 K. A 3X beam expander ensured a uniform illumination of the sample tube during freezing.

Values for the zero-field splitting parameter D were estimated using a previously described protocol (*23*). The populations of the two Kramers doublets of the $S = 3/2$ ground state were estimated at g-values of 4.4 and 5.4. A plot of the natural logarithm of the ratio of the peak intensities vs. the inverse of the absolute temperature is fit to a straight line, the slope of which yields the energy separation, Δ, of the two Kramers doublets of the $S = 3/2$ ground state.

3.3.5 *Mössbauer Spectroscopy*

Mössbauer spectra were recorded on spectrometers from WEB Research (Edina, MN) operating in the constant acceleration mode in transmission geometry. Spectra were recorded with the temperature of the sample at 4.2 K maintained by a liquid helium cryostat. For low-field spectra, the sample was kept inside a SVT-400 dewar (Janis, Wilmington, MA) and a magnetic field of 40 mT was applied parallel to the γ-beam. For high-field spectra, the sample was kept inside a 12SVT dewar (Janis, Wilmington, MA), which houses a superconducting magnet that allows for application of variable fields between 0 and 8 T parallel to the γ-beam. The isomer shifts quoted are relative to the centroid of the spectrum of a metallic foil of Fe at room temperature. Data analysis was performed using the program WMOSS from WEB Research (Edina, MN). Some of the simulations are based on the spin Hamiltonian formalism, given by the following equation, in which the first term describes the electron Zeeman effect, the second term represents the interaction between the electric field gradient with the nuclear quadrupole

moment, the third term describes the magnetic hyperfine interactions of the electronic spin with the ^{57}Fe nuclei, and the last term represents the nuclear Zeeman interaction. Simulations for both spectroscopically distinct sites (diferrous pair and mixed-valent pair) of the [4Fe-4S]$^{+}$ cluster were carried out with respect to the electronic spin of the ground state, $S = 3/2$.

$$\mathbf{H} = \beta \mathbf{S} \bullet \mathbf{g} \bullet \mathbf{B} + \sum_{\mathbf{i}=1}^{2} \frac{\mathbf{eQV}_{\mathbf{zz,i}}}{4} \left[\mathbf{I}_{\mathbf{z,i}}^{2} - \frac{I_i(I_i+1)}{3} + \frac{\eta}{3}\left(\mathbf{I}_{\mathbf{x,i}}^{2} - \mathbf{I}_{\mathbf{y,i}}^{2}\right) \right] + \sum_{\mathbf{i}=1}^{2} \mathbf{S} \bullet \mathbf{A}_{\mathbf{i}} \bullet \mathbf{I}_{\mathbf{i}} - \sum_{\mathbf{i}=1}^{2} g_n \beta_{\mathbf{n}} \mathbf{B} \bullet \mathbf{I}_{\mathbf{i}}$$

3.4 RESULTS

3.4.1 *The Reduction of Acceptor 'X' in HbRC Cores by Photoaccumulation*

HbRC cores were prepared by stripping PshB from HbRC complexes with 1 M KCl followed by ion-exchange chromatography (*20*). As shown in Figure 3.1 (top), the flash-induced absorption change at 798 nm in the resulting HbRC core decays monotonically with a lifetime of 16-ms. The absence of the ca. 75-ms decay component indicates that the PshB protein, which contains the F_A and F_B clusters, has been removed within limits of detection. I tentatively denote the electron acceptor responsible for the 16-ms kinetic transient in purified HbRC cores as component 'X'. Prolonged exposure to air does not alter the amplitude or kinetics of the flash-induced transient, indicating that unlike F_A and F_B, 'X' is stable to dioxygen. Because the addition of 2 mM sodium dithionite at pH 10.0 did not alter the amplitude or kinetics of the 16-ms component on a single turnover flash, 'X' cannot be reduced chemically. However, the application of successive laser flashes to the sample resulted in a progressive loss of amplitude of the 16-ms decay component such that 50% of the absorbance change was lost after 9 flashes, and 85% of the absorbance change was lost after 90 flashes (Figure 3.1b). A continuous beam of white light produced the same effect; as shown in Figure 3.1 (bottom), over 95% of the amplitude of the 15-ms decay component was lost after 1 min of illumination. The missing amplitude represents either rapid charge separation followed by recombination between P798 and an electron acceptor that precedes 'X' or it represents a damaged HbRC core. When the pH was lowered to 7.0 by addition of aerobic buffer, the 16-ms phase returned (data not shown), indicating that 'X' is reduced rather than damaged. Under both illumination protocols, a kinetic transient with a lifetime of 23 μs becomes visible (Figure 3.1, bottom), the magnitude of which does not depend on the loss of amplitude of the 16-ms decay phase. Because its amplitude is a function of the laser flash intensity (data not shown), this component is tentatively assigned to the decay of an antenna chlorophyll triplet.

3.4.2 *As-Isolated HbRC Cores Contain a [4Fe-4S]$^{2+}$ Cluster*

To determine whether 'X' is an Fe/S cluster, as-isolated ^{57}Fe-enriched HbRC cores were studied by Mössbauer spectroscopy. The spectrum, which was recorded at 4.2 K in an externally applied 40-mT magnetic field oriented parallel to the γ-beam, is shown in Figure 3.2 (top) as hashed marks. It shows a sharp (linewidth, Γ_{left} = 0.25 mm/s and Γ_{right} = 0.29 mm/s) quadrupole doublet with parameters typical of [4Fe-4S]$^{2+}$ clusters: isomer shift δ = 0.45 ± 0.02 mm/s and quadrupole splitting parameter ΔE_Q = 1.07 ± 0.02 mm/s (Figure 3.2, top, solid line). This quadrupole doublet accounts for 97±3 % of the total intensity of the spectrum. The spectrum of this sample recorded in an external 8-T magnetic field oriented parallel to the γ-beam is shown in Figure 3.2 (bottom). By using the Mössbauer parameters obtained from the 40-mT spectrum, it is possible to determine the effective magnetic field experienced by the ^{57}Fe nuclei to be 8 T, *i.e.,* the magnitude of the effective magnetic field equals that of the externally applied magnetic field. This means that the internal magnetic field is zero and that the Fe sites have a diamagnetic (S = 0) ground state. A simulation using the spin Hamiltonian formalism assuming diamagnetism, values of δ and ΔE_Q determined from the 40-mT spectrum, and the asymmetry parameter (η) = 0.4 ± 0.1 is shown as a solid line overlaid with the experimental data. Without exception, [4Fe-4S]$^{2+}$ clusters have a diamagnetic ground state, and consequently, the 8-T spectrum is in full conformity with the presence a [4Fe-4S]$^{2+}$ cluster in as-isolated HbRC cores. Other Fe species, such as different Fe/S cluster types or adventitiously bound Fe represent less than 3% of the total Fe contained in the sample.

3.4.3 *Cytochrome Content of HbRC Cores*

The Type I homodimeric reaction center from *Chlorobium limicola* contains a bound cytochrome c_{553} (*24*). Similar to other prokaryotic cytochromes, the axial ligands are a His and a Met. The related cytochrome c_{551} from *Pseudomonas aeruginosa*, which also has a His/Met-ligated heme, has in its low-spin ferrous form Mössbauer parameters, δ = 0.45 mm/s and ΔE_Q = 1.29 mm/s, which are almost identical to those observed for HbRC cores (see above) (*25*). Moreover, low-spin ferrous heme centers have a

diamagnetic ground state, and therefore the Mössbauer spectroscopic features associated with the HbRC do not rule out the presence of a His/Met-ligated low-spin ferrous heme. To resolve this issue, HbRC cores were studied using biophysical methods that are capable of detecting the presence of a heme-containing cofactor. The *c*-Type cytochrome found in the RC from *Chlorobium* has a midpoint potentials of approximately 150 mV, and can be oxidized to the EPR-active ferric form. Oxidized *P. aeruginosa* cytochrome c_{551}, for example, contains a low-spin ferric heme, which exhibits EPR resonances with *g*-values of 3.2 and 2.05 (*26*). HbRC complexes and HbRC cores that were oxidized with ammonium persulfate in the presence of air showed no evidence for either a high-spin or a low-spin cytochrome in either sample by EPR spectroscopy (data not shown). Heme cofactors display an intense feature in the visible region; the so-called Soret band has a maximum located in the 550 nm to 555 nm range for *c*-type cytochromes (*27*), a region in which BChl *g* minimally absorbs. I failed to find any evidence for the presence of a *c*-type cytochrome in HbRC cores by optical spectroscopy. Heme proteins can be identified by staining with benzidine dyes (*28*). I separated the polypeptides in the HbRC cores by SDS-PAGE followed by staining with 3, 3', 5, 5'-tetramethylbenzidine and found no evidence for a *c*-type cytochrome. I conclude that a bound *c*-type cytochrome is absent in my preparations of HbRC cores from *Hm*. Thus, the Mössbauer spectra of as-isolated HbRC cores emanate from $[4Fe\text{-}4S]^{2+}$ clusters and not from a low-spin ferrous *c*-type cytochrome.

3.4.4 *Non-Heme Iron and Bacteriochlorophyll g Content of HbRC Cores*

Iron and BChl *g* concentrations were measured on six HbRC core samples ranging from 1.0 mM Bchl *g* to 15 mM Bchl *g*. Five identical samples were analyzed at each bacteriochlorophyll concentration. In a total of 30 samples, the ratio of BChl *g* / Fe was found to be 5.49 ± 0.27 (mean and standard deviation). The Mössbauer-spectroscopic results indicate that 97% of the Fe in as-isolated HbRC cores is in form of $[4Fe\text{-}4S]^{2+}$ clusters, which translates to a ratio of BChl *g* / $[4Fe\text{-}4S]^{2+}$ as 21.6 ± 1.1 (mean and standard deviation).

3.4.5 *Reduced 'X' is a [4Fe-4S]$^{1+}$ Cluster with an S = 3/2 Ground State*

Highly concentrated HbRC cores were subject to a similar photoaccumulation protocol (described in Materials and Methods) and examined by low-temperature EPR spectroscopy. As shown in Figure 3.3 (top), resonances from F_A and F_B are present around 3500 G in membranes and solubilized membranes, but as expected, they are missing in HbRC cores. In all three samples, a broad, intense signal is present between 1200 and 2000 G. At 4.2 K, the low-field resonance shows two distinctive features: a peak at g = 5.4 and a shoulder at g = 4.4 (Figure 3.3, bottom). As the temperature is increased to 12 K, the g = 5.4 peak decreases in intensity, while the g = 4.4 shoulder increases in intensity. These resonances can be assigned to a [4Fe-4S]$^{1+}$ cluster with a ground spin state of S = 3/2. The temperature dependence suggests that the g = 5.4 signal emanates from the ground Kramers doublet, whereas the g = 4.4 feature is associated with the excited Kramers doublet of the S = 3/2 spin manifold. The energy difference, Δ, between the two Kramers doublets from the relative intensity of the two signals is approximately 3 cm^{-1} +/- 0.7 (Figure 3.3b). Because □ is related to the zero-field splitting parameters D and E/D (Equation 1), we estimate $|D|$ □ 1.5 cm^{-1}.

The g-values of approximately 5.4 and 4.4 are expected for a S = 3/2 spin system exhibiting a rhombicity, E/D, of approximately 0.2 (see also Mössbauer studies below). Assuming D < 0, such a system exhibits g-values of 5.8, 1.3, and 1.0 for the ground doublet and 5.0, 2.7, and 1.8 for the excited doublet. The fact that g-values are not well resolved suggests significant heterogeneity of the sample, which could result in a distribution of E/D values and broadened spectra. Rhombograms are derived for the case D >> g□B. However, based on the temperature dependence of the signal, D is estimated to be small. The broadness of these EPR features could also be caused by mixing of the ZFS interaction and the Zeeman interaction. A simulation of the EPR spectrum based on diagonalization of the spin Hamiltonian matrix (*29-31*) and assuming discrete values of E/D = 0.2 and D = -1.5 cm^{-1} yields a spectrum similar to that predicted by g-values obtained from a rhombograms for D >> g□B (not shown). This suggests that the observed EPR features are not due to the small ZFS parameters, but rather result as a consequence of a distribution of ZFS parameters.

The feature in the g = 2 region is characteristic of a $[4Fe\text{-}4S]^{1+}$ cluster with a ground spin state of S = 1/2. One possibility is that this signal emanates from a small amount of PshB (containing reduced F_A and F_B) that has not been removed from the HbRC complex. In support of this proposal, the g-values of 2.04 and 1.90, as well as the spin relaxation properties, as inferred from the temperature dependence of the resonances (not shown), are similar to those of reduced F_A/F_B in HbRC complexes (*20*). A second possibility is that reduced 'X' may exist in different conformations with S = 3/2 and S = 1/2 ground states. In the case of the Fe protein of *Av* nitrogenase, the addition of 50% ethylene glycol favors the S = 1/2 ground state, whereas the addition of 0.4 M urea favors the S = 3/2 ground state (*32*). In HbRC cores, however, no alteration in the relative populations of the g = 5.4 / 4.4 and g = 1.94 resonances were found in HbRC cores after addition of ethylene glycol or urea. The origin of the $g \sim 2$ signals, therefore, remains unresolved, although the integrated intensity of the resonances corresponds to less than 2% of the amount of F_A and F_B present in intact HbRC complexes.

The identical sample of photoaccumulated HbRC cores was characterized further by Mössbauer spectroscopy (Figure 3.4). The 4.2-K/40-mT Mössbauer spectrum (left panel, top spectrum) exhibits, in addition to two sharp lines, a broad and featureless absorption extending from -1.5 mm/s to + 2.0 mm/s. Comparison of this spectrum to the 4.2-K/40-mT spectrum of as-isolated HbRC cores (solid line) reveals that the two sharp lines emanate from a non-reduced $[4Fe\text{-}4S]^{2+}$ cluster. Analysis of the spectrum reveals that 35 ± 5% of the total intensity is attributable to $[4Fe\text{-}4S]^{2+}$ clusters. (Unlike the optical studies depicted in Figure 1, the EPR and Mössbauer studies require much higher chlorophyll concentrations, which preclude quantitative photoreduction of the sample.) Removal of its spectral contribution results in the reference spectrum of reduced 'X' (Figure 3.4, bottom, left), which is broad and featureless. The broadening is caused by the magnetic hyperfine interactions between the electronic spin and the ^{57}Fe nuclei. Detection of magnetically split Mössbauer spectra in a small (40 mT) magnetic field is typical of Fe centers having a half-integer electron spin ground state and electronic fluctuation rates slower than the ^{57}Fe nuclear Larmor frequency. It is possible that the broad and featureless spectrum is a consequence of the intermediate relaxation regime, and recorded the spectrum of this sample at 2 K in a 40-mT magnetic field. Since this spectrum (data

not shown) is essentially identical to that recorded at 4.2 K, it can be concluded that the broad features are not a consequence of intermediate relaxation.

At higher temperatures and without applied magnetic field, the Mössbauer features of $[4Fe\text{-}4S]^{1+}$ clusters typically collapse into quadrupole doublets. The 100-K/zero-field spectrum of photoaccumulated HbRC cores, which is shown in Figure 3.4, (top right, as hashed marks), shows these collapsed quadrapole doublets. Plotted as a solid line is the 100-K/zero-field spectrum of as-isolated HbRC cores scaled to 35% of the total intensity. Removal of this contribution results in the 100-K/zero-field reference spectrum of reduced 'X' (Figure 3.4, bottom right). This spectrum exhibits a broad line at +0.14 mm/s and two sharp, well-resolved lines at +0.86 mm/s and +1.14 mm/s. Importantly, the latter two lines have similar intensity and width, suggesting the presence of two quadrupole doublets of equal intensity. The low-energy lines of the two quadrupole doublets overlap and give rise to the more intense peak at +0.14 mm/s. This spectrum has been analyzed with two symmetrical ($\Box_{left} = \Box_{right}$) quadrupole doublets of equal intensity and width. Two fits of equal quality are obtained, depending on how the four lines are paired. The first fit involves combining the inner lines to one quadrupole doublet and the outer lines to the other quadrupole doublet, yielding the following parameters: $\Box(1) = +0.54$ mm/s, $|\Box E_Q(1)| = 0.65$ mm/s, $\Box(2) = +0.60$ mm/s, and $|\Box E_Q(2)| = 1.08$ mm/s. For the second fit lines one and three are paired to the first quadrupole doublet, and lines two and four to the second quadrupole doublet: $\Box(1) = +0.46$ mm/s, $|\Box E_Q(1)| = 0.80$ mm/s, $\Box(2) = +0.68$ mm/s, and $|\Box E_Q(2)| = 0.93$ mm/s. This simulation is shown as a solid line in Figure 4.4, bottom right, and the individual contribution of the first (second) quadrupole doublet are shown as dashed (dotted) lines for clarity.

Of these two possibilities, the second is favored for the following reason. The fact that two at least partially resolved quadrupole doublets of equal intensity are observed suggests that the spectrum of the $[4Fe\text{-}4S]^{1+}$ cluster is comprised of two distinct pairs of Fe ions. The Mössbauer parameters of the first pair, $\Box(1) = +0.46$ mm/s and $|\Box E_Q(1)| = 0.80$ mm/s, are typical of a valence-delocalized $Fe^{2.5}$-$Fe^{2.5}$ unit. The other diiron pair then has to be a diferrous pair. The Mössbauer parameters of the second pair, $\Box(2) = +0.68$ mm/s, and $|\Box E_Q(2)| = 0.93$ mm/s, in particular the high isomer shift, support this assignment. For example, the isomer shifts of the Fe-sites of the all-ferrous $[4Fe\text{-}4S]^{0}$

cluster from *Av* Fe-protein is +0.68 mm/s (at 4.2 K) (*33*), in good agreement with the isomer shift for the quadrupole doublet assigned to the diferrous pair of the $[4Fe\text{-}4S]^{1+}$ cluster.

To further study the electronic structure of the $[4Fe\text{-}4S]^{1+}$ cluster, the 4.2-K/8-T Mössbauer spectrum of the photoaccumulated HbRC cores was recorded (Figure 3.4, top middle, hashed marks). Again, the 4.2-K/8-T spectrum of non-reduced 'X', scaled to 35% of the total intensity of the hashed marked spectrum, is overlaid as a solid line. Removal of this component yields the 4.2-K/8-T reference spectrum of reduced 'X' (Figure 3.4, bottom middle, hashed marks), which is broad and featureless. Importantly, the overall splitting of this spectrum is similar to that of the 4.2 K/40 mT spectrum (Figure 3.4, bottom left). The 4.2-K reference spectra can be simulated using the spin Hamiltonian formalism in the slow relaxation limit with an electronic spin of $S = 3/2$ with zero-field splitting (ZFS) parameters estimated from the analysis of the EPR spectra: $D = -1.5$ cm^{-1}, $E/D = 0.2$. Furthermore, the isomer shifts and quadrupole splitting parameters determined from the 100 K/zero-field spectrum were used. The **A**-tensors were assumed to be isotropic in order to reduce the number of variables. The solid lines overlaid with the reference spectra are simulations using the following parameters: $S = 3/2$, $D_{3/2} = -1.5$ cm^{-1}, $(E/D)_{3/2} = 0.2$, $g = 2.0$, $\delta(1) = +0.46$ mm/s, $|\Delta E_Q(1)| = 0.80$ mm/s, $\eta(1) = 0.8$, $A_{iso}(1)/g_N\beta_N = -8.6$ T, $\delta(2) = +0.68$ mm/s, and $|\Delta E_Q(2)| = 0.93$ mm/s, $\eta(2) = -10$, $A_{iso}(2)/g_N\beta_N = -2.9$ T. The individual components of the diferrous (site 2) and mixed-valent pair (site 1) are shown as dashed and dotted lines, respectively. These parameters are not uniquely determined due to the lack of spectral resolution and the large number of variables. For example, a fit in which the larger **A**-tensor component is associated with the mixed-valent sites ($A_{iso}(1)/g_N\beta_N = -3.9$ T) and the smaller **A**-tensor component is associated with the diferrous sites ($A_{iso}(2)/g_N\beta_N = -9.2$ T) results in simulations of similar quality and cannot be ruled out. However, the overall shape and splitting of the two 4.2-K reference spectra requires the **A**-tensor components to be approximately -8 T and -3 T. The **A**-tensors determined are those with respect to the total electronic spin of the ground state, $S = 3/2$. They are related to the intrinsic **a**-tensors of the i-th iron site, $\mathbf{a}_i$, by the following equation, in which c_{ij} is the vector coupling coefficient for the i-th Fe site and j-th spin state.

$$\mathbf{A}_{ij} = c_{ij} \cdot \mathbf{a}_i \quad (1)$$

Theoretical analysis of hyperfine coupling tensors in Fe/S clusters allowed Mouesca et al. (*34*) to estimate typical values for the intrinsic **a**-tensors of the mixed-valent pair and the diferrous pair of $[4Fe\text{-}4S]^{1+}$ clusters with either $S = 1/2$ or $S = 3/2$ ground states as $a/g_{N\_N} = -17.5$ T. Since the experimentally observed A/g_{N_N} values span an approximate range from -3T to -8T, the spin coupling coefficients of all four Fe sites are small and positive. By adopting a spin coupling scheme, in which the spin of the diferrous pair, $\mathbf{S}_{diferrous}$, is coupled to the spin of the mixed-valent pair, $\mathbf{S}_{mixed\text{-}valent}$, to yield the total spin, **S**, the spin projection coefficients for all 15 states with $S = 3/2$ ground state is calculated. Several of the states have spin coupling coefficients that are in accordance with the parameters deduced from the Mössbauer analysis. As can be seen from Table 1 (see Supplemental Material), there are $S = 3/2$ states that have positive spin coupling coefficients for *all four* Fe sites. Given that the spin coupling coefficients are calculated for pure spin states, *i.e.* without considering mixing with other spin states, and that the spin coupling coefficients cannot be determined accurately experimentally, it can be concluded that the Mössbauer spectroscopic results are fully consistent with the description of reduced 'X' as a $[4Fe\text{-}4S]^{1+}$ cluster with a $S = 3/2$ spin state.

3.5 DISCUSSION

3.5.1 *Assignment of the [4Fe-4S] Cluster in HbRC Cores as F_X*

F_X is defined as the interpolypeptide [4Fe-4S] cluster ligated to the PsaA/PsaB heterodimer of PS I of plants, algae and cyanobacteria, and to the PscA/PscA homodimer of the reaction center of green sulfur bacteria. It functions as the immediate electron donor to the F_A and F_B clusters, which are found in all Type I reaction centers (*20, 35*). Using a combination of biophysical techniques, I have studied *Hm* HbRC cores from which the PshB protein has been removed by treatment with 1 M KCl. Mössbauer spectroscopy reveals that 97±3% of the total Fe associated with HbRC cores is in form of $[4Fe\text{-}4S]^{2+}$ clusters. I have demonstrated by a combination of time-resolved optical, EPR, and Mössbauer spectroscopies that the [4Fe-4S] cluster in HbRC cores can be reduced by illumination of the sample in the presence of dithionite. The Fe/S cluster

stoichiometry can be deduced from the amino acid sequence of the PshA protein of the closely related organism *Heliobacillus mobilis*, which shows a conserved F_X binding motif (FPCxGPxxGGTC) that contains the two cysteines residues that coordinate the interpolypeptide [4Fe-4S] cluster (*17*). Because only one such F_X binding site exists per PshA dimer, one [4Fe-4S] cluster exists per reaction center. All known classes of Type I reaction centers, both heterodimeric and homodimeric, therefore contain an F_X interpolypeptide [4Fe-4S] cluster. It should be noted that this [4Fe-4S] cluster is likely to be the origin of the time-resolved optical difference spectrum around 430 nm reported by Kleinherenbrink et al. *(16)* in urea-treated reaction centers from *H. mobilis*.

3.5.2 *Reduced F_X in HbRC Cores has a S = 3/2 Ground Spin State*

In PS I of cyanobacteria and plants, and in the photosynthetic reaction center from *Chlorobium*, reduced F_X is a $[4Fe\text{-}4S]^{1+}$ cluster with a $S = 1/2$ ground spin state and is observed as a set of rhombic resonances around $g = 2$ (*35*). In contrast, reduced F_X of the HbRC from *Hm* has a $S = 3/2$ ground state at low temperature. The difficulty in observing resonances from $[4Fe\text{-}4S]^{1+}$ clusters with a $S = 3/2$ ground spin state is most likely the reason that F_X in heliobacteria had not been detected by EPR. $[4Fe\text{-}4S]^{+}$ clusters with $S = 3/2$ ground state typically exhibit temperature-dependent resonances in the range $g \approx 4$ to $g \approx 6$, which emanate from the two Kramers doublets of the $S = 3/2$ ground state (*23, 32, 36-38*). The value of $D \approx -1.5$ cm^{-1} for *Hm* F_X is similar to D-values of other $[4Fe\text{-}4S]^{+}$ clusters with $S = 3/2$ ground states, which range from $|D| \approx 0.7$ cm^{-1} to 4 cm^{-1} (*23, 32, 37, 38*). The Mössbauer-spectroscopic features of F_X in *Hm* are similar to those of the $[4Fe\text{-}4S]^{+}$ cluster observed in the urea-treated Fe-protein from *Av* nitrogenase (*32*). Both clusters exhibit magnetically split spectra at 4.2 K in external magnetic field. The splitting is comparably small in both weak (40-mT) and strong (8-T) external fields, suggesting that the spin projection factors are small and positive. At higher temperatures, the magnetically split spectra collapse into quadrupole doublets. For *Hm* F_X, two partially resolved quadrupole doublets of equal intensity, with parameters typical of a mixed-valence pair and a diferrous pair are observed. In contrast, the 50-K / zero-field spectrum of the *Av* Fe-protein yields one broad quadrupole doublet.

It has been found that $[4Fe\text{-}4S]^{+}$ clusters with $S = 3/2$ ground state may also exist in another conformation, which exhibits a $S = 1/2$ ground state. For example, the relative proportions of the $S = 1/2$ and $S = 3/2$ forms of *Av* Fe-protein depend on the solution properties. Addition of 50% ethylene glycol favors the $S = 1/2$ ground state, whereas the addition of 0.4 M urea favors the $S = 3/2$ ground state (*32*). Based on the X-ray structure of the *Av* Fe-protein, which shows that the [4Fe-4S] cluster is accessible to solvent (*39*), Johnson and co-workers suggested that the presence of either glycerol or urea may induce slightly different conformations of the $[4Fe\text{-}4S]^{+}$ cluster with different spin ground states (*23, 40*). The observation that addition of ethylene glycol or urea does not perturb the cluster may also indicate that F_X of HbRC is not solvent accessible. This is consistent with the finding that this [4Fe-4S] cluster is also stable to dioxygen.

3.5.3 *Antenna size of Bchl* g *in HbRC Complexes*

Because the iron present in HbRC cores is entirely within F_X, and because F_X has been shown to be a [4Fe-4S] cluster, the non-heme iron content can be used as a reliable metric for quantifying the number of antenna BChl *g* molecules associated with each reaction center. HbRC cores therefore contain 21.6 ± 1.1 BChl *g*/F_X. This value should be considered an upper limit; any denaturation of F_X in the course of sample isolation would lead to a higher rather than lower ratio of Bchl *g* / P798. In previous work, Nuijs et al. (*41*) assumed the *in vivo* extinction coefficients of Bchl *g* in the absorption maximum at 788 nm and that of the bleaching of P798 at 799 nm to be equivalent and estimated the antenna size in membrane fragments of *H. chlorum* to be 30 BChl *g* / P798. Kobayashi et al. (*42*) arrived at a Bchl *g* to Bchl *g'* ratio of 14.1 in reaction centers from *H. chlorum*. Assuming two Bchl *g'* per P798, this corresponds to 28.2 Bchl *g'* per P798. Kleinherenbrink et al. *(16)* assumed the extinction coefficients for the primary donor, P800, and the antenna BChl *g* are equal ($\Delta\_ = 100\ mM^{-1}\ cm^{-1}$), and estimated 24 BChl *g* / P800 in urea-treated reaction centers from *H. mobilis*. These values are in reasonable agreement with my value of 21.6 ± 1.1 BChl *g* / P798 in HbRC cores from *H. modesticaldum*. The consensus opinion, therefore, is that HbRC complexes have a small antenna complement, which is in contrast to 96 Chl *a*/P700 in cyanobacterial PS I *(3)*. A small antenna size is also consistent with my qualitative observation (*20*) that

considerably higher light intensities are required to reduce the Fe/S clusters in HbRC complexes than in cyanobacterial PS I.

3.6 SUMMARY

This study provides incontrovertible evidence for the presence of the interpolypeptide Fe/S cluster F_X in reaction centers of *Heliobacterium modesticaldum* By incubating HbRC cores with dithionite in the presence of the light, I found the 15-ms charge recombination phase is replaced with a kinetic transient in the sub-µs time domain. This change in kinetics is consistent with the reduction of an electron acceptor. HbRC cores treated in this manner show a broad and intense EPR signal at g = 5. This signal is characteristic of a $[4Fe\text{-}4S]^{1+,2+}$ cluster with a ground spin state of S = 3/2. The Mössbauer spectrum in the as-isolated HbRC core shows that all of the Fe is present in the form of a $[4Fe\text{-}4S]^{2+}$ cluster. After reduction with sodium dithionite in the presence of light, approximately 65% of the Fe appears in the form of a $[4Fe\text{-}4S]^{1+}$ cluster; the remainder is in the $[4Fe\text{-}4S]^{2+}$ state These results indicated that the EPR signal at g = 5 was in fact originating from a $[4Fe\text{-}4S]^{1+,2+}$ cluster with a ground spin state of S=3/2. The EPR spectrum does not show any contaminating ferric iron or any other reduced clusters. Overnight incubation of the HbRC cores with oxygen and APS also does not indicate that cytochromes are present and therefore all iron in the HbRC core sample originates from F_X. By assigning one [4Fe-4S]/P798, an antenna size of 21.6 ± 1.1 Bchl g molecules was estimated for the HbRC core.

3.7 LIST OF TABLES

Table 3.1. Spin coupling coefficients for $S = 3/2$ states with positive spin coupling coefficients for all four Fe sites of the $[4Fe\text{-}4S]^{+}$ cluster. The spin coupling coefficients were calculated using the following spin coupling scheme and methods, as described e.g. in "A. Bencini and D. Gatteschi, *EPR of Exchange Coupled Systems*, Springer Verlag, Berlin, 1990". The spin projection factor of the mixed-valent unit was calculated as the average of the spin projection factors of the ferrous and ferric sites (c_3 and c_4) that comprise this unit, according to e.g. G. Blondin and J. J. Girerd, Chem. Rev. (1990) *90*, 1359-1376.

$$\mathbf{S_1} + \mathbf{S_2} = \mathbf{S_{diferrous}}$$
$$\mathbf{S_3} + \mathbf{S_4} = \mathbf{S_{mixed\text{-}valent}}$$
$$\mathbf{S_{diferrous}} + \mathbf{S_{mixed\text{-}valent}} = \mathbf{S}$$
$$\mathbf{S_1} = \mathbf{S_2} = \mathbf{S_3} = 2,\ \mathbf{S_4} = 5/2$$

$\lvert S_{diferrous}, S_{mixed\text{-}valent}, S\rangle$	$c_{diferrous}$	$c_{mixed\text{-}valent}$	$A_{diferrous}/g_{N\_N}$ [T] [a]	$A_{mixed\text{-}valent}/g_{N\_N}$ [T]
$\lvert 1, 1/2, 3/2\rangle$	1/3	1/6	-5.8	-2.9
$\lvert 1, 3/2, 3/2\rangle$	2/15	11/30	-2.3	-6.4
$\lvert 2, 3/2, 3/2\rangle$	2/5	1/10	-7.0	-1.8
$\lvert 2, 5/2, 3/2\rangle$	1/15	13/30	-1.2	-7.6
$\lvert 3, 5/2, 3/2\rangle$	7/15	1/30	-8.2	-0.6

[a] calculated based on the intrinsic a-values for a diferrous (mixed-valent) pair of a $[4Fe\text{-}4S]^{+}$ cluster with $S = 3/2$ ground state: $a_{diferrous}/g_{N\_N} = a_{mixed\text{-}valent}/g_{N\_N} = -17.5$ T, as given by Mouesca et al., Inorg Chem. (1995), *34*, 4347-4359.

3.8 REFERENCES

(1) Deisenhofer, J., Epp, O., Sinning, I., and Michel, H. (1995) Crystallographic refinement at 2.3 Ångstrom resolution and refined model of the photosynthetic reaction centre from *Rhodopseudomonas viridis*. *J Mol Biol 246*, 429-457.

(2) Deisenhofer, J., Epp, O., Miki, K., Huber, R., and Michel, H. (1984) X-ray structure analysis of a membrane protein complex. Electron density map at 3 Å resolution and a model of the chromophores of the photosynthetic reaction center from *Rhodopseudomonas viridis*. *J Mol Biol 180*, 385-398.

(3) Jordan, P., Fromme, P., Witt, H. T., Klukas, O., Saenger, W., and Krauß, N. (2001) Three-dimensional structure of cyanobacterial photosystem I at 2.5 A resolution,*Nature 411,* 909-917.

(4) Ben-Shem, A., Frolow, F., and Nelson, N. (2003) Crystal structure of plant photosystem I. *Nature 426*, 630-635.

(5) Kamiya, N., and Shen, J. R. (2003) Crystal structure of oxygen-evolving photosystem II from *Thermosynechococcus vulcanus* at 3.7 Å resolution. *Proc Natl Acad Sci USA 100*, 98-103.

(6) Zouni, A., Witt, H. T., Kern, J., Fromme, P., Krauss, N., Saenger, W., and Orth, P. (2001) Crystal structure of photosystem II from *Synechococcus elongatus* at 3.8 Å resolution. *Nature 409*, 739-743.

(7) Ferreira, K. N., Iverson, T. M., Maghlaoui, K., Barber, J., and Iwata, S. (2004) Architecture of the photosynthetic oxygen-evolving center. *Science 303*, 1831-1838.

(8) Noguchi, T., Fukami, Y., Oh-Oka, H., and Inoue, Y. (1997) Fourier transform infrared study on the primary donor P798 of *Heliobacterium modesticaldum*: Cysteine S-H coupled to P798 and molecular interactions of carbonyl groups. *Biochemistry 36*, 12329-12336.

(9) Prince, R. C., Gest, H., and Blankenship, R. E. (1985) Thermodynamic properties of the photochemical reaction center of *Heliobacerium chlorum*. *FEBS Lett 182*, 345-349.

(10) Liebl, U., Lambry, J. C., Breton, J., Martin, J. L., and Vos, M. H. (1997) Spectral equilibration and primary photochemistry in *Heliobacillus mobilis* at cryogenic temperature. *Biochemistry 36*, 5912-5920.

(11) Lin, S., Chiou, H. C., Kleinherenbrink, F. A. M., and Blankenship, R. E. (1994) Time-resolved spectroscopy of energy and electron transfer processes in the photosynthetic bacterium *Heliobacillus mobilis*. *Biophys J 66*, 437-445.

(12) Trost, J. T., and Blankenship, R. E. (1989) Isolation of a photoactive photosynthetic reaction center-core antenna complex from *Heliobacillus mobilis*. *Biochemistry 28*, 9898-9904.

(13) Brok, M., Vasmel, H., Horikx, J. T. C., and Hoff, A. J. (1986) Electron transport components of *Heliobacterium chlorum* investigated by EPR spectroscopy at 9 and 34 GHz. *FEBS Lett 194*, 322-326.

(14) Muhiuddin, I. P., Rigby, S. E., Evans, M. C., Amesz, J., and Heathcote, P. (1999) ENDOR and special TRIPLE resonance spectroscopy of photoaccumulated semiquinone electron acceptors in the reaction centers of green sulfur bacteria and heliobacteria. *Biochemistry 38*, 7159-7167.

(15) Brettel, K., Leibl, W., and Liebl, U. (1998) Electron transfer in the heliobacterial reaction center: evidence against a quinone-type electron acceptor functioning analogous to A_1 in photosystem I. *Biochim Biophys Acta 1363*, 175-181.
(16) Kleinherenbrink, F. A., Chiou, H. C., LoBrutto, R., and Blankenship, R. E. (1994) Spectroscopic evidence for the presence of an iron-sulfur center similar to F_X of Photosystem I in *Heliobacillus mobilis*. *Photosynth Res 41*, 115-123.
(17) Liebl, U., Mockensturm-Wilson, M., Trost, J. T., Brune, D. C., Blankenship, R. E., and Vermaas, W. (1993) Single core polypeptide in the reaction center of the photosynthetic bacterium *Heliobacillus mobilis*: Structural implications and relations to other photosystems. *Proc Natl Acad Sci USA 90*, 7124-7128.
(18) Nitschke, W., Feiler, U., and Rutherford, A. W. (1990) Photosynthetic reaction center of green sulfur bacteria studied by EPR. *Biochemistry 29*, 3834-3842.
(19) Kimble, L. K., Mandelco, L., Woese, C. R., and Madigan, M. T. (1995) *Heliobacterium modesticaldum*, sp-Nov, a thermophilic heliobacterium of hot-springs and volcanic soils. *Arch Microbiol 163*, 259-267.
(20) Heinnickel, M., Shen, G., Agalarov, R., and Golbeck, J. H. (2005) Resolution and reconstitution of a bound Fe-S protein from the photosynthetic reaction center of *Heliobacterium modesticaldum*. *Biochemistry 44*, 9950-9960.
(21) Neerken, S., and Amesz, J. (2001) The antenna reaction center complex of heliobacteria: composition, energy conversion and electron transfer. *Biochim Biophys Acta 1507*, 278-290.
(22) Kennedy, M. C., Kent, T. A., Emptage, M., Merkle, H., Beinert, H., and Munck, E. (1984) Evidence for the formation of a linear [3Fe-4S] cluster in partially unfolded aconitase. *J Biol Chem 259*, 14463-14471.
(23) Duderstadt, R. E., Brereton, P. S., Adams, M. W., and Johnson, M. K. (1999) A pure S = 3/2 $[Fe_4S_4]^+$ cluster in the A33Y variant of *Pyrococcus furiosus* ferredoxin. *FEBS Lett 454*, 21-26.
(24) Albouy, D., Sturgis, J. N., Feiler, U., Nitschke, W., and Robert, B. (1997) Membrane-associated c-type cytochromes from the green sulfur bacterium *Chlorobium limicola forma thiosulfatophilum*: purification and characterization of cytochrome c_{553}. *Biochemistry 36*, 1927-1932.
(25) Debrunner, P. G. (1989) Mössbauer spectroscopy of iron porphyrins. *Physical Bioinorganic Chemistry Series 4*, 137-234.
(26) Dwivedi, A., Toscano Jr., W. A., and Debrunner, P. G. (1979) Mössbauer studies of cytochrome c_{551}. Intrinsic heterogeneity related to g-strain. *Biochim Biophys Acta 576*, 502-508.
(27) Blankenship, R. (2002) *Molecular Mechanisms of Photosynthesis*, Blackwell Science, Ltd, London.
(28) Holloway, P. J., Maclean, D. J., and Scott, K. J. (1987) Measurement of cytochrome *f* in thylakoids of higher plants using quantitative gel electrophoresis. *Anal Biochem 164*, 31-34.
(29) Glerup, J., and Weihe, H. (1991) Magnetic susceptibility and EPR spectra of m-cyano-bis[pentaamminechromium(III)] perchlorate. *Acta Chem. Scand. 45*, 444-448.

(30) Glerup, J., and Weihe, H. (1997) Magnetic susceptibility and EPR spectra of (m-hydroxo)bis[pentaamminechromium(III)] chloride monohydrate. *Inorg. Chem. 36*, 2816-2819.

(31) Jacobsen, C. J. H., Pedersen, E., Villadsen, J., and Weihe, H. (1993) ESR characterization of trans-diacidatotetrakis(pyridine)vanadium and -manganese trans-VII$(py)_4X_2$ and trans-MnII$(py)_4X_2$ (X = NCS, Cl, Br, I; py = pyridine). *Inorg. Chem. 32*, 1216-1221.

(32) Lindahl, P. A., Day, E. P., Kent, T. A., Orme-Johnson, W. H., and Munck, E. (1985) Mössbauer, EPR, and magnetization studies of the *Azotobacter vinelandii* Fe protein. Evidence for a $[4Fe\text{-}4S]^{1+}$ cluster with spin S = 3/2. *J Biol Chem 260*, 11160-11173.

(33) Yoo, S. J., Angove, H. C., Burgess, B. K., Hendrich, M. P., and Munck, E. (1999) Mossbauer and integer-spin EPR studies and spin-coupling analysis of the $[4Fe\text{-}4S]^0$ cluster of the Fe protein from *Azotobacter vinelandi*i nitrogenase. *J Amer Chem Soc 121*, 2534-2545.

(34) Mouesca, J.-M., Noodleman, L., Case, D. A., and Lamotte, B. (1995) Spin densities and spin coupling in iron-sulfur clusters: A new analysis of hyperfine coupling constants. *Inorg. Chem. 34*, 4347-4359.

(35) Vassiliev, I. R., Antonkine, M. L., and Golbeck, J. H. (2001) Iron-sulfur clusters in Type I reaction centers. *Biochim Biophys Acta 1507*, 139-160.

(36) Zambrano, I. C., Kowal, A. T., Mortenson, L. E., Adams, M. W., and Johnson, M. K. (1989) Magnetic circular dichroism and electron paramagnetic resonance studies of hydrogenases I and II from *Clostridium pasteurianum*. *J Biol Chem 264*, 20974-20983.

(37) Conover, R. C., Kowal, A. T., Fu, W. G., Park, J. B., Aono, S., Adams, M. W., and Johnson, M. K. (1990) Spectroscopic characterization of the novel iron-sulfur cluster in *Pyrococcus furiosus* ferredoxin. *J Biol Chem 265*, 8533-8541.

(38) Koehler, B. P., Mukund, S., Conover, R. C., Dhawan, I. K., Roy, R., Adams, M. W. W., and Johnson, M. K. (1996) Spectroscopic characterization of the tungsten and iron centers in aldehyde ferredoxin oxidoreductases from two hyperthermophilic archaea. *J Am Chem Soc 118*, 12391-12405.

(39) Georgiadis, M., Komiya, H., Chakrabarti, P., Woo, D., Kornuc, J., and Rees, D. (1992) Crystallographic structure of the nitrogenase iron protein from *Azotobacter vinelandii*. *Science 257*, 1653-1659.

(40) Duderstadt, R. E., Staples, C. R., Brereton, P. S., Adams, M. W., and Johnson, M. K. (1999) Effects of mutations in aspartate 14 on the spectroscopic properties of the $[Fe_3S_4]^{+,0}$ clusters in *Pyrococcus furiosus* ferredoxin. *Biochemistry 38*, 10585-10593.

(41) Nuijs, A. M., van Dorssen, R. J., Duysens, L. N. M., and Amesz, J. (1985) Excited states and primary photochemical reactions in the photosynthetic bacterium *Heliobacerium chlorum*. *Proc. Natl. Acad. Sci. USA 82*, 6865-6868.

(42) Kobayashi, M., van de Meent, E. J., Erkelens, C., Amesz, J., Ikegami, I and Watanage, T. (1991) Bacteriochlorophyll *g* epimer as a possible reaction center component of heliobacteria. *Biochim Biophys Acta 1057*, 89-96.

3.9 FIGURE LEGENDS

Figure 3.1 Flash induced absorption changes of $P798^+$ in HbRC cores in the presence of 1 mM ascorbate, 50 mM MOPS pH 7.0 (top) and 2 mM dithionite, 100 mM glycine pH 10.0 and illumination for 1 minute (bottom). Both samples had an optical transmittance at 788 nm of 0.80 OD. The plots depict an average of 16 traces acquired at 10 s intervals. Time is plotted on a logarithmic scale in which a deviation from the horizontal represents a kinetic phase. The computer-generated exponential fit is shown as a *solid line.* Results of the exponential fits are displayed as fit curves, where each individual component is plotted with vertical offset relative to the next component (with a longer lifetime) or the base line, the offset being equal to the amplitude of the latter component. The relative contributions of each kinetic phase can be judged by the intersection of the fit line with the *abscissa*. The residual of the fit is depicted above the main trace.

Figure 3.1b Time resolved optical decay of a bleaching at 798 nm. The sample was flashed 230 times. The "3 flash", "9 flash", and "30 flash" traces are the average of 3 flashes beginning at flash number 3, 6, and 9 respectively. The 90 and 210 flash are the average of 10 flashes beginning with flash number 90 and 210 respectively. The 12-ms phase clearly decreases as the flash number is increased.

Figure 3.2 Mössbauer spectra of ^{57}Fe-enriched HbRC cores recorded at 4.2 K in externally applied magnetic fields of 40 mT (top) and 8 T (bottom). The orientation of the magnetic field is parallel to the γ-beam. The experimental spectra are shown as hashed marks. The solid line overlaid with the 40-mT spectrum is a quadrupole doublet with the following parameters: δ = 0.45 mm/s, ΔE_Q = 1.07 mm/s, Γ_{left} = 0.25 mm/s, and Γ_{right} = 0.29 mm/s. The solid line overlaid with the 8-T spectrum is a spin Hamiltonian simulation, using the above values for δ and ΔE_Q, η = 0.4, and assuming diamagnetism.

Figure 3.3 (Top) EPR spectra of photoaccumulated membranes, solubilized membranes, and HbRC cores at a temperature of 4.2 K. The spectra represent four averages of 1000 total data points. (Bottom) EPR spectra of photoaccumulated HbRC cores measured at

temperatures from 4.2 K to 12 K. The spectra represent 10 averages of 8000 total data points. The effective *g*-values of the resonances are depicted. EPR conditions: microwave power, 126 mW; microwave frequency, 9.47 GHz; receiver gain, 2 x 10^4; modulation amplitude, 10 G at 100 kHz.

Figure 3.3b Plot of the natural logarithm of the ratio of the amplitudes at $g = 5.4$ and $g = 4.4$ vs the inverse of the absolute temperature. Peak intensities were determined as described in Materials and Methods of the manuscript. The slope of the line was used to determine the energy separation of the two Kramers doublets of the $S = 3/2$ state.

Figure 3.4 Mössbauer spectra of ^{57}Fe-enriched photoaccumulated HbRC cores recorded at 4.2 K in a 40-mT magnetic field (left panel), 4.2 K in an 8-T magnetic field (middle panel), and 100 K without applied field (right panel). The experimental spectra are shown on top as hashed marks. The solid lines are spectra of as-isolated HbRC cores recorded under the same experimental conditions and scaled to 35% of the intensity of the respective hashed-marked spectrum. Removal of the contribution of the $[4Fe\text{-}4S]^{2+}$ clusters of non-reduced HbRC results in the reference spectra of reduced 'X', the $[4Fe\text{-}4S]^{+}$ cluster with $S = 3/2$ ground spin state (hashed marked spectra on bottom of each panel). The solid lines overlaid with the reference spectra are simulations of the $[4Fe\text{-}4S]^{+}$ cluster described in the text. Individual contributions from the diferrous and mixed-valent site of the cluster are shown dotted and dashed, respectively. Simulations of the 4.2-K data were generated by using the spin Hamiltonian formalism in the slow relaxation limit with the following parameters: $S = 3/2$, $D_{3/2} = -1.5$ cm^{-1}, $(E/D)_{3/2} = 0.2$, $g = 2.0$, $\delta(1) = 0.46$ mm/s, $|\Delta E_Q(1)| = 0.80$ mm/s, $\eta(1) = 0.8$, $A_{iso}(1)/g_N\beta_N = -8.6$ T, $\delta(2) = 0.68$ mm/s, and $|\Delta E_Q(2)| = 0.93$ mm/s, $\eta(2) = -10$, $A_{iso}(2)/g_N\beta_N = -2.9$ T. The 100-K data was simulated with two quadrupole doublets with the following parameters: $\delta(1) = 0.46$ mm/s, $|\Delta E_Q(1)| = 0.80$ mm/s (dashed), $\delta(2) = 0.68$ mm/s, and $|\Delta E_Q(2)| = 0.93$ mm/s (dotted).

Figure 3.1

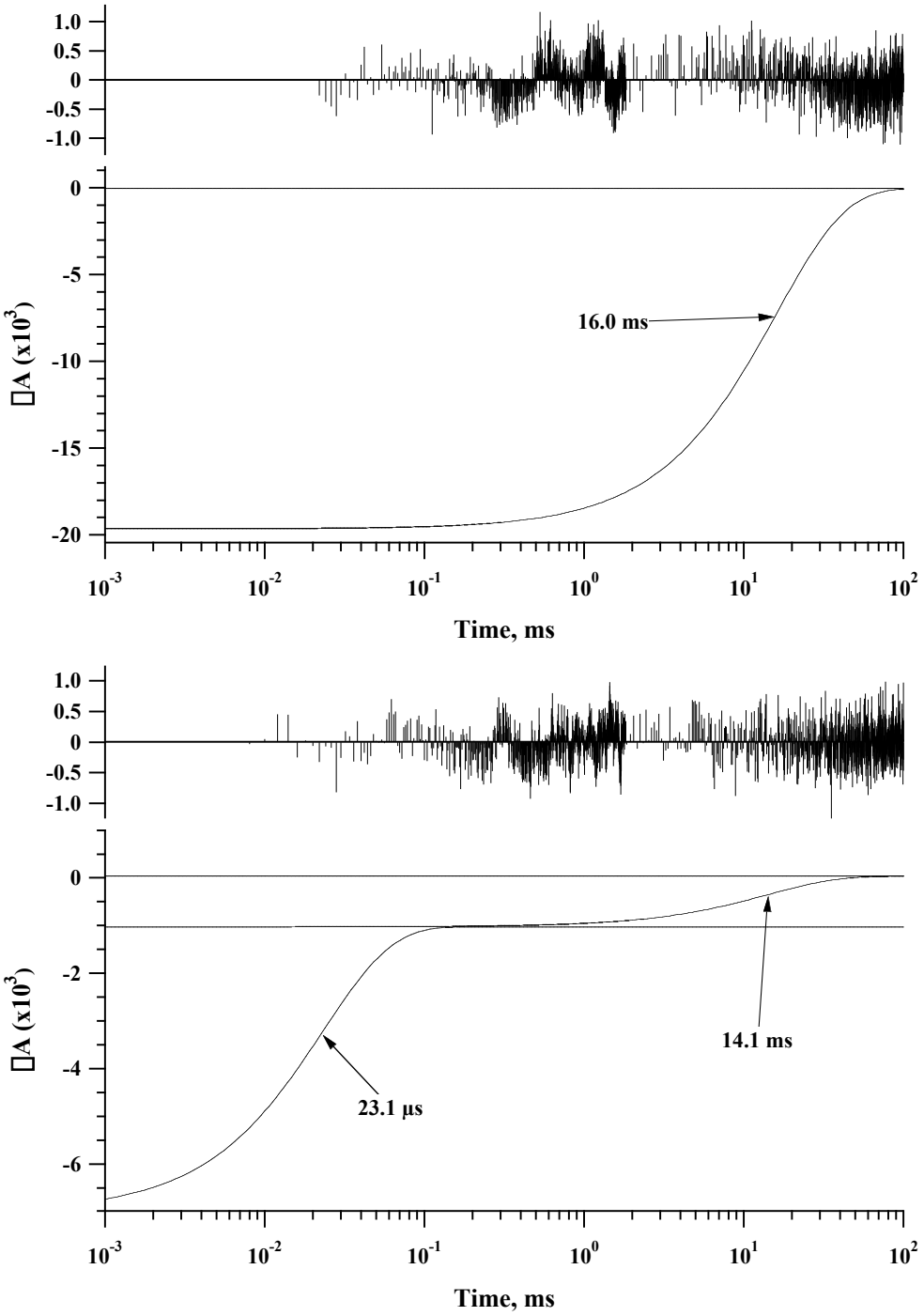
1.0
0.5
0
-0.5
-1.0
0
-5
-10
-15
-20
ΔA (x10^3)
16.0 ms
10^-3
10^-2
10^-1
10^0
10^1
10^2
Time, ms
1.0
0.5
0
-0.5
-1.0
0
-2
-4
-6
ΔA (x10^3)
14.1 ms
23.1 µs
10^-3
10^-2
10^-1
10^0
10^1
10^2
Time, ms

Figure 3.1b

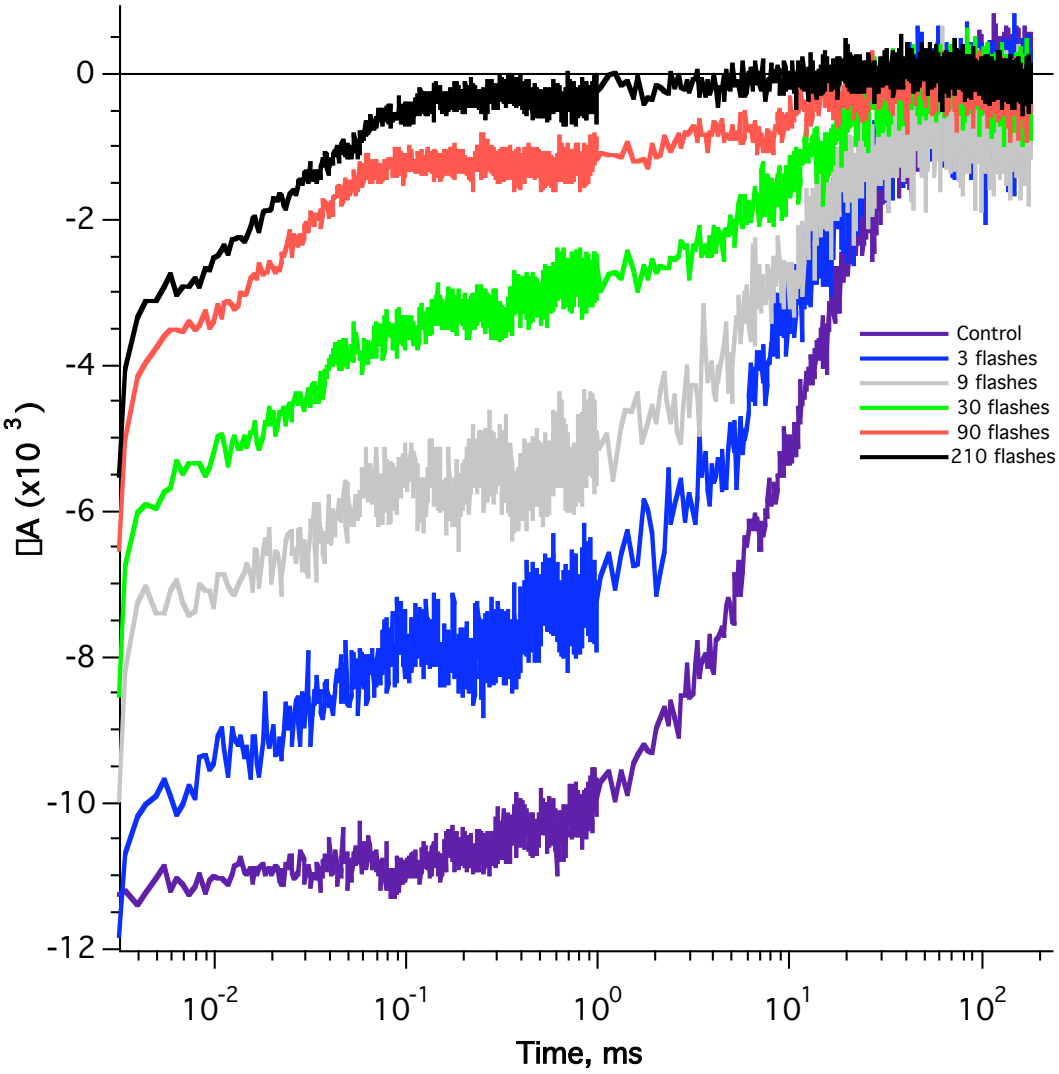
0
-2
-4
-6
-8
-10
-12
ΔA (x10 3)
10-2
10-1
100
101
102
Time, ms
Control
3 flashes
9 flashes
30 flashes
90 flashes
210 flashes

Figure 3.2

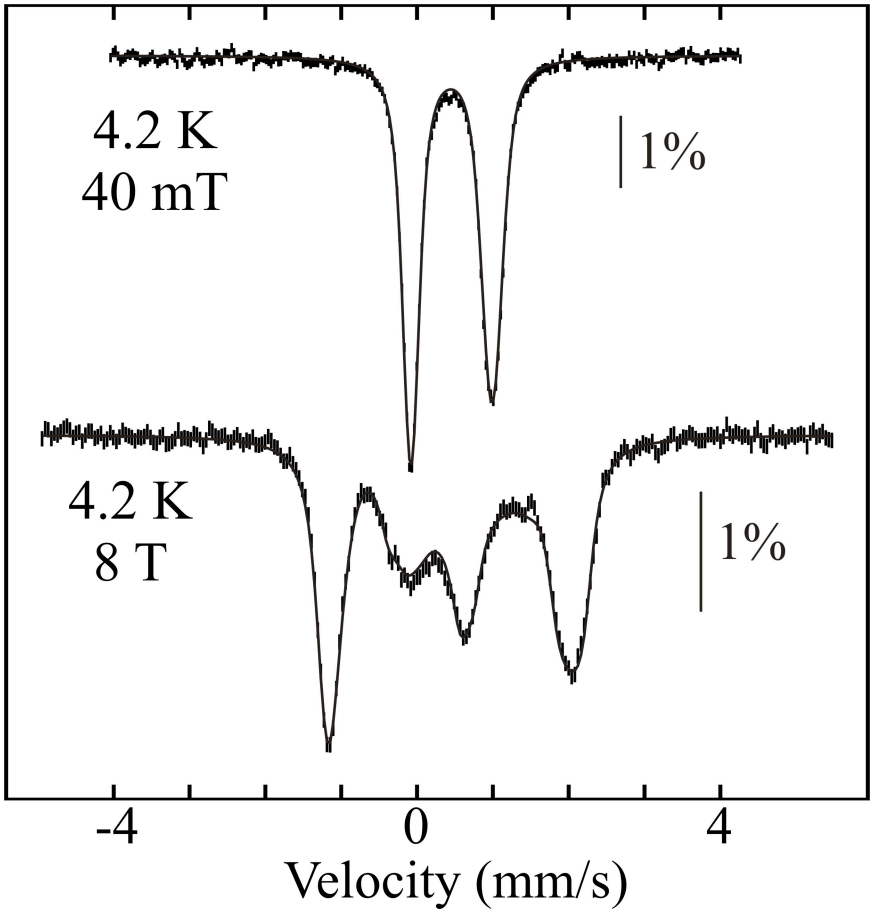

Figure 3.3

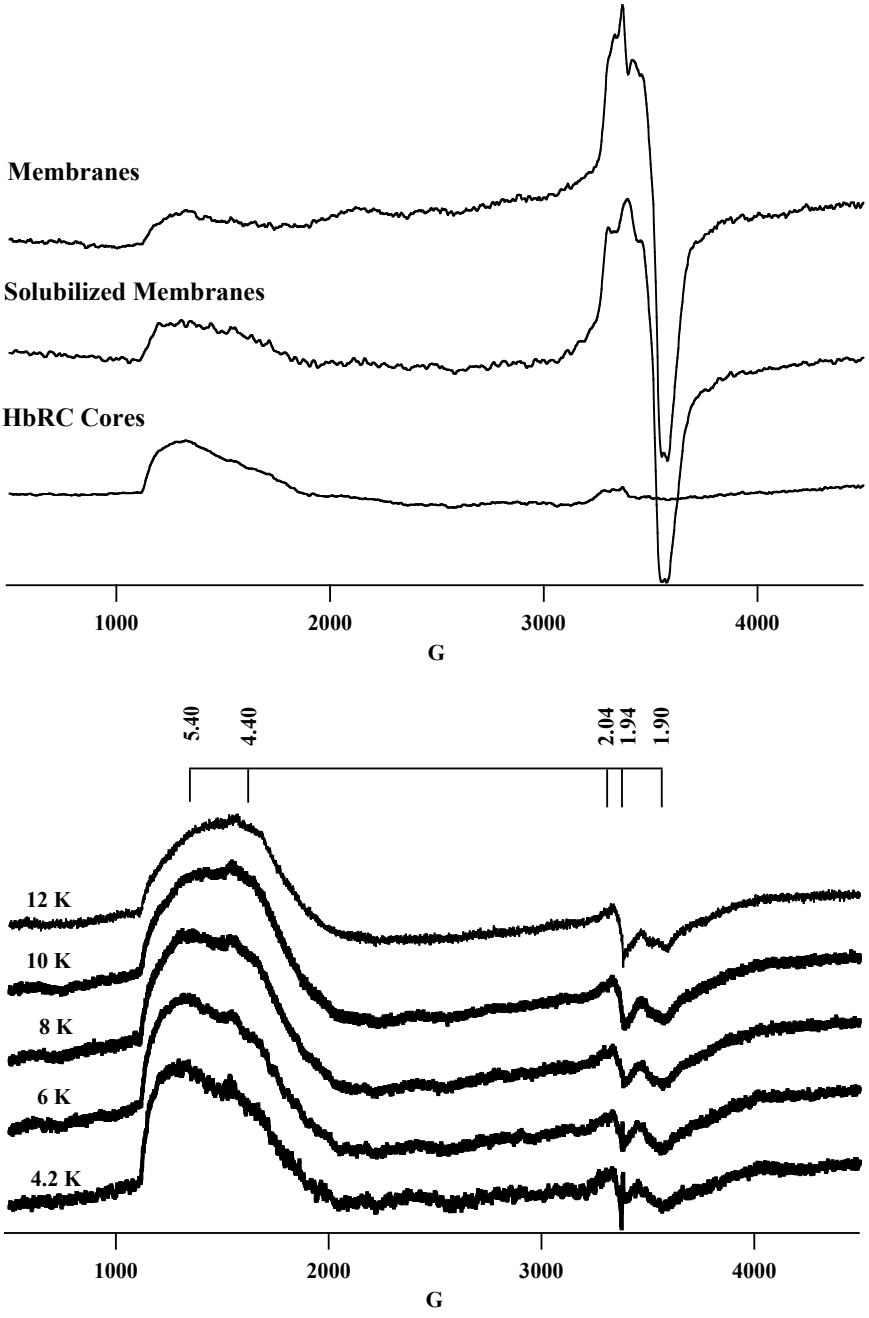
Membranes
Solubilized Membranes
HbRC Cores
1000
2000
3000
4000
G
5.40
4.40
2.04
1.94
1.90
12 K
10 K
8 K
6 K
4.2 K
1000
2000
3000
4000
G

Figure 3.3b

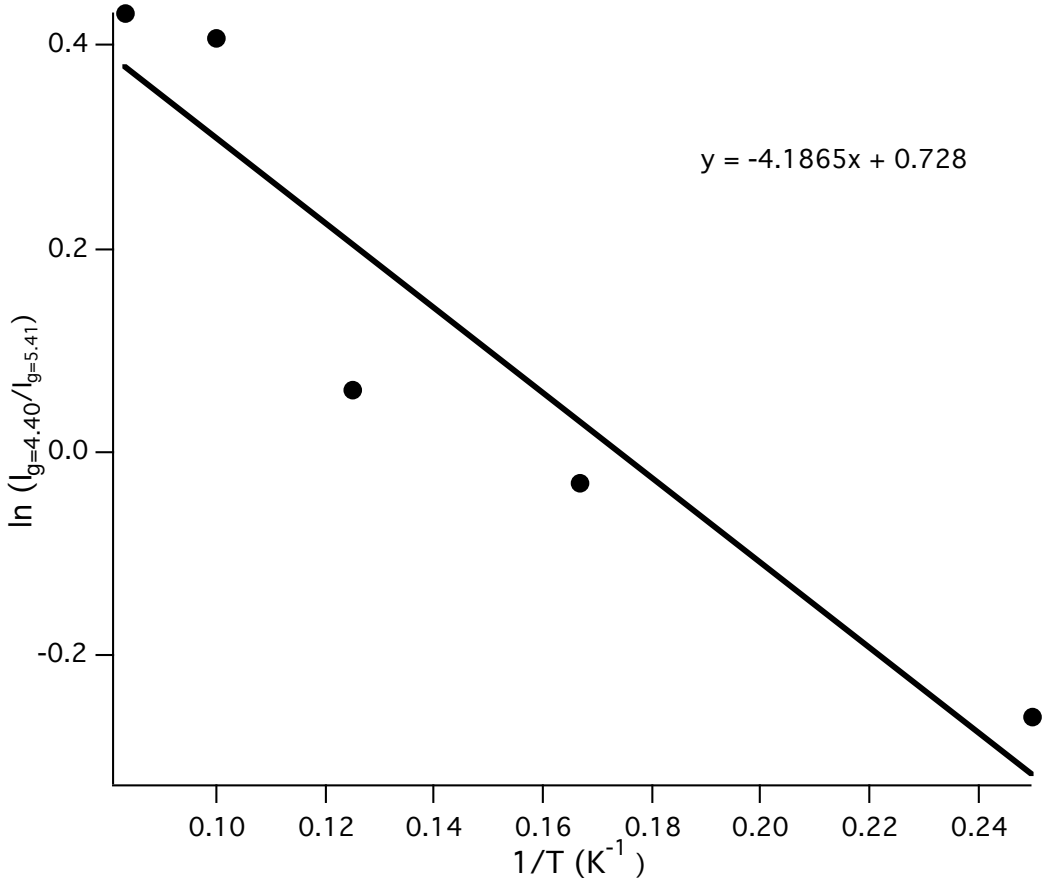
y = -4.1865x + 0.728
0.4
0.2
0.0
-0.2
ln (Ig=4.40/Ig=5.41)
0.10
0.12
0.14
0.16
0.18
0.20
0.22
0.24
1/T (K-1)

Figure 3.4

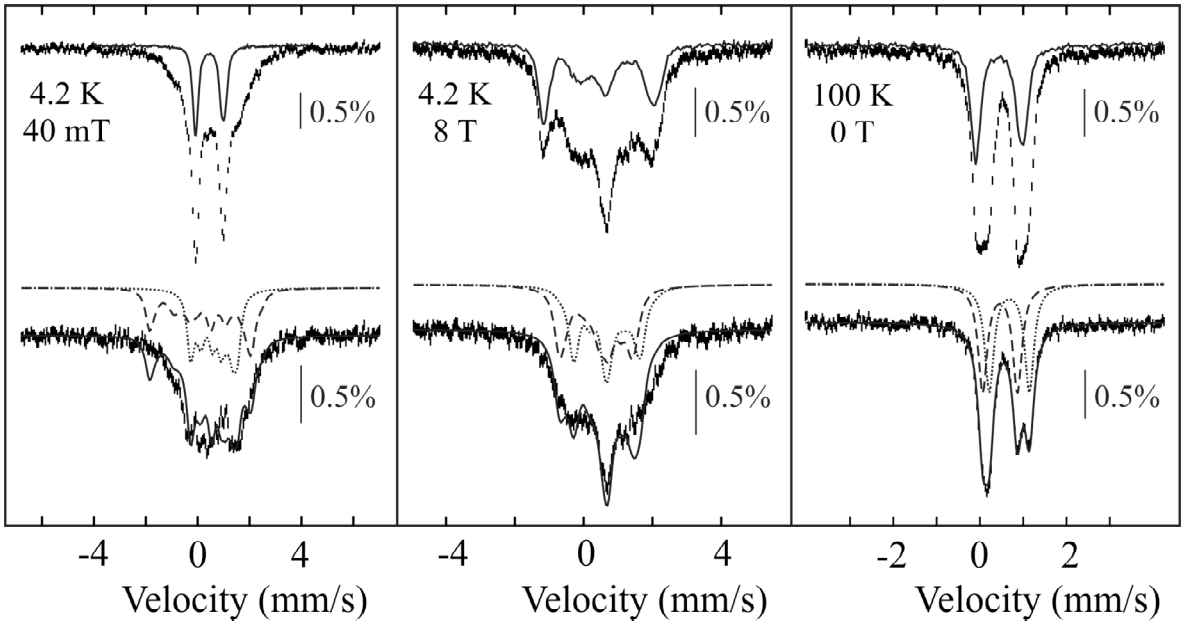
4.2 K
40 mT
0.5%
0.5%
4.2 K
8 T
0.5%
0.5%
100 K
0 T
0.5%
0.5%
-4
0
4
Velocity (mm/s)
-4
0
4
Velocity (mm/s)
-2
0
2
Velocity (mm/s)

Chapter 4

Identification and Characterization of PshB, the Dicluster Ferredoxin that Harbors the Terminal Electron Acceptors F_A and F_B in *Heliobacterium modesticaldum*

[Submitted in part as a paper entitled "Identification and Characterization of PshB, the Dicluster Ferredoxin that Harbors the Terminal Electron Acceptors F_A and F_B in *Heliobacterium modesticaldum*" by Mark Heinnickel, Gaozhong Shen, and, John H. Golbeck (2007) Biochemistry (in press)]

4.1 ABSTRACT

In chapter 2, I developed a method to remove and isolate the PshB protein that harbors the F_A and F_B iron-sulfur clusters from RCs of *Heliobacterium modesticaldum*. In this chapter, I report the cloning of a candidate gene and the properties of its product. Genuine PshB was dissociated from the reaction center with 1 M NaCl and purified using an affinity strategy. After acquiring its N-terminal amino acid sequence, an *fd2*-like gene encoding a 5.5-kDa dicluster ferredoxin was identified from the literature as a candidate for PshB. The Fd2-like apoprotein was expressed in *Escherichia coli* with a His tag, and the Fe/S clusters were inserted using inorganic reagents. The optical absorbance and EPR spectra of the Fd2-like holoprotein were similar to genuine PshB. The Fd2-like holoprotein was co-eluted with HbRC cores on both G-75 gel filtration and Ni affinity columns. Consistent with binding, the EPR resonances at g = 2.067, 1.933 and 1.890 from $[F_A/F_B]^-$ were restored after illumination at 15 K, and the long-lived, room temperature charge recombination kinetics between $P798^+$ and $[F_A/F_B]^-$ re-appeared on a laser flash. These characteristics indicate that the long-sought gene and polypeptide harboring the F_A- and F_B-like clusters in heliobacteria has been identified. The amino acid sequence of PshB indicates an entirely different mode of binding with the reaction center core than PsaC, its counterpart in Photosystem I.

4.2 INTRODUCTION

Photosynthetic RCs are membrane-bound, protein-pigment complexes that convert light energy into a stable charge-separated state. Two types occur in nature: Type I RCs have Fe/S clusters as the terminal electron acceptors, and Type II RCs have mobile quinones as the terminal electron acceptors. Type I RCs can be further subdivided into two groups: homodimeric RCs, which are found in anaerobic bacteria of the families *Chlorobiaecae* and *Heliobacteriaceae*, and PS I, heterodimeric RCs which are found in plants, algae, and cyanobacteria. Type II RCs can similarly be subdivided into two groups, the heterodimeric bacterial RC and PS II, a heterodimeric RC which is found in plants, algae, and cyanobacteria. X-ray crystal structures are available for the bacterial RC (*1*), PS II (*2-4*), and PS I (*5, 6*), but no high resolution structural information exists for Type I homodimeric RCs.

Heliobacteria are soil-dwelling phototrophs frequently found in rice fields (*7*). They are the only gram-positive photosynthetic bacteria (*8*) and the only spore-forming photosynthetic bacteria (*7*). They have a number of intriguing characteristics, including an entirely novel pigment, bacteriochlorophyll *g* (Bchl *g*), that gives the microorganism its characteristic brown color (*9*). However, little is known about the polypeptide composition of the HbRC apart from the fact that it consists of a homodimer of the PshA protein (*10*).

The PshA homodimer incorporates all of the antenna bacteriochlorophylls as well as the primary electron donor, P798, a Bchl *g´* homodimer (*11, 12*); the primary electron acceptor A_0, a 8^1-OH-chlorophyll a_F monomer[1] (*13*); and the interpolypeptide electron acceptor F_X (*10, 14*), a $[4Fe\text{-}4S]^{1+,2+}$ cluster with a ground spin state of S = 3/2 (*15*) (however, see also (*16*)). The PshA homodimer also contains up to two menaquinones, but their function remains unknown (*17-20*). To date, there is no convincing evidence for the participation of a quinone as a secondary electron acceptor in heliobacteria. The intact HbRC also contains a separate polypeptide, termed PshB (*21*), that harbors two $[4Fe\text{-}4S]^{1+,2+}$ clusters similar to F_A and F_B in PS I (*12, 21, 22*). However, there is no reliable data on the identity of the gene that encodes for PshB in heliobacteria. Further

[1] The subscript F refers to a farnesyl rather than phytyl tail, see ref. (13).

complicating the picture is a report that the major photosynthesis gene cluster in *Heliobacillus mobilis* does not include a gene that would code for a low molecular mass dicluster ferredoxin (*23*).

In Chapter 2, I showed that PshB can be removed from the reaction center complex of *Heliobacterium modesticaldum* with 1.0 M NaCl. The PshB-depleted reaction center was labeled 'P798-F_X' core. Upon removing PshB, the flash-induced kinetics accelerates from a ~75-ms lifetime to a ~15-ms lifetime, indicating that the former arises from the recombination of $P798^+$ with $[F_A/F_B]^-$. The latter was shown to arise from the recombination of $P798^+$ with F_X^- (*15*). I isolated PshB and succeeded in rebinding it to HbRC cores. The reconstituted HbRC was fully functional in terms of promoting light-induced electron transfer between P798 and F_A/F_B. In this chapter, I report the cloning and identification of a candidate gene for PshB from *H. modesticaldum* and the expression and properties of the recombinant PshB protein in *Escherichia coli.*

4.3 MATERIALS AND METHODS

4.3.1 *Isolation of Heliobacterial Reaction Centers*

A culture of *H. modesticaldum* was generously provided by Dr. Michael Madigan (Southern Illinois University). Liquid cultures of *H. modesticaldum* were grown anaerobically in PYE media as described in (*24*) except that resazurin, an oxygen reporter dye, was added to a final concentration of 0.001%. The medium was degassed and allowed to incubate in an anaerobic chamber with an atmosphere of 10% H_2 and 90% N_2 (Coy Labs, Grass Lake, MI) until the color of the resazurin indicated it was devoid of oxygen. The bottles were inoculated using the Hungate technique and the culture was allowed to grow under illumination for 48 hrs at 43°C. Banks of eight fluorescent bulbs provided white light illumination. All biochemical manipulations were performed anaerobically. Plasticware and glassware were placed in the anaerobic chamber three hours prior to use and were tested with resazurin to verify that any residual oxygen had been removed. Cells grown to late-exponential phase were harvested anaerobically at 10,000 x *g* and resuspended in 50 mM MOPS buffer, pH 7. Whole cells were lysed by sonication, and membranes were pelleted by centrifugation at 200,000 x *g*. Membranes

were solubilized with 1% *n*-dodecyl-_-D-maltopyranoside for one hour; insoluble fragments were removed by centrifugation at 200,000 x *g*. HbRC cores devoid of PshB were isolated by passing detergent-solubilized membranes over a diethylaminoethyl cellulose ion-exchange column equilibrated in 50 mM MOPS, pH 7.0.

4.3.2 *Purification of PshB, the Bound Fe/S Protein containing F_A and F_B*

Solubilized membranes were incubated with 1 M NaCl for one hour and ultrafiltered over a 30-kDa molecular mass cutoff membrane (PM 30, Millipore). The proteins that passed through the membrane were collected, and the filtrate was concentrated over a 3-kDa molecular mass cutoff membrane (YM-3, Millipore) and desalted on a PD-10 column (Amersham Biosciences). After purification, the PshB protein was resolved by SDS-PAGE and was blotted onto a PVDF membrane. N-terminal sequencing was carried out in the Macromolecular Core Facility of The Pennsylvania State University (Hershey, PA).

4.3.3 *Cloning of the* pshB *Gene*

Chromosomal DNA was isolated from *H. modesticaldum* using a previously published protocol (*25*). The DNA fragment containing the *pshB* gene was amplified using the chromosomal DNA of *H. modesticaldum* as template and PCR primers, which were designed based on a sequence comparison with the Fd2 protein from *H. mobilis* (*26*). The 5' DNA oligo was AACGGAGGTGAACATATGTATAAAATC with generation of a *Nde* I site, and the 3' primer was TGGTTAGGATCCATTAGGCTTTGATGGCGTC with generation of a *Bam*HI site. The PCR fragment was purified and cloned into a pET16b expression vector after digestion with *Nde*I and *Bam*HI. The cloned DNA fragment unintentionally contained the *fd1* and *fd2* genes encoding two different ferredoxins, which were verified by DNA sequencing. For expression of the second ferredoxin-like protein (Fd2), a DNA fragment was amplified from this plasmid using the primers 5' AGGCAGGTGAAAAGACATATGGCTTACAAA and 3' CAAAAAACCCCTCCAGACCCGTTTAGAGGCCCCAAGGGGTTATGCTAG. The

PCR fragment was cloned into a pET16b expression vector after digestion with *Bam*HI and *Nde*I and verified by DNA sequencing.

4.3.4 *Protein Expression and Purification*

The pET16bFd2 plasmid was transformed into BL21 (DE3) cells for expression. *E. coli* cells were grown in LB media to an $OD_{600\ nm}$ of 0.6, and IPTG was added to a final concentration of 200 M. After 6 hours of growth, cells were spun down at 10,000 x *g* and lysed using a French Press. Unlysed cells were removed by centrifugation at 10,000 x *g*. The sodium chloride concentration in the cell lysate was brought to 300 mM, and imidazole was added to a final concentration of 10 mM. The cell lysate was loaded onto NTA resin that was equilibrated in 300 mM NaCl, 10 mM imidazole, and 50 mM Tris (pH 8.3), the column was washed extensively with the same buffer, and, the apoprotein was eluted with 250 mM imidazole, 300 mM NaCl, and 50 mM Tris (pH 8.3).

4.3.5 *Reconstitution of the Fe/S Clusters*

The Fe/S apoprotein was incubated for 20 minutes with 100 mM _-mercaptoethanol in 50 mM Tris buffer (pH 8.3). Ferrous ammonium sulfate was added dropwise to a final concentration of 180 µM and the solution was allowed to incubate for 20 minutes. After the mixture turned brown, sodium sulfide was added dropwise to a final concentration of 180 µM and the solution was allowed to incubate overnight at 4°C. The reconstituted Fe/S protein was desalted and concentrated by ultrafiltration over a YM-3 membrane (*21*).

4.3.6 *Low Temperature X-band EPR Spectroscopy*

Low temperature EPR spectroscopy was performed using a Bruker ECS-106 X-band spectrometer equipped with an Oxford liquid helium cryostat and temperature controller. The recombinant protein was chemically reduced with 10 mM sodium hydrosulfite in 100 mM glycine at pH 10.0. A difference spectrum was constructed by subtracting the oxidized spectrum (no additions) from the chemically-reduced spectrum. HbRC complexes were illuminated with an argon-ion laser, which was operated at 2.5 W in all-lines mode. A 3-fold beam expander was used to fill the grid of the resonator. A

difference spectrum was constructed by subtracting the dark-adapted spectrum from the light-induced spectrum.

4.3.7 *Time Resolved Optical Spectroscopy in the near-IR*

The kinetics of $P798^+$ reduction were measured by monitoring the flash-induced absorbance change after a laser flash. The sample was probed with a continuous measuring beam at 798 nm isolated from a 400-W tungsten-halogen lamp with a 1/4 meter monochromator. A shutter admitted the measuring beam 10 ms prior to the laser flash. The measuring beam was monitored using a reverse-biased Si photodiode that was shielded from stray light with an 800 nm interference filter. The signal from the photodiode was amplified using a Tektronix AM502 differential amplifier and digitized using a DSA601 Tektronix digital oscilloscope. The data were sent to a Macintosh computer via an IEEE-488 bus (National Instruments). The electronic bandwidth of the detection system was 1 MHz. The sample was excited by an Nd-YAG laser operating in the second harmonic (λ = 532 nm) with a 7 ns pulse duration and an energy of ~ 2 mJ/cm^2. Typically 8 to 16 transients were recorded and averaged. Samples were placed in a quartz anaerobic cuvette with an optical path of 10 mm. The samples were in 50 mM MOPS pH 7.0 buffer at an absorbance of 1.0 OD at 788 nm. The kinetic traces were analyzed by fitting a multiexponential decay using the Marquardt least-squares algorithm (Igor Pro, Lake Oswego, OR).

4.4 RESULTS

4.4.1 *N-terminal Amino Acid Sequencing of Genuine PshB*

The PshB protein is weakly bound to HbRCs, and can be removed with 1.0 M NaCl followed by ultrafiltration over a 30-kDa cutoff membrane. To identify PshB unambiguously, an affinity technique was devised in which the ultrafiltrate was added to HbRC cores to reconstitute an HbRC complex. The rebinding of PshB was confirmed by the restoration of the flash-induced long-lived charge recombination kinetics between $P798^+$ and $[F_A/F_B]^-$. The HbRC complexes were separated from unbound PshB and other contaminating proteins by passage over a G-75 gel filtration column, and collected. The

HbRC complexes were then treated with 1% SDS and the polypeptides were resolved on a 15% SDS-PAGE gel and stained with silver. The polypeptide composition of the HbRC complexes includes a band at ~10 kDa which was not present in HbRC cores (Figure 4.1). The ~10 kDa polypeptide was blotted onto a PVDF membrane, and the N-terminal sequence was determined to be AYKITD.

4.4.2 *Cloning and Sequencing of the Gene Encoding a Dicluster Ferredoxin*

The N-terminal sequence of genuine PshB is similar to the N-terminal sequences of Fd2 and Fd1, ferredoxins that were previously isolated from *H. mobilis* (*26*). Fd1 is a 5513 Da polypeptide with the N-terminal sequence MAKYDASI and Fd2 is a 5575 Da polypeptide with the N-terminal sequence MAYKISD. Both contain two CxxCxxCxxxC binding motifs for two $[4Fe\text{-}4S]^{1+,2+}$ clusters. Table I shows a comparison of the products of the *fd1* and *fd2* genes from *H. mobilis* and the products of the *fd1*-like and *fd2*-like genes from the unpublished genome sequence of *H. modesticaldum* (R. Blankenship, personal communication). The N-terminal sequence of genuine PshB is a perfect match to the deduced amino acid sequence of the Fd2-like protein in *H. modesticaldum*. The *fd2*-like gene was cloned from *H. modesticaldum* and expressed with an N-terminal His tag.

4.4.3 *Comparison of Genuine PshB and the Expressed Fd2-like Protein*

The Fd2 apoprotein of *H. modesticaldum* was overproduced in *E. coli,* purified by Ni-chelation chromatography, and the iron-sulfur clusters were inserted using inorganic techniques. The optical absorbance spectra of PshB and the Fd2-like holoprotein were shown to be similar (Figure 4.2, right). Both have a broad absorbance maximum at 400 nm and a ratio of 280 nm to 400 nm of ~2.1 to 1, and both lose one-half of their absorbance in the visible after addition of sodium dithionite at pH 10 (data not shown). The low temperature EPR spectra of PshB and the Fd2 protein were also shown to be similar (Figure 4.2, left). Both show a complex ‘interaction spectrum’ after reduction with dithionite characteristic of bacterial dicluster ferredoxins that contain two closely-spaced $[4Fe\text{-}4S]^{1+,2+}$ clusters.

4.4.4 *Interaction of the Expressed Fd2-like Protein with HbRC cores*

If the recombinant Fd2 protein is equivalent to PshB, it should bind to HbRC cores. In the first experiment, the His-tagged recombinant Fd2 holoprotein was added to HbRC cores and the mixture was subject to chromatography on a G-75 gel filtration column. The eluate containing the brown-colored reaction center was collected and the polypeptide composition was analyzed by SDS-PAGE (Figure 4.3, lane 1). The band visible at ~55 kDa was previously shown to be PshA (*10, 27*). An additional band is present at ~10-kDa, indicating that the recombinant Fd2 protein binds to HbRC cores under the low ionic strength conditions of this experiment. (The mass of the Fd2-like protein with the added His tag is 7879 Da.) In the second experiment, the His-tagged recombinant Fd2 protein was first bound to a Ni-affinity column and then HbRC cores were loaded. The column was washed until the eluate was free of protein, imidazole was added to displace the bound Fd2 protein, and the polypeptide composition of the eluate was analyzed by SDS-PAGE (Figure 4.3, lane 2). The presence of a band at ~10-kDa as well as ~55 kDa indicates that HbRC cores bind the Fd2-like protein, thereby reconstituting the HbRC complex. It should be noted that HbRC cores alone are not retained on the Ni-affinity column.

4.4.5 *Time-Resolved Optical Kinetics of HbRC Cores with Expressed Fd2-like Protein*

To determine whether the reconstituted HbRC complex is functionally active at room temperature, the kinetics between $P798^+$ and $[F_A/F_B]^-$ were measured using time-resolved optical spectroscopy. Freshly-isolated HbRC complexes were shown previously to have biphasic kinetics; a ~15-ms kinetic phase originates from charge recombination between $P798^+$ and F_X, and a ~75 ms kinetic phase originates from charge recombination between $P798^+$ and $[F_A/F_B]^-$ (*21*). The ratio between the two kinetic phases is approximately 1:1 in both detergent-solubilized membranes and freshly isolated HbRC complexes (*21*). The HbRC cores used in the reconstitution studies (Figure 4.4, top) show mono-exponential charge recombination of ~15 ms, indicating that PshB has been completely removed by anion exchange chromatography. When genuine PshB is added to the HbRC cores in 25-fold molar excess, a long-lived kinetic phase with a lifetime of 96 ms appears, corresponding to 56% of the total amplitude (Figure 4.4, middle). When the

Fd2 protein is added to the HbRC cores in 50-fold molar excess, a long-lived kinetic phase with a lifetime of ~114 ms appears, corresponding to 52% of the total amplitude (Figure 4.4, bottom). This percentage can be raised to ~85% by adding a 150-fold molar excess of the Fd2 protein; however, when the mixture is subjected to gel filtration to remove the unbound proteins, the contribution of the slow kinetic phase returns to ~50% of the total absorption change (data not shown). I found that a ~ 2-fold larger molar excess of the Fd2-like protein relative to genuine PshB is required to achieve the same level of reconstitution.

4.4.6 *Low Temperature EPR spectrum of HbRC Cores with recombinant Fd2*

To determine whether the reconstituted HbRC complex is functionally active at low temperature, the EPR spectrum of the terminal Fe/S clusters was measured after illumination at 15 K. Freshly-isolated HbRCs, were shown previously to have a rhombic set of resonances at g = 2.067, 1.933 and 1.890, similar to that in whole cells (*21*). When PshB is removed, these resonances disappear, and only a derivative-shaped resonance at g = 2.003 is present from $P798^{+}$ (Figure 4.5, top and bottom, broken line). The electron acceptor under these conditions is iron-sulfur cluster F_X; however, it is in a ground spin state of S = 3/2, and is only visible downfield as a relatively weak doublet between g = 4 and 6 (*15*). When genuine PshB is incubated with the HbRC cores in 25-fold molar excess, a rhombic set of resonances at g = 2.067, 1.933 and 1.890 is seen after illumination at 15 K (Figure 4.5, top, solid line). When the expressed Fd2-like protein is incubated with the HbRC cores in 50-fold molar excess, an identical rhombic set of resonances at g = 2.067, 1.933 and 1.890 is seen after illumination at 15 K (Figure 4.5, bottom, solid line). Because the experiment was carried out at low temperature, no diffusion is possible, consistent with the proposal that the Fd2 protein is bound to the HbRC cores.

4.5 DISCUSSION

The primary aims of this work were to identify the *pshB* gene in *H. modesticaldum*, to determine the amino acid sequence its product, and to partially

characterize that product. To date, the only protein that has been shown to be an actual component of the HbRC complex is PshA (*10*). A homodimer of PshA binds the Bchl *g* antenna molecules, the primary donor P798, the primary acceptor A_0, and the [4Fe-4S]$^{1+,2+}$ cluster F_X (*10, 15*). The number of Bchl *g* antenna molecules in the HbRC is between 28 by HPLC analysis of pigments (*28*) and 22 by a comparison of chlorophyll and iron concentrations (*15*). It has been long known that F_A- and F_B-like iron-sulfur clusters function as terminal electron acceptors (*12, 22*); however, a dicluster ferredoxin protein similar to PsaC was not present in purified HbRC preparations (*11, 29*). Recently, I succeeded in isolating an HbRC complex from *H. modesticaldum* that contains PshB, the polypeptide that harbors the F_A and F_B clusters (*21*). My strategy to identify its gene focused on isolating the genuine PshB protein and determining its N-terminal amino acid sequence. I was assisted by the report that two ferredoxins, Fd1 and Fd2, had been isolated previously from *H. mobilis* and their gene sequences determined (*26*). I constructed primers based on the N-terminal and C-terminal amino acid sequence of *fd2* from *H. mobilis*, and using these primers I cloned the counterparts of *fd1* and *fd2* from *H. modesticaldum* as a single fragment. The deduced N-terminal amino acid sequence of the Fd2-like protein from *H. modesticaldum* matched perfectly the N-terminal amino acid sequence of genuine PshB. I cloned the corresponding *fd2* gene from *H. modesticaldum* into an expression vector, overproduced the protein with a His-affinity tag, and showed that the product binds to HbRC cores. The reconstituted HbRC was found to be fully functional in promoting light-induced electron transfer between P798 and F_A/F_B. A 2-fold higher concentration of the recombinant Fd2 protein is required to achieve a level of reconstitution comparable to genuine PshB. This could be due to known differences between the two proteins: the recombinant Fd2 protein contains a 2.5 kDa affinity tag consisting of 21 residues, including 10 consecutive His residues, on the N-terminus, and it terminates with the residues KA instead of IPG (the preceding 51 amino acids, however, are identical). The alteration at the C-terminus is because the primers were constructed using the sequence of the *fd2* gene from *H. mobilis* in the absence of the C-terminal amino acid sequence of genuine PshB. These additional amino acids at the N-terminus and changes at the C-terminus could result in a different binding affinity than genuine PshB. Nevertheless, the properties of the expressed Fd2-like protein indicate that

the long-sought gene that codes for the F_A/F_B polypeptide in heliobacterial reaction centers has been identified.

Fd2 in *H. modesticaldum* (hereafter termed PshB) has a predicted molecular weight of 5440 (54 amino acids), and is therefore considerably smaller than PsaC, which has a molecular weight of 8829 (81 amino acids). Both are acidic proteins with estimated pIs of 4.06 and 5.5, respectively. Both contain two traditional CxxCxxCxxxC binding motifs for the $[4Fe\text{-}4S]^{1+,2+}$ clusters; however, in PsaC, a Pro follows the terminal Cys residue in both Fe/S cluster binding motifs, whereas in PshB, a Cys follows the terminal Cys in the N-terminal Fe/S cluster binding motif (Table I). Although it is not uncommon for a dicluster ferredoxin to contain a residue other than Pro in this position, a Cys is highly unusual. It is not known if the Cys•Cys motif has any structural or functional significance. A database search shows that PshB is a member of a family of a large number of bacterial dicluster ferredoxins that are highly acidic and have nearly the same mass and number of amino acids. A number of high resolution X-ray and NMR structures are available for several bacterial dicluster ferredoxins (PDB entries 1FDX (now replaced with 1DUR), 1CLF, 1FDN, 2FDN, 1BLU, 1FCA, 5FD1, 1BC6, 1BQX, 1RGV) (*30-40*), including PsaC (PDB entry 1K0T) (*41*). In bacterial dicluster ferredoxins as well as PsaC, both $[4Fe\text{-}4S]^{1+,2+}$ cluster binding motifs and the clusters themselves exhibit a local pseudo-C_2-symmetry. All show a very similar set of protein folds characterized by a two-stranded anti-parallel β-sheet arrangement of N- and C-termini and the two $[4Fe\text{-}4S]^{1+,2+}$ clusters separated by a single α-helical turn. These central structural features are common to all dicluster ferredoxins characterized thus far, and they can be expected to be present in the highly similar PshB from *H. modesticaldum*. Conspicuously absent is the insertion of 8 residues in the middle of the loop connecting the two consensus iron-sulfur binding motifs, and the C-terminal extension of 14 or 15 residues present in PsaC. The amino acids in the loop insertion region of PsaC are considered to be involved in ferredoxin/flavodoxin binding (*42, 43*) and those in the C-terminus in binding to the PsaA/PsaB core and to other stromal subunits (*44*). Most significantly, the two Arg and one Lys residue that binds PsaC to the PsaA/PsaB heterodimer of PS I are not present in PshB from *H. modesticaldum;* all are replaced by neutral residues (Table I). This

indicates a different mode of binding with the HbRC core, but details await a high-resolution crystal structure of the HbRC replete with PshB.

Acknowledgments

The authors thank Dr. Robert Blankenship for generously providing the genomic sequence of *Heliobacterium modesticaldum* prior to publication. The Phototrophic ProkaryoteSequencing Project <http://genomes.tgen.org/funded>http://genomes.tgen.org/ was funded by the NSF Microbial Genome Sequencing Program.

4.6 SUMMARY

In this Chapter, I reported the cloning of the gene *pshB*, and I showed when it is overexpressed and the Fe/S clusters inserted, PshB can bind HbRC cores and function as an electron acceptor. PshB was co-purified with HbRC cores on a G-75 gel filtration column. The protein was blotted to a PVDF membrane and its N-terminal sequence was determined. The N-terminal sequence was found to be quite similar to a ferredoxin protein cloned from *Heliobacillus mobilis*, called Fd2. The gene encoding an Fd2 homolog was cloned from *H. modesticaldum* and overexpressed in *E. coli* with a His affinity tag. Fe/S clusters were reconstituted into Fd2 by incubation with iron, sulfide, and 2-mercaptoethanol under anaerobic conditions. The absorbance and EPR spectra were found to be comparable to the PshB protein purified from *H. modesticaldum*. Fd2 copurifies with HbRC cores on a G-75 gel filtration column, and a Ni-affinity column. Fd2 was also capable of light-induced electron transfer as seen by time resolved optical spectroscopy and low-temperature EPR spectroscopy. I therefore rename the protein formerly known as Fd2 as PshB, the protein in the HbRC that harbors the terminal electron acceptors. Amino acid sequence analysis of this gene product indicates it is very similar to clostridial dicluster ferredoxins. PshB is missing two evolutionary adaptions present in PsaC, the Z-loop and the C-terminal extension. The Z-loop has been implicated in ferredoxin binding, whereas the C-terminal extension is known to bind to the PsaA/PsaB heterodimer in PS I. As indicated by the fact that these proteins sequences are missing, the HbRC may have significant differences in functionality and stability when compared to PSI.

4.7 LIST OF TABLES

Table 4.1. Comparison of the N-terminal amino acid sequences of PshB from *H. modesticaldum* with amino acid sequences of Fd1 and Fd2 from *H. mobilis* and *H. modesticaldum*, as well as PsaC from *Thermosynechococcus elongatus* BP-1.

N-terminal sequences		AYKITD	
PshB *H.mod.*	1	MAYKITDACTACGACMDGCCVGAIVEGK----------KYSITSDCVDCGVCADKCPVDAIIPG	55
Fd2 *H.mob.*	1	MYKIDASQCTGCGACVSGCYTNAIVEANG----------KYTITDDCVDCGVCQDSCPVDAIKA	54
Fd1 *H.mod.*	1	VVYKISDACVACGACEDACPVNAIIKG-D----------VYSITDACIDCGTCADTCPAGAISEG	55
Fd1 *H. mob.*	1	AYKISDACVNCGSCVDACPVGAIEKGSD----------IYCINDTCIDCGSCVDTCPAGAISEG	54
PsaC BP-1	1	MAHTVKIYDTCIGCTQCVRACPTDVLEMVPWDGCKAGQIASSPRTEDCVGCKRCETACPTDFLSIRVYLGAETTRSMGLAY	81
		* * * * * * * *	

4.8 REFERENCES

(1) Deisenhofer, J., Epp, O., Miki, K., Huber, R., and Michel, H. (1984) X-ray structure analysis of a membrane protein complex. Electron density map at 3 Å resolution and a model of the chromophores of the photosynthetic reaction center from *Rhodopseudomonas viridis*. *J Mol Biol 180*, 385-98.

(2) Loll, B., Kern, J., Saenger, W., Zouni, A., and Biesiadka, J. (2005) Towards complete cofactor arrangement in the 3.0 Å resolution structure of photosystem II. *Nature 438*, 1040-4.

(3) Iwata, S., and Barber, J. (2004) Structure of photosystem II and molecular architecture of the oxygen-evolving centre. *Curr Opin Struct Biol 14*, 447-53.

(4) Zouni, A., Witt, H. T., Kern, J., Fromme, P., Krauss, N., Saenger, W., and Orth, P. (2001) Crystal structure of photosystem II from *Synechococcus elongatus* at 3.8 Å resolution. *Nature 409*, 739-43.

(5) Jordan, P., Fromme, P., Witt, H. T., Klukas, O., Saenger, W., and Krauss, N. (2001) Three-dimensional structure of cyanobacterial photosystem I at 2.5 Å resolution. *Nature 411*, 909-17.

(6) Ben-Shem, A., Frolow, F., and Nelson, N. (2003) Crystal structure of plant photosystem I. *Nature 426*, 630-5.

(7) Madigan, M. T., and Ormerod, J. G. (1995) Taxonomy, physiology, and ecology of heliobacteria, in *Anoxygenic Photosynthetic Bacteria* (Blankenship, R. E., Madigan, M. T., and Bauer, C. E. Eds.), pp 17-30 Kluwer , Dordrecht, The Netherlands

(8) Woese, C. R., Debrunner-Vossbrinck, B. A., Oyaizu, H., Stackebrandt, E., and Ludwig, W. (1985) Gram-positive bacteria: possible photosynthetic ancestry. *Science 229*, 762-5.

(9) Gest, H., Favinger, JL. (1983) *Heliobacterium chlorum*, an anoxygenic brownish-green photosynthetic bacterium containing a "new" form of bacteriochlorophyll. *Arch of Microbiol.136*, 11-16.

(10) Liebl, U., Mockensturm-Wilson, M., Trost, J. T., Brune, D. C., Blankenship, R. E., and Vermaas, W. (1993) Single core polypeptide in the reaction center of the photosynthetic bacterium *Heliobacillus mobilis*: structural implications and relations to other photosystems. *Proc Natl Acad Sci U S A 90*, 7124-8.

(11) Trost, J. T., and Blankenship, R. E. (1989) Isolation of a photoactive photosynthetic reaction center-core antenna complex from *Heliobacillus mobilis*. *Biochemistry 28*, 9898-904.

(12) Prince, R. C., Gest, H., Blankenship, R. E,. (1985) Thermodynamic properties of the photochemical reaction center of *Heliobacterium chlorum*. *Biochim Biophys Acta 810*, 377-384.

(13) van de Meent, E. J., Kobayashi, M., Erkelens, C., van Veelen, P.A., Amesz, J., Watanabe, T. (1991) Identification of 8'-hydroxychlorophyll *a* as a functional reaction center pigment in heliobacteria. *Biochim Biophys Acta 1058*, 356-62.

(14) Kleinherenbrink, F. A. M., Chiou, H. C., LoBrutto, R., and Blankenship, R. E. (1994) Spectroscopic evidence for the presence of an iron-sulfur center similar to F_X of Photosystem I in *Heliobacillus mobilis*. *Photosynth Res 41*, 115-23.

(15) Heinnickel, M., Agalarov, R., Svensen, N., Krebs, C., and Golbeck, J. H. (2006) Identification of FX in the heliobacterial reaction center as a [4Fe-4S] cluster with an S = 3/2 ground spin state. *Biochemistry 45*, 6756-64.

(16) Miyamoto, R., Iwaki, M., Mino, H., Harada, J., Itoh, S., and Oh-Oka, H. (2006) ESR signal of the iron-sulfur center F_X and its function in the homodimeric reaction center of *Heliobacterium modesticaldum*. *Biochemistry 45*, 6306-16.

(17) Muhiuddin, I. P., Rigby, S. E., Evans, M. C., Amesz, J., and Heathcote, P. (1999) ENDOR and special TRIPLE resonance spectroscopy of photoaccumulated semiquinone electron acceptors in the reaction centers of green sulfur bacteria and heliobacteria. *Biochemistry 38*, 7159-67.

(18) Brettel, K., Leibl, W., and Leibl, U. (1998) Electron transfer in the heliobacterial reaction center: Evidence against a quinone-type electron acceptor functioning analogous to A(1) in photosystem I. *Biochim. Biophys. Acta 1363*, 175-81.

(19) Kleinherenbrink, F. A. M., Ikegami, I., Hiraishi, A., Otte, S. C. M., Amesz, J. (1993) Electron Transfer in Menaquinone Depleted Membranes of *Heliobacterium chlorum*. *Biochim Biophys Acta 1142*, 69-73.

(20) van der Est, A., Hager-Braun, C., Leibl, W., Hauska, G., and Stehlik, D. (1998) Transient electron paramagnetic resonance spectroscopy on green-sulfur bacteria and heliobacteria at two microwave frequencies. *Biochim. Biophys. Acta 1409*, 87-98.

(21) Heinnickel, M., Shen, G., Agalarov, R., and Golbeck, J. H. (2005) Resolution and reconstitution of a bound Fe/S protein from the photosynthetic reaction center of *Heliobacterium modesticaldum*. *Biochemistry 44*, 9950-60.

(22) Nitschke, W., Setif, P., Liebl, U., Feiler, U., and Rutherford, A. W. (1990) Reaction center photochemistry of *Heliobacterium chlorum*. *Biochemistry 29*, 11079-88.

(23) Xiong, J., Inoue, K., and Bauer, C. E. (1998) Tracking molecular evolution of photosynthesis by characterization of a major photosynthesis gene cluster from *Heliobacillus mobilis*. *Proc Nat Acad Sci USA 95*, 14851-14856.

(24) Kimble, L. K., Mandelco, L., Woese C. R., Madigan, M. T. (1995) *Heliobacterium modesticaldum*, sp. nov., a thermophilic heliobacterium of hot springs and volcanic soils. *Arch of Microbiol. 163*, 259-267.

(25) Murphy, R. C., Gasparich, G. E., Bryant, D. A., and Porter, R. D. (1990) Nucleotide sequence and further characterization of the *Synechococcus* sp. strain PCC 7002 *recA* gene: complementation of a cyanobacterial *recA* mutation by the *Escherichia coli recA* gene. *J Bacteriol 172*, 967-76.

(26) Hatano , A., Seo, D., Kitashima, M., Sakurai, H., and Inoue, K. (2004) in *24th International Congress on Photosynthesis* (van der Est, A. a. B., D., Ed.), Montreal.

(27) Trost, J., Brune, D., and Blankenship, R. E. (1992) Protein sequences and redox titrations indicate that the electron acceptors in reaction centers from heliobacteria are similar to Photosystem-I. *Photosynth Res 32*, 11-22.

(28) Kobayashi, M., van de Meent, E. J., Erkelens, C., Amesz, J., Ikegami, I., and Watanabe, T. (1991) Bacteriochlorophyll *g* epimer as a possible reaciton center component of heliobacteria. *Biochim Biophys Acta 1057*, 89-96.

(29) van de Meent, E. J., Kleinherenbrink, F. A. M., Amesz, J. (1990) Purification and properties of an antenna-reaction center complex from heliobacteria. *Biochim Biophys Acta 1015*, 223-230.
(30) Adman, E. T., Sieker, L. C., and Jensen, L. H. (1973) The structure of a bacterial ferredoxin. *J. Biol. Chem. 248*, 3987-3996.
(31) Adman, E. T., Sieker, L. C., and Jensen, L. H. (1976) Structure of *Peptococcus aerogenes* ferredoxin. Refinement at 2 Å resolution. *J Biol Chem 251*, 3801-3806.
(32) Bertini, I., Donaire, A., Feinberg, B. A., Luchinat, C., Piccioli, M., and Yuan, H. P. (1995) Solution structure of the oxidized 2[4Fe-4S] ferredoxin from *Clostridium pasteurianum*. *Eur J Biochem 232*, 192-205.
(33) Duee, E. D., Fanchon, E., Vicat, J., Sieker, L. C., Meyer, J., and Moulis, J. M. (1994) Refined crystal structure of the 2[4Fe-4S] ferredoxin from *Clostridium acid urici* at 1.84 Å resolution. *J Mol Biol 243*, 683-695.
(34) Dauter, Z., Wilson, K. S., Sieker, L. C., Meyer, J., and Moulis, J. M. (1997) Atomic resolution (0.94 Å) structure of *Clostridium acidurici* ferredoxin. Detailed geometry of [4Fe-4S] clusters in a protein. *Biochemistry 36*, 16065-16073.
(35) Moulis, J. M., Sieker, L. C., Wilson, K. S., and Dauter, Z. (1996) Crystal structure of the 2[4Fe-4S] ferredoxin from *Chromatium vinosum*: Evolutionary and mechanistic inferences for [3/4Fe-4S] ferredoxins. *Protein Sci 5*, 1765-1775.
(36) TranQui, D., and Jesior, J. C. (1995) Structure of the ferredoxin from *Clostridium acidiurici* - model at 1.8 Å resolution. *Acta Crystallogr. D. Biol. Crystallogr. 51*, 155-159.
(37) Stout, C. D. (1993) Crystal Structures of Oxidized and Reduced *Azotobacter vinelandii* Ferredoxin at pH-8 and 6. *J Biol Chem 268*, 25920-25927.
(38) Aono, S., Bentrop, D., Bertini, I., Donaire, A., Luchinat, C., Niikura, Y., and Rosato, A. (1998) Solution structure of the oxidized Fe_7S_8 ferredoxin from the thermophilic bacterium *Bacillus schlegelii* by ^{1}H NMR spectroscopy. *Biochemistry 37*, 9812-9826.
(39) Aono, S., Bentrop, D., Bertini, I., Cosenza, G., and Luchinat, C. (1998) Solution structure of an artificial Fe8S8 ferredoxin: the D13C variant of *Bacillus schlegelii* Fe7S8 ferredoxin. *Eur. J. Biochem. 258*, 502-514.
(40) Unciuleac, M., Boll, M., Warkentin, E., and Ermler, U. (2004) Crystallization of 4-hydroxybenzoyl-CoA reductase and the structure of its electron donor ferredoxin. *Acta Crystallogr. D-Biol Crystallogr. 60*, 388-391.
(41) Antonkine, M. L., Liu, G., Bentrop, D., Bryant, D. A., Bertini, I., Luchinat, C., Golbeck, J. H., and Stehlik, D. (2002) Solution structure of the unbound, oxidized Photosystem I subunit PsaC, containing [4Fe-4S] clusters F_A and F_B: a conformational change occurs upon binding to Photosystem I. *J Biol Inorg Chem 7*, 461-72.
(42) Fischer, N., Hippler, M., Setif, P., Jacquot, J. P., and Rochaix, J. D. (1998) The PsaC subunit of photosystem I provides an essential lysine residue for fast electron transfer to ferredoxin. *EMBO J 17*, 849-858.
(43) Fischer, N., Setif, P., and Rochaix, J. D. (1999) Site-directed mutagenesis of the PsaC subunit of photosystem I. F_B is the cluster interacting with soluble ferredoxin. *J Biol Chem 274*, 23333-23340.

(44) Antonkine, M. L., Jordan, P., Fromme, P., Krauss, N., Golbeck, J. H., and Stehlik, D. (2003) Assembly of protein subunits within the stromal ridge of Photosystem I. Structural changes between unbound and sequentially PS I-bound polypeptides and correlated changes of the magnetic properties of the terminal iron sulfur clusters. *J Mol Biol 327*, 671-97.

4.9 FIGURE LEGENDS

Figure 4.1. 15% SDS-PAGE gel of HbRC cores purified with bound PshB. Lane 1 –HbRC cores. Lane 2 –HbRC cores purifed with PshB on a G-75 column. The PsaA protein is absent because the sample was extracted with organic solvent to remove the chlorophylls prior to SDS treatment; this improved resolution of the other bands, but it led to the precipitation of PshA. Lane 3 – Molecular weight markers.

Figure 4.2 Low temperature EPR spectra (left) and room temperature absorbance spectra (right) of PshB (top) and the Fd2-like protein (bottom). EPR spectra are on the right, and absorbance spectra are on the left. For EPR the samples were treated with 33 mM dithionite in 100 mM glycine (pH 10) to reduce the iron-sulfur clusters. The spectrometer conditions were: temperature, 20 K; power, 126 mW; microwave frequency, 9.47 GHz; receiver gain, 2 x 10^4; modulation amplitude, 10 G at 100 kHz.

Figure 4.3 SDS-PAGE analysis of HbRC cores co-purified with His-tagged Fd2-like protein. Lane 1 - HbRC cores + Fd2-like protein after purification on a G-75 gel filtration column; Lane 2 –HbRC cores + Fd2-like protein after elution from the Ni affinity column with 250 mM imidazole; Lane 3 – Molecular weight markers

Figure 4.4 Flash-induced absorption changes at 798 nm of HbRC cores purified by DEAE ion-exchange chromatography (top), HbRC cores with a 25-fold molar excess of genuine PshB (middle), and HbRC cores with a 50-fold molar excess of reconstituted Fd2-like protein (bottom). The experimental data represents the average of 8 scans except for the Fd2-like protein (bottom), which is the average of 16 scans. The data are fitted using the Marquardt algorithm; the residuals (difference between experimental and fit curve) are shown in the upper panel.

Figure 4.5 Light-induced EPR difference spectra of HbRC cores purified by DEAE ion-exchange chromatography reconstituted with a 25-fold molar excess of genuine PshB (top) and reconstituted with a 50-fold molar excess of reconstituted Fd2-like protein

(bottom). The EPR spectrum of HbRC complexes prior to addition of PshB and the Fd2-like protein are depicted as dotted lines (top and bottom). The spectrometer conditions were: temperature, 20 K; power, 126 mW; microwave frequency, 9.47 GHz; receiver gain, 2 x 10^4; modulation amplitude, 10 G at 100 kHz. The optical absorbance at 788 nm of the sample was 45.

Figure 4.1

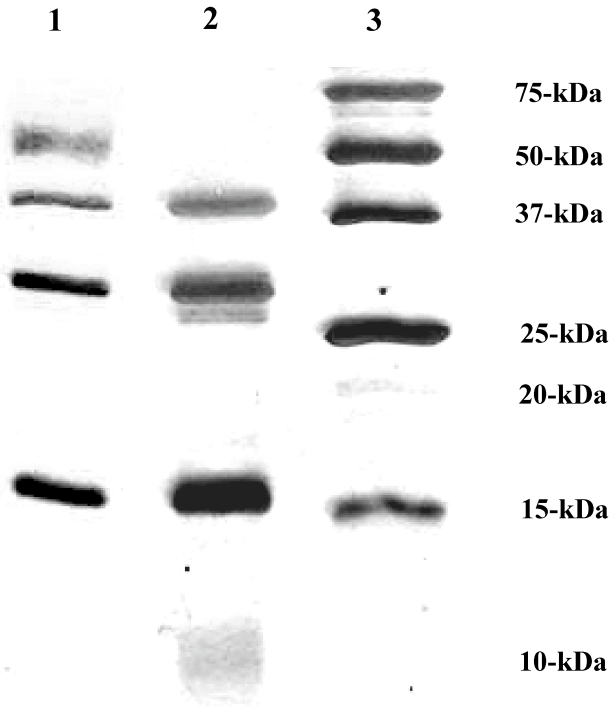

Figure 4.2

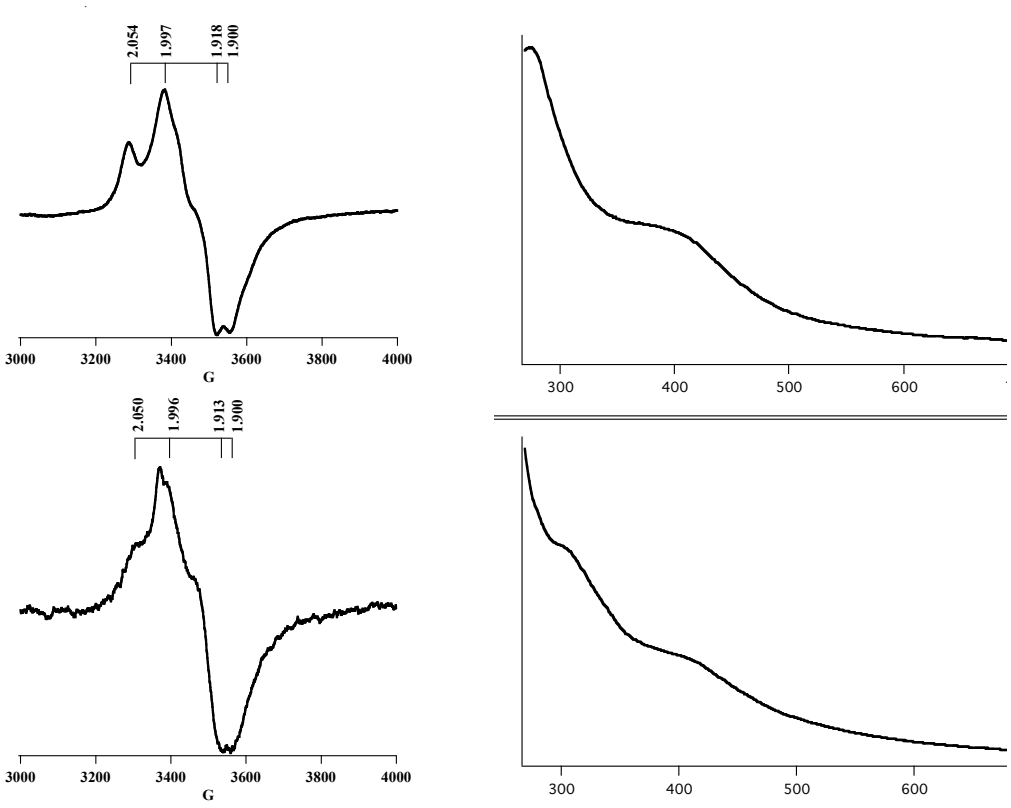
2.054
1.997
1.918
1.900
3000
3200
3400
3600
3800
4000
G
2.050
1.996
1.913
1.900
3000
3200
3400
3600
3800
4000
G
300
400
500
600
300
400
500
600

Figure 4.3

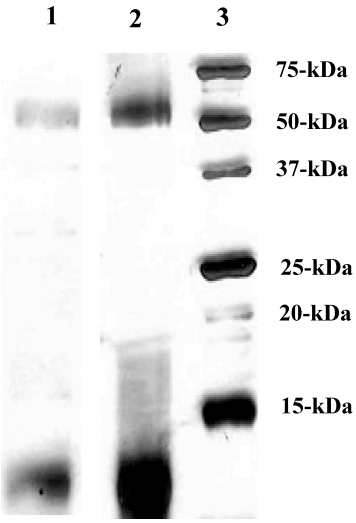

Figure 4.4

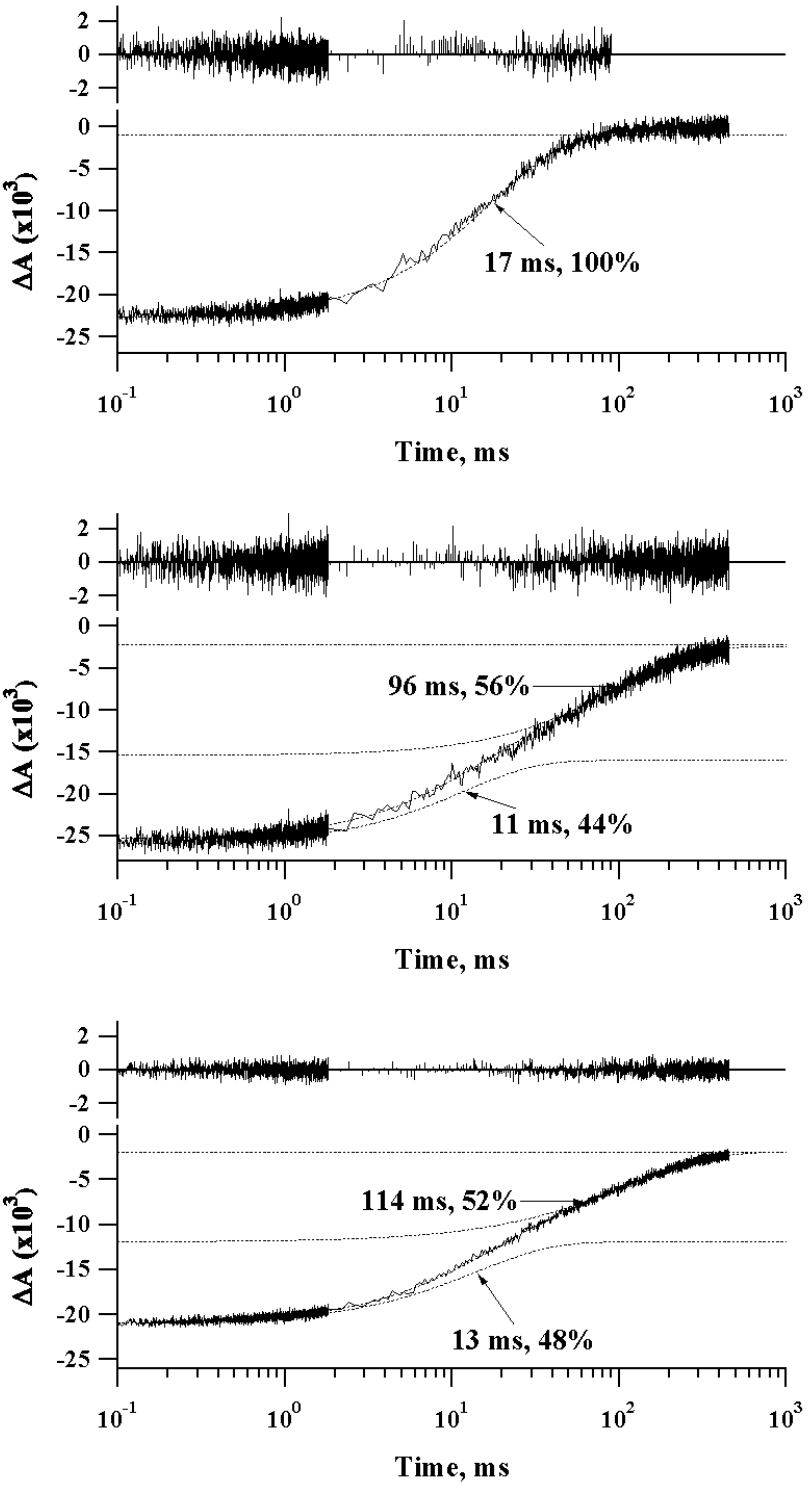
ΔA (x10³)
17 ms, 100%
Time, ms
96 ms, 56%
11 ms, 44%
Time, ms
114 ms, 52%
13 ms, 48%
Time, ms

Figure 4.5

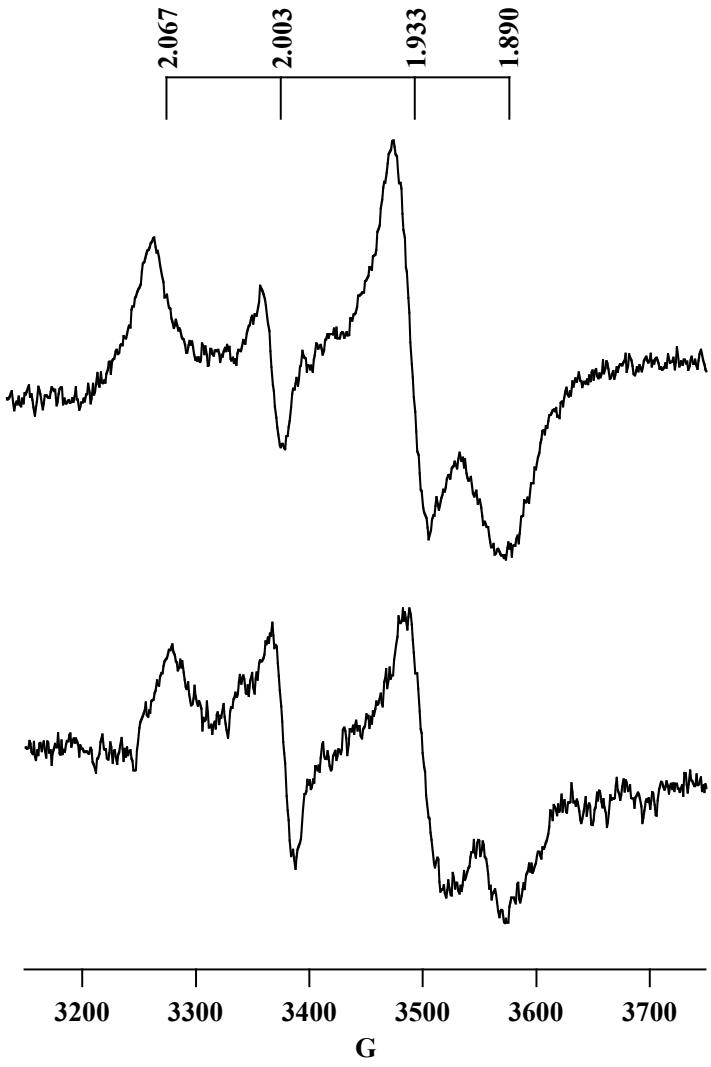

Chapter 5

Concluding Remarks

The work presented in this dissertation provides the foundation for further work on the structure and function of the HbRC. Now that the *pshB* gene has been indentified, the PshB protein can be overexpressed and purified for further structural analysis. HbRC cores purified from the membrane can also be employed for structural analysis.

The electron transfer cofactors in heliobacteria have been a matter of controversy. Although the primary donor and primary acceptor are well understood, the Fe/S clusters and quinone intermediate in the complex are the subject of intense debate. Even though I have performed a comprehensive study on the Fe/S clusters in the HbRC complex, the function of the quinone is still in question. It is possible that an atomic resolution crystal structure could clarify the situation. This work is ongoing in the Golbeck laboratory in collaboration with Dr. Petra Fromme.

Because of its absence in purified HbRCs, the existence of the PshB protein has been questioned several times in the literature. My work clearly shows this existence has been questioned because the binding of PshB to the PshA homodimer is sensitive to ionic strength. Although pulldown experiments based on PshB indicate that only PshA and PshB are present in the HbRC complex, it is possible there are additional, weakly bound proteins that similarly dissociate during purification. A method that could be used to resolve this issue could be to His-tag PshA *in vivo*, and to purify all HbRCs using a Ni-affinity column. In order to attempt an experiment of this type, one would need to be able to perform site-directed mutagenesis in heliobacteria. Prof. Kevin Redding, a collaborator of the Golbeck laboratory, is currently working to develop a genetic system in heliobacteria to make such a variant.

Although PshB in heliobacteria serves a function similar to PsaC in cyanobacteria, their amino acid sequences show distinct differences. Most notably, PshB is missing the C-terminal extension that enables PsaC to bind tightly to PS I. It seems conceivable that PsaC was at one time in evolution a soluble ferredoxin that acquired a C-terminal extension to make a more stable protein complex with PS I. Indeed, this may

be considered additional biochemical evidence that the HbRC is an evolutionary precursor to PS I.

A comparison of the iron and bacteriochlorophyll content reveal the HbRC has far fewer antenna pigments than does PS I. The low pigment content is curious, considering that in soil, their native environment, heliobacteria may recieve less light than plants, which are recieve far more light. A more appropriate situation appears to occur in green sulfur bacteria, wherein large chlorosomes have evolved to capture the small amount of light that is available in the deep water environment of these organisms. One explanation for this phenomenon could be that heliobacteria do not depend as heavily on photosynthesis for survival as do cyanobacteria or green sulfur bacteria.

To summarize, this work provides information on the structure and function of the F_X, F_A, and F_B iron-sulfur clusters in the HbRC. The major conclusions are: (1) HbRC loosely binds a ferredoxin-like protein, PshB, that binds the iron-sulfur clusters F_A and F_B. (2) PshB can be purified from HbRC complexes at high ionic strength, and rebound to HbRC cores to form a functional complex. (3) HbRC cores bind an interpolypeptide Fe/S cluster, termed F_X. When HbRC cores are incubated with sodium dithionite in the presence of light, F_X undergoes a one-electron reduction. (4) Mossbauer and EPR data indicate the reduced cluster has a ground spin state of S = 3/2. (5) Analysis of the non-heme iron content shows that the HbRC has approximately 21.1 +/- 1.1 Bchl *g*/F_X cluster. (6) The gene encoding the PshB protein was cloned from *H. modesticaldum* based upon an N-terminal sequence that was similar to that of fd2, a previously-described soluble ferredoxin from *Heliobacillis mobilis*.

MARK L. HEINNICKEL

Education

2007 PhD, Biochemistry and Molecular Biology, Penn State University
2001 B. Sci., Chemistry, St. Vincent College, Latrobe, Pennsylvania

Honors/Awards

2004 R. Adams Ducher Travel Grant. The Pennsylvania State University
2003 2nd prize, Outstanding Graduate Assistant Teaching Award
2001-2002. University Graduate Fellowship. The Pennsylvania State University

Publications

1. **Heinnickel, M**., Golbeck. (2007) Heliobacterial Photosynthesis. *Photosynth Res* (*in press)*

2. **Heinnickel, M.**, Shen, G., Golbeck JH. (2007) Identification of the *pshB* gene coding for the terminal Fe/S protein in the photosynthetic reaction center of *Heliobacterium modesticaldum*. *Biochemistry*. 49(6): 2530-6

3. Noks, P., Krasil'nikov P., **Heinnickel M**, Rubin AB. Kinetics of pigment-acceptor interaction induced by steady-state illumination in Synechocystis spaeroides photosystem I preparations cooled to 160 K in the dark and on light. *Biofizika*. 2006 51(1):65-72.

4. **Heinnickel, M.,** Agalarov, R., Svensen, N., Krebs, C., Golbeck, JH. (2006) The Identification of FX in the Heliobacterial Reaction Center as a [4Fe-4S] Cluster with a Ground Spin State of S = 3/2. *Biochemistry*. 45(21): 6756-6764

5. **Heinnickel, M**., Shen, G., Agalarov, R., Golbeck, JH. (2005) The Photosynthetic Reaction Center from *Heliobacterium modesticaldum*. In: *Photosynthesis: Fundamental Aspects to Global Perspectives*. Proceedings of the XIIIth International Congress on Photosynthesis, Montreal, (August 2004), A. van der Est and D. Bruce, eds., pp. 57-59. Allen Press, Lawrence, KS, USA

6. **Heinnickel, M.,** Shen, G., Agalarov, R, Golbeck, JH. (2005) Resolution and Reconsitutuion of a bound Fe/S protein. *Biochemistry*. 44(29):9950-60.

7. Knox, PP, **Heinnickel, M**, Rubin, A. (2004) Effect of low temperatures on photochemical activity of PS1 reaction centers from Synechocystis sp. frozen under illumination. *Biochemistry (Moscow)* 69(12):1399-402.

8. Knox, PP, **Heinnickel, M,** Rubin, A. (2004) Effect of oxygen on temporary stabilization of photoreduced quinone acceptors in Rhodobacter sphaeroides reaction centers. *Biochemistry (Moscow)* 69(3):281-4.